الجمهورية الجزائرية الديمقراطية الشعبية

Democratic and Popular Republic of Algeria

Ministry of Higher Education and Scientific Research

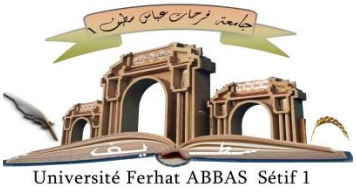

FERHAT ABBAS SETIF 1 UNIVERSITY

FACULTY OF TECHNOLOGY

Thesis

Submitted to the Process Engineering Department

for the degree of

DOCTORATE

Domain : Sciences and Technology

Field: Process Engineering **Option : Polymer engineering**

By

AOUISSI Tahar

Development, characterization and numerical simulation of the effect of incorporating a compatibilizer on the properties of bio-sourced polymer blends: PLA/PS and PLA/LDPE.

Defended on 22/05/2024 Front of the Jury:

GUESSOUM Melia	**Professor**	**Univ. Ferhat Abbas Sétif 1**	**President**
HELLATI Abdelhak	**Professor**	**Univ. M.B. EL Ibrahimi BBA**	**Supervisor**
BENANIBA Mohamed Tahar	**Professor**	**Univ. Ferhat Abbas Sétif 1**	**Co-Supervisor**
NEKKAA Sorya	**Professor**	**Univ. Ferhat Abbas Sétif 1**	**Examiner**
DADACHE Derradji	**M.C. A**	**Univ. M.B. EL Ibrahimi BBA**	**Examiner**
BENACHOUR Djafer	**Professor**	**Univ. Ferhat Abbas Sétif 1**	**Invited**

الجمهورية الجزائرية الديمقراطية الشعبية

République Algérienne Démocratique et Populaire

Ministère de L'Enseignement Supérieur et de la Recherche Scientifique

Université Ferhat ABBAS Sétif 1

UNIVERSITÉ FERHAT ABBAS - SETIF1

FACULTÉ DE TECHNOLOGIE

THÈSE

Présentée au Département de Génie des Procédés

Pour l'obtention du diplôme de

DOCTORAT

Domaine : Sciences et Technologie

Filière : Génie des Procédés **Option : Génie des polymères**

Par

AOUISSI Tahar

THÈME

Développement, caractérisation et simulation numérique de l'effet d'incorporation d'un compatibilisant sur les propriétés des mélanges à base de polymères biosourcés : PLA/PS et PLA/PEBD

Soutenue le 22/05/2024 devant le Jury :

GUESSOUM Melia	**Professeur**	**Univ. Ferhat Abbas Sétif 1**	**Présidente**
HELLATI Abdelhak	**Professeur**	**Univ M. B. El Ibrahimi BBA**	**Directeur de thèse**
BENANIBA Mohamed Tahar	**Professeur**	**Univ. Ferhat Abbas Sétif 1**	**Co-Directeur**
NEKKAA Sorya	**Professeur**	**Univ. Ferhat Abbas Sétif 1**	**Examinatrice**
DADACHE Derradji	**M.C.A**	**Univ M. B. El Ibrahimi BBA**	**Examinateur**
BENACHOUR Djafer	**Professeur**	**Univ. Ferhat Abbas Sétif 1**	**Membre invité**

ACKNOWLEDGEMENTS

All the praises and thanks go to Allah Almighty for giving me the strength, patience, and courage to accomplish this study.

Undertaking this Doctorate has been a life-changing experience for me. It would not have been completed without the contributions of many people to whom I would like to express all my recognition.

First, I would like to express my sincere gratitude to my supervisor, Pr. HELLATI Abdelhak and my co-supervisor, Pr. BENANIBA Mohamed Tahar, Pr. BENACHOUR Djafer for their continuous guidance over these last five years, patience, motivation, and constant feedback.

I thank the committee members, Pr. GUESSOUM Melia, Pr. NEKKAA Sorya and Dr. DADACHE Derradji, for their valuable time and insightful comments throughout the examination of this thesis. A special thanks go to Pr. Yacine BENGUERBA and Dr. Ali ZERRIOUH helped me in the simulation field.

I want to thank Dr. Dario CAVALLO for agreeing to help me with my current and future research and for including me in his research laboratory.

I would also like to thank Ibtissam SARROUB TS of the LCPHP laboratory and Moncef KHITAS, engineer of the LMPMP laboratory, for their guidance, suggestions, and invaluable help while completing this work.

I wish to extend my warmest thanks to Dr. Touffik BAOUZ for providing me with some of the products I needed to complete this work.

Last but not least, I would like to warmly thank my family and friends for the love and support they have provided by my, as well as all those who have contributed either directly or indirectly to the fulfillment of this study, and all those who have given me more than I could ever express in words.

DEDICATIONS

This thesis work is dedicated to those who sacrificed a lot of their time for my happiness and success, those who accompanied me throughout my life, the dearest and closest in the world, and who symbolize courage and tenderness; my very special parents, God keep them for me.

To my dear brothers.

To my dear sisters.

To all my cousins and their families.

To all my very dear friends: "Moustapha, Walid, Khalil, Yasser, Mathil, Issam, Kheider, Houssam, Miloud, Redouane, Nadire, Billal, Mosaab, and Fayçal".

To all my friends and everyone I know, near or far.

TAHAR

TABLE OF CONTENTS

Chapter I. Biodegradable polymers

Chapter II. polymer blends based on PLA

Chapter III. Materials and Methodology

Chapter IV. Compatibility Enhancement of (PLA/PS) Blends by Incorporating SEBS-g-MAH as a Compatibilizer Agent: experimental and simulation study

Chapter V. Effect of the SEBS-g-MAH on (PLA/LDPE) biolends: Morphological and thermal properties at the microscopic scale

FIGURES LIST

Chapter I

Chapter II

Chapter III

Chapter IV

Chapter V

TABLES LIST

Chapter I

Chapter III

Chapter IV

Chapter V

LIST OF ABBREVIATIONS AND SYMBOLS

PLA	Poly (lactic acide)
LDPE	Low density polyethylene
PS	Polystyrene
SEBS-g-MAH	Maleic anhydride grafted styrene-ethylene-butylene-styrene
SEM	Scanner electron microscopy
DSC	Differential Scanning Calorimetry
FTIR	Fourier Transform Infrared
XRD	X-ray Diffraction
TGA	Thermogravimetric Analysis
$\mathbf{T_{onset}}$	Extrapolated start temperature of degradation
Tg	Glass transition temperature
Tm	Melting temperature
$\mathbf{T_{1max}}$	Maximum degradation temperature in the first stage
$\mathbf{T_{2max}}$	Maximum degradation temperature in the second stage
$\mathbf{\Delta G_m}$	Gibb's free energy of mixing
$\mathbf{\Delta H_m}$	Enthalpy of mixing
$\mathbf{\Delta S_m}$	Entropy of mixing
COMPASS	Condensed-phase Optimized Molecular Potentials for Atomistic Simulation Studies
$\mathbf{V_{dW}}$**:**	Van der Waals forces
NPT:	Constant temperature, constant pressure thermodynamic ensemble
NVT:	Constant temperature, constant volume thermodynamic ensemble
$\mathbf{E_{non-\ bond}}$**:**	Energy of non-bond
$\mathbf{E_{VdW}}$**:**	Energy of van der Waals
$\mathbf{E_{electrostatic}}$**:**	Electrostatic energy
DFT	Density functional theory
MDS	Molecular dynamic Simulation
COSMO-RS	Conductor-like Screening Model for Real Solvents
HBAs	Hydrogen bond acceptors
HBDs	Hydrogen bond donors

General Introduction

GENERAL INTRODUCTION

Consumers are drawn to traditional plastics derived from fossil fuels because of their affordability and favorable mechanical properties. However, these plastics also present environmental challenges due to their resistance to biodegradation by microorganisms [1,2]. In response, biodegradable plastics have emerged as promising alternatives to traditional plastics, offering comparable properties and the potential to transform into non-toxic materials. Biomaterials and polymer bioblends are commonly utilized as biodegradable polymers to meet this criterion [3].

Poly (lactic acid) (PLA) is a biodegradable and biocompatible polymer that possesses mechanical qualities on par with fossil-based polymers. It has recently gained significant attention due to its desirable attributes, such as relatively high stiffness and strength at ambient temperature [4,5]. PLA finds widespread application in various industries, including biology, pharmaceuticals, and food [6]. Despite PLA's advantages over petroleum-based plastics, such as renewability, biodegradability, and reduced carbon footprint, it does have certain limitations [7,8]. One major limitation is its relatively low heat resistance and mechanical strength compared to other plastics, restricting its use in high-temperature environments or under significant mechanical stresses [8,9]. Consequently, many researchers are exploring methods to produce plastics from renewable sources by blending them with polymers derived from fossil fuels, with PLA being a prominent candidate for such applications [10,11]. When in a molten state, PLA can be combined with various biodegradable and non-biodegradable polymers, including poly(ε-caprolactone) (PCL) [12], poly (ethylene terephthalate) (PET) [13], polypropylene (PP) [14], polystyrene (PS) [6,15–18], and elastomers [19–21].

To enhance the properties of PLA blends. various blending methods with fossil polymers have been employed [22,23]. For instance, blending polylactic acid (PLA) with PS could be a favorable approach to meet cost-effectiveness concerns while improving the biodegradability of PS [15]. Blending PLA and LDPE also have potential uses in packaging, agriculture, and biomedical engineering. Low-density polyethylene (LDPE) and poly (lactic acid) can be combined to produce a biodegradable polymer with better mechanical properties and greater environmental friendliness. In contrast, LDPE is a petroleum-based thermoplastic with exceptional flexibility and strength [24,25-29].

The absence of compatibility between the two components in this blend leads to reduced malleability, lower resilience, and restricted use. Furthermore, several investigations have shown the enhancement of compatibility and improved interfacial adhesion via different compatibilizers [30-33]. Researchers have also explored the use of macromolecular compatibilizers to improve the interfacial adhesion between PLA and PS phases [34,35]. However, due to the immiscibility of PLA and PS, multiple-phase separation occurs in their blends, negatively affecting the blend's properties. addition of polylactide-polystyrene (PLA-co-PS) graft copolymers to polylactide (PLA). The newly created PLA-co-PS graft copolymer enhanced the compatibility between PLA and PS blends. While the authors recognize the potential applicability of specific blends using this methodology, more study is required to substantiate these findings [36]. Research was also conducted to enhance the durability of PLA by studying the compatibility of PLA/LDPE polymer blends that do not mix well [32]. Blends with varying proportions of PLA were created by a melt mixing technique, with the addition of glycidyl methacrylateGMA and polyethylene grafted with glycidyl methacrylate (PE-GMA) as reactive compatibilizers, to achieve this objective. These compatibilizers decrease the interfacial tension and improve the adhesion between the various components of the blend. The chemical reactivity of the included compatibilizers may be readily characterized in the following manner. The compatibilizer must possess some degree of compatibility with PE.

With the advancement of computational technology, molecular dynamics (MD) has been more significant in material modeling and subsequent technology development. MD has the advantage of effectively uncovering the underlying processes of the microscopic phase, as shown by recent research [37,38]. Over the last decade, MD simulation has been effectively used to compute the interaction mechanism [39] , mechanical characteristics[40], and forecast the miscibility [41] of polymer blends. These results demonstrate that MD is a suitable and dependable technique for analyzing the structural performance and mutual interaction in polymer blends [42].

This thesis investigates the effects of adding styrene ethylene-butylene-styrene grafted maleic anhydride (SEBS-g-MAH) at different concentrations (2.5, 5, 7.5, and 10 wt%) on the compatibility of (polylactic acid / polystyrene) (PLA/PS) and (polylactic acid low-density polyethylene) (PLA/LDPE) bioblends, with a weight ratio of (75/25) and (20/80) respectively. Various characterization methods were employed to examine the morphological, thermal, and thermal degradation properties and mechanical parameters relevant to producing

(PLA/PS) and (PLA/LDPE). The primary objective is to gain a deeper understanding of the role of SEBS-g-MAH as a binding agent between the two polymers. Theoretical computation, specifically molecular modeling, offers an alternative approach to obtaining results regarding structural and spectroscopic properties [43,44]. These results can be compared to experimental findings. Exploring the intermolecular bonding within blends through practical techniques is generally challenging. However, molecular dynamics simulations provide a reliable, cost-effective, and efficient tool to overcome this limitation. Atomic-level simulations have frequently been employed to predict the physical properties and interaction mechanisms in polymer blend compatibilization [45–48]. This theoretical investigation is crucial in comprehending and explaining the diverse effects of the compatibilization agent's efficacy on the blend's properties [49].

Our thesis is divided into five main chapters:

Chapter I and II: represents the bibliographic part of this thesis, covering the general theory around Biodegradable polymers and Poly (lactic acid). Followed by an overview and recent research in polymer blends based on PLA.

Chapter III describes the materials used, the preparation methods and the various techniques used during characterization (experimental and Computational study).

Chapter IV: reports on the study of Blends (PLA/PS) by Incorporating SEBS-g-MAH as a Compatibilizer Agent

Chapter V aims to investigate the results and discuss the effect of the SEBS-g-MAH on (PLA/LDPE) blends.

Finally, we conclude our work with a general conclusion and perspectives.

REFERENCES

[1] N. P. Thanh, Y. Matsui, and T. Fujiwara, “Assessment of plastic waste generation and its potential recycling of household solid waste in Can Tho City, Vietnam,” Environ. Monit. Assess., vol. 175, no. 1–4, pp. 23–35, 2011.

[2] N. Newaj and M. H. Masud, “Utilization of Waste Plastic to Save the Environment,” Icmiee-Pi-140291, pp. 1–4, 2014, [Online]. Available: http://www2.kuet.ac.bd/icmiee2014/wp-content/uploads/2015/02/ICMIEE-PI-140291.pdf.

[3] A. Ammala et al., An overview of degradable and biodegradable polyolefins, vol. 36, no. 8. Elsevier Ltd, 2011.

[4] A. K. Agrawal, Spinning of Poly(Lactic Acid) Fibers.pp,323-341, 2010.

[5] K. Hashima, S. Nishitsuji, and T. Inoue, “Structure-properties of super-tough PLA alloy with excellent heat resistance,” Polymer (Guildf)., vol. 51, no. 17, pp. 3934–3939, 2010.

[6] B. O. Leung, A. P. Hitchcock, J. L. Brash, A. Scholl, and A. Doran, “Phase segregation in polystyrene-polylactide blends,” Macromolecules, vol. 42, no. 5, pp. 1679–1684, 2009.

[7] A. Deghiche et al., “Effect of the stearic acid-modified TiO2 on PLA nanocomposites: Morphological and thermal properties at the microscopic scale,” J. Environ. Chem. Eng., vol. 9, no. 6, pp. 106541, 2021.

[8] T. Narancic et al., “Biodegradable Plastic Blends Create New Possibilities for End-of-Life Management of Plastics but They Are Not a Panacea for Plastic Pollution,” Environ. Sci. Technol., vol. 52, no. 18, pp. 10441–10452, 2018.

[9] E. Balla et al., “Poly(lactic acid): A versatile biobased polymer for the future with multifunctional properties-from monomer synthesis, polymerization techniques and molecular weight increase to PLA applications,” Polymers (Basel)., vol. 13, no. 11,pp 1822, 2021.

[10] J. C. C. Lima, E. A. G. Araújo, P. Agrawal, and T. J. A. Mélo, “PLA/SEBS Bioblends: Influence of SEBS Content and of Thermal Treatment on the Impact Strength and Morphology,” Macromol. Symp., vol. 383, no. 1, pp. 1–6, 2019.

[11] R. Nehra, S. N. Maiti, and J. Jacob, “Analytical interpretations of static and dynamic mechanical properties of thermoplastic elastomer toughened PLA blends,” J. Appl. Polym. Sci., vol. 135, no. 1, pp. 1–13, 2018.

[12] X. Zhang, Y. Xiao, and M. Lang, “Synthesis and degradation behavior of miktoarm poly(ε-caprolactone) 2 -b-poly(L-lactone) 2 microspheres,” Polym. J., vol. 45, no. 4, pp. 420–426, 2013.

[13] X. You, M. R. Snowdon, M. Misra, and A. K. Mohanty, “Biobased Poly(ethylene

terephthalate)/Poly(lactic acid) Blends Tailored with Epoxide Compatibilizers," ACS Omega, vol. 3, no. 9, pp. 11759–11769, 2018.

[14] E. Z. E. Zawawi, A. H. N. Hafizah, A. Z. Romli, N. Y. Yuliana, and N. N. Bonnia, "Effect of nanoclay on mechanical and morphological properties of poly(lactide) acid (PLA) and polypropylene (PP) blends," Mater. Today Proc., vol. 46, no. pp. 1778–1782, 2020.

[15] K. Hamad, M. Kaseem, and F. Deri, "Rheological and mechanical properties of poly(lactic acid)/polystyrene polymer blend," Polym. Bull., vol. 65, no. 5, pp. 509–519, 2010.

[16] K. Hamad, M. Kaseem, F. Deri, and Y. G. Ko, "Mechanical properties and compatibility of polylactic acid/polystyrene polymer blend," Mater. Lett., vol. 164, pp. 409–412, 2016.

[17] G. Biresaw and C. J. Carriere, "Interfacial tension of poly(lactic acid)/polystyrene blends," J. Polym. Sci. Part B Polym. Phys., vol. 40, no. 19, pp. 2248–2258, 2002.

[18] X. Liao, H. Zhang, Y. Wang, L. Wu, and G. Li, "Unique interfacial and confined porous morphology of PLA/PS blends in supercritical carbon dioxide," RSC Adv., vol. 4, no. 85, pp. 45109–45117, 2014.

[19] C. Xu, D. Yuan, L. Fu, and Y. Chen, "Physical blend of PLA/NR with co-continuous phase structure: Preparation, rheology property, mechanical properties and morphology," Polym. Test., vol. 37, pp. 94–101, 2014.

[20] T. Talbamrung, C. Kasemsook, W. Sangtean, S. Wachirahuttapong, and C. Thongpin, "Effect of Peroxide and Organoclay on Thermal and Mechanical Properties of PLA in PLA/NBR Melted Blend," Energy Procedia, vol. 89, pp. 274–281, 2016.

[21] N. Candau, O. Oguz, N. León Albiter, G. Förster, and M. L. Maspoch, "Poly (Lactic acid)/ground tire rubber blends using peroxide vulcanization," Polymers (Basel)., vol. 13, no. 9, pp. 1–20, 2021.

[22] J. Z. Liang, L. Zhou, C. Y. Tang, and C. P. Tsui, "Crystalline properties of poly(L-lactic acid) composites filled with nanometer calcium carbonate," Compos. Part B Eng., vol. 45, no. 1, pp. 1646–1650, 2013.

[23] M. Zhang, Y. Huang, M. Kong, H. Zhu, G. Chen, and Q. Yang, "Morphology and rheology of poly(l-lactide)/polystyrene blends filled with silica nanoparticles," J. Mater. Sci., vol. 47, no. 3, pp. 1339–1347, 2012.

[24] K. S. Anderson, K. M. Schreck, and M. A. Hillmyer, "Toughening polylactide," Polym. Rev., vol. 48, no. 1, pp. 85–108, 2008.

[25] K. Hamad, M. Kaseem, and F. Deri, "Poly(lactic acid)/low density polyethylene polymer blends: preparation and characterization," Asia-Pacific J. Chem. Eng., vol. 7, no.pp 310-316, 2012.

[26] R. M. Rasal, A. V. Janorkar, and D. E. Hirt, "Poly(lactic acid) modifications," Prog. Polym. Sci., vol. 35, no. 3, pp. 338–356, 2010.

[27] B. Boubekeur, N. Belhaneche-Bensemra, and V. Massardier, “Valorization of waste jute fibers in developing low-density polyethylene /poly lactic acid bio-based composites,” J. Reinf. Plast. Compos., vol. 34, no. 8, pp. 649–661, 2015.

[28] B. Boubekeur, N. Belhaneche-Bensemra, and V. Massardier, “Low-Density Polyethylene/Poly(Lactic Acid) Blends Reinforced by Waste Wood Flour,” J. Vinyl Addit. Technol., vol. 26, no. 4, pp. 443–451, 2020.

[29] H. Zhou, M. Zhao, Z. Qu, J. Mi, X. Wang, and Y. Deng, “Thermal and Rheological Properties of Poly(lactic acid)/Low-Density Polyethylene Blends and Their Supercritical CO2 Foaming Behavior,” J. Polym. Environ., vol. 26, no. 9, pp. 3564–3573, 2018.

[30] K. S. Anderson and M. A. Hillmyer, “The influence of block copolymer microstructure on the toughness of compatibilized polylactide/polyethylene blends,” Polymer (Guildf)., vol. 45, no. 26, pp. 8809–8823, 2004.

[31] G. Singh, H. Bhunia, A. Rajor, R. N. Jana, and V. Choudhary, “Mechanical properties and morphology of polylactide, linear low-density polyethylene, and their blends,” J. Appl. Polym. Sci., vol. 118, no. 1, pp. 496–502, 2010.

[32] Y. F. Kim, C. N. Choi, Y. D. Kim, K. Y. Lee, and M. S. Lee, “Compatibilization of immiscible poly(l-lactide) and low density polyethylene blends,” Fibers Polym., vol. 5, no. 4, pp. 270–274, 2004.

[33] K. S. Anderson, S. H. Lim, and M. A. Hillmyer, “Toughening of polylactide by melt blending with linear low-density polyethylene,” J. Appl. Polym. Sci., vol. 89, no. 14, pp. 3757–3768, 2003.

[34] B. Wang et al., “Effect of poly(styrene-ran-methyl acrylate) inclusion on the compatibility of polylactide/polystyrene-b-polybutadiene-b-polystyrene blends characterized by morphological, thermal, rheological, and mechanical measurements,” Polymers (Basel)., vol. 11, no. 5, 2019.

[35] X. Gong et al., “Compatibilization of poly(lactic acid)/high impact polystyrene interface using copolymer poly(stylene-ran-methyl acrylate),” J. Appl. Polym. Sci., vol. 135, no. 6, pp. 1–7, 2018.

[36] S. Gazzotti, K. H. Adolfsson, M. Hakkarainen, H. Farina, A. Silvani, and M. A. Ortenzi, “DOX mediated synthesis of PLA-co-PS graft copolymers with matrix-driven self-assembly in PLA-based blends,” Eur. Polym. J., vol. 170, no. pp. 111157, 2022.

[37] P. Khakbaz and J. B. Klauda, “Investigation of phase transitions of saturated phosphocholine lipid bilayers via molecular dynamics simulations,” Biochim. Biophys. Acta - Biomembr., vol. 1860, no. 8, pp. 1489–1501, 2018.

[38] R. S. Katiyar and P. K. Jha, “Phase behavior of aqueous polyacrylic acid solutions using atomistic molecular dynamics simulations of model oligomers,” Polymer (Guildf)., vol. 114, pp. 266–276, 2017.

[39] S. Khan et al., “Exploring molecular insights into the interaction mechanism of cholesterol derivatives with the Mce4A: A combined spectroscopic and molecular dynamic simulation studies,” Int. J. Biol. Macromol., vol. 111, pp. 548–560, 2018.

[40] M. Wei, P. Xu, Y. Yuan, X. Tian, J. Sun, and J. Lin, “Molecular dynamics simulation on the mechanical properties of natural-rubber-: Graft -rigid-polymer/rigid-polymer

systems," Phys. Chem. Chem. Phys., vol. 20, no. 12, pp. 8228–8240, 2018.

[41] Q. Wei et al., "Study the bonding mechanism of binders on hydroxyapatite surface and mechanical properties for 3DP fabrication bone scaffolds," J. Mech. Behav. Biomed. Mater., vol. 57, pp. 190–200, 2016.

[42] H. Cai et al., "Experimental and computational investigation on performances of the thermoplastic elastomer SEBS/Poly(lactic acid) blends," Mater. Today Commun., vol. 35, no, pp. 105600, 2023.

[43] A. Zerriouh, A. Deghiche, W. Bououden, D. Cavallo, A. Erto, and N. Haddaoui, "A computational and experimental investigation of TEOS-treated graphene oxide-PVA interaction: molecular dynamics simulation and COSMO-RS insights," J. Mol. Liq., vol. 382, no. pp. 121914, 2022.

[44] L. Otmani, R. Doufnoune, Y. Benguerba, and A. Erto, "Experimental and theoretical investigation of the interaction of sulfonated graphene oxide with polyvinylalcohol/poly (4-styrenesulfonic) complex," J. Mol. Liq., vol. 284, pp. 599–606, 2019.

[45] M. Bichara Abderaman, "A Molecular Dynamics Study on the Miscibility of Polyglycolide with Different Polymers," Int. J. Mater. Sci. Appl., vol. 7, no. 4, pp. 126, 2018.

[46] Y. Li, Q. Wang, and S. Wang, "A review on enhancement of mechanical and tribological properties of polymer composites reinforced by carbon nanotubes and graphene sheet: Molecular dynamics simulations," Compos. Part B Eng., vol. 160, pp. 348–361, 2019.

[47] R. Bo, J. Wang, C. Wang, Y. Wang, P. He, and Z. Han, "Selective distribution of BaTiO3 and graphene in PS/PVDF blends: Molecular dynamics simulations," Mater. Today Commun., vol. 34, pp. 105247,2023.

[48] K. L. Ngai, S. Valenti, and S. Capaccioli, "Molecular dynamic in binary mixtures and polymer blends with large difference in glass transition temperatures of the two components: A critical review," J. Non. Cryst. Solids, vol. 558, pp. 119573, 2021.

[49] Q. Wei et al., "Multi-scale investigation on the phase miscibility of polylactic acid/o-carboxymethyl chitosan blends," Polymer (Guildf)., vol. 176, no. pp. 159–167, 2019.

Chapter I. Biodegradable Polymers

Chapter I. Biodegradable polymers

I.1. Introduction

In recent years, the growing use of petroleum-derived synthetic plastics has yielded several benefits for society and contributed to economic progress. In the 1950s, there were only 1.5 million tons of plastic produced annually. However, by 2018, this amount had risen to around 400 million tonnes. It is projected that the yearly worldwide plastic production will reach a quantity of 1800 million tons by the year 2050. Nevertheless, although they have valuable possessing commendable attributes including affordability, exceptional resilience, ease of manipulation, and reduced weight, the majority of synthetic plastics exhibit a limited duration of usefulness prior to their disposal, particularly those used in packaging and as disposable items. The combination of a short service life and improper waste disposal practices has resulted in significant environmental challenges, including the exacerbation of global warming and the proliferation of plastic pollution [1,2]. Approximately 70 million tons of anthropogenic plastic, out of a total of 90 million tons, are deposited in the natural environment, where they will undergo progressive degradation into microplastics. This process poses significant health risks that need attention and concern. Global warming has been further exacerbated due to the unregulated release of greenhouse gases (GHGs), notably carbon dioxide (CO_2). The concentration of CO2 and global temperature in the year 2019 exceeded 400 parts per million (ppm) and experienced an increase of 1 degree Celsius, respectively. This situation poses a significant environmental concern. According to current projections, the concentration of carbon dioxide (CO2) is anticipated to exceed 450 parts per million (ppm) during the next 20 to 40 years [2–5].The global temperature is projected to see a rise of 1.5 °C. Research and development of biodegradable polymers have been spurred by growing oil costs and increased activity on environmental and pollution avoidance. According to a recent study [6], the market for biodegradable plastics, including poly (lactic acid) (PLA), polycaprolactone (PCL), starch blends, regenerated cellulose, polybutylene succinate (PBS), and poly (butyl acrylate) (PBA), was valued at 19.54 billion USD in 2016.

I.2. General information on biodegradation of polymers

I.2.1 Methods of polymer degradation

Generally, the techniques used for polymer degradation may be classified into two main groups: "abiotic" and "biotic" approaches. There are five distinct mechanisms through which synthetic polymers can undergo degradation, which are influenced by external factors. These mechanisms include photodegradation caused by UV radiation or high-energy radiation (an abiotic process), oxidation (an abiotic process) enhanced by chemical, thermal degradation at elevated temperatures (an abiotic process), mechanical degradation (an abiotic process), and biodegradation catalyzed by organisms (a biotic process). It is worth noting that photodegradation can be considered environmentally friendly if it occurs in the absence of high-energy radiation. Microorganisms, namely bacteria and fungi or their symbiotic relationships, have the greatest polymer degradation capacity for of all existing organisms. The use of the polymer as a nutritional resource is facilitated by their sophisticated enzymatic mechanisms. Another crucial element to consider is that of the metabolites, namely the organic acids associated with the tricarboxylic acid cycle, specifically oxaloacetic acid, citric acid, and succinic acid. The metabolites generated by bacteria produce persistent deleterious effects even after death [7].

The process of polymer biodegradation in the environment, i.e. in soil and seawater, is a multi-faceted phenomenon. At the same time, the polymer undergoes mechanical damage due to environmental factors such as UV rays, high temperatures, humidity and others, which promotes the biodegradation process[7].

I.2.2 Scheme and stages of polymer biodegradation

The process of polymer biodegradation involves many stages, including the initial adhesion of microorganisms to the polymer surface the subsequent adaption of these microbes, the depolymerization of the polymer, and finally, the mineralization of the resulting residues [8].

The first step involves the adsorption of the microbe onto the polymer surface. It is interesting to note that colonization is greater in samples with more developed external surfaces. During the adaptation phase, the second step microbial colonies develop and multiply. Thirdly, extracellular enzymes (i.e., exoenzymes) systematically break down the main macrochains into mono- and oligomeric components since polymer macromolecules cannot penetrate the semi-permeable cell wall of micro-organisms. The general overview of polymer biodegradation shown in FigureI.1 [9] .

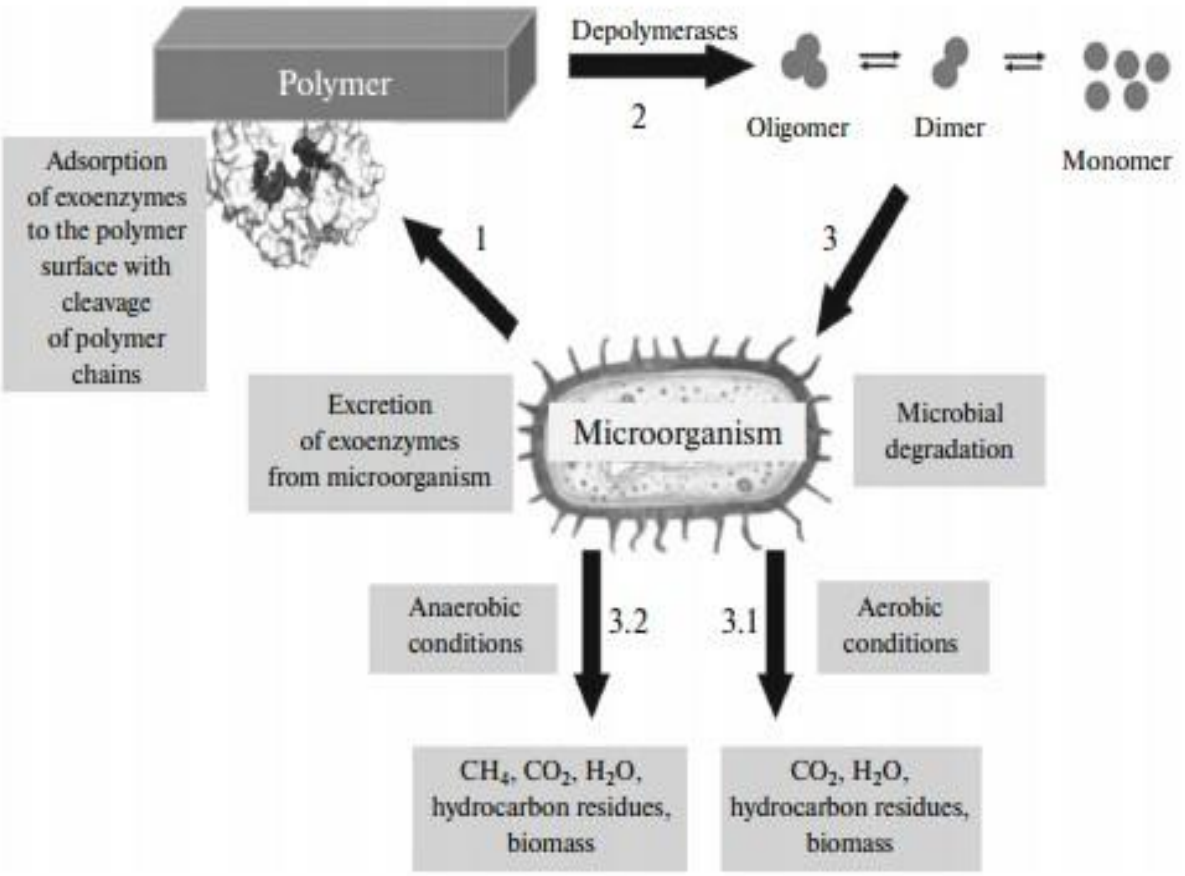

Figure I.1. General scheme of polymer biodegradation[9].

The term "depolymerases" refers to the enzymes that break down polymer chains. Within a species, depolymerases may differ in terms of both their qualitative and quantitative makeup. Because they need to create certain enzymes or metabolites that may start the polymer depolymerization cycle, not all microbes are able to degrade any particular polymer. Finally, the low-molecular-weight pieces that have been acquired break through the cell wall and are mineralized by endoenzymes, which are intracellular enzymes. This process produces the final products, which include carbon dioxide, water, salts, and methane. In this instance, microbes exploit low-molecular-weight fragments as sources of energy and/or carbon. It should be mentioned that the rate of polymer biodegradation seldom exceeds 100% since most of the polymer ends up leaking into other materials like humus and biomass[10].

I.2.3 Mechanisms of Polymer Biodegradation

Polymer biodegradation occurs via two distinct mechanisms: biological oxidation and biological hydrolysis [8]. There is a synergistic impact from these methods.

Biological hydrolysis is a biochemical process that takes place via the catalytic activity of certain enzymes known as hydrolases. The resultant products of biological hydrolysis exhibit similarities to the analogous products of chemical hydrolysis, with the main distinction being in the catalyst used.

During the production of hydrocarbon polymers, oxidation reactions occur, resulting in the formation of hydroperoxides. The quantity of hydroperoxides formed plays a significant role in determining the rate of thermal and photooxidation that takes place during the following usage of these polymers. The involvement of hydroperoxides in the radical oxidation mechanisms of synthetic polymers is of significant importance [8].Figure I.2 shows the polymer biodegradation pathways using various mechanisms [11].

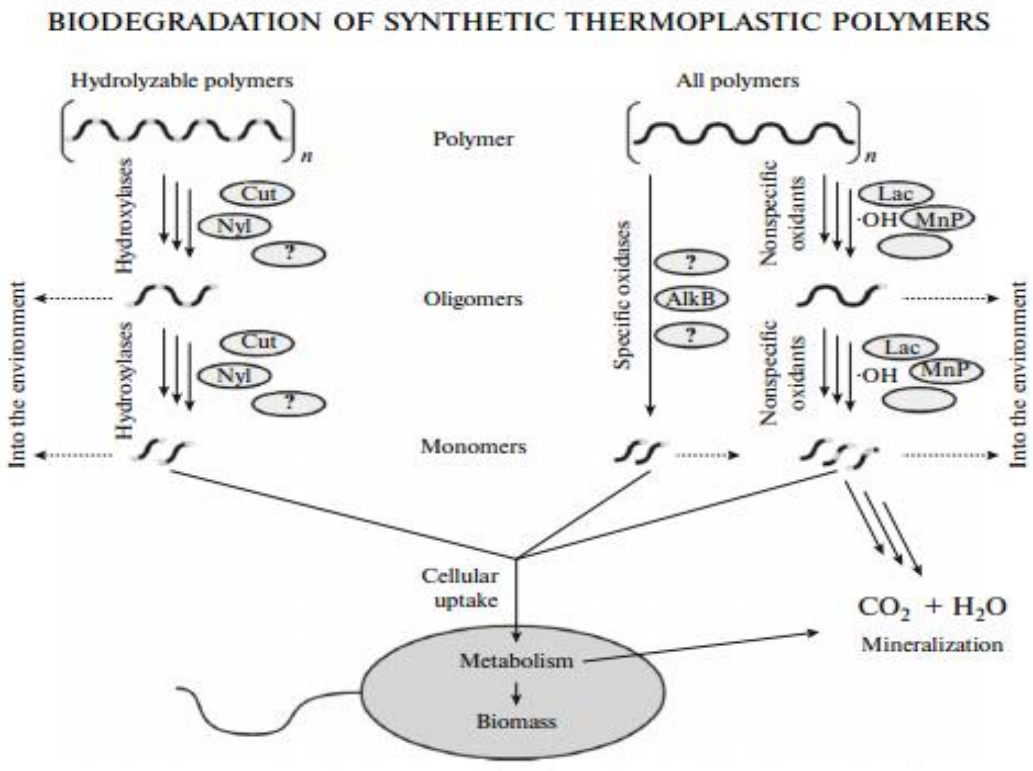

Figure I.2. Mechanisms of polymer biodegradation [9]: question mark, hitherto unknown enzymes; Cut, cutinase; Nyl, nylon hydrolase; AlkB, alkane hydroxylase; Lac, laccase; and MnP, manganese peroxidase.

I.2.4 Factors Affecting Polymer Biodegradation

The biodegradation process is influenced by many key factors, including the inherent characteristics and features of the polymer, the conditions present in the environment, and the specific attributes of the microorganism involved Figure I.3.

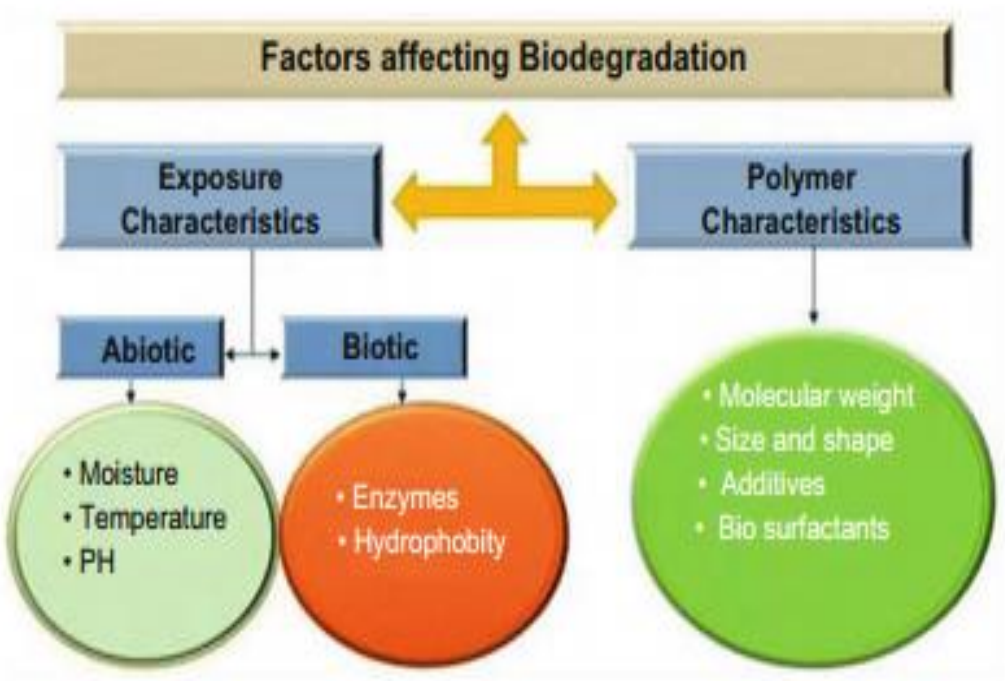

Figure I.3. Factors affecting the biodegradation process [12].

I.2.4.1 Nature and Properties of a Polymer

The main factor of the biodegradation process is the polymer's nature. Therefore, unlike polyesters or polycarbonates, polyolefins biodegrade under quite different circumstances.

a) **Molecular weight of a polymer:** The microbial degradation of a polymer is inversely proportional to its molecular weight. The reduction in solubility of the polymer is a consequence of its increased molecular weight, hence leading to complications in depolymerization when exposed to the relevant enzymes [9].
b) **Size, shape, and surface condition of polymer samples**: The rate of biodegradation is directly proportional to the surface area and level of development of the polymer. The ASTM D6400-04 provides the prescribed specifications for the form and dimensions of several categories of biodegradable polymers[13].
c) **Polymer structure:** The biodegradability of the polymer is enhanced by the inclusion of hydrophilic functional groups. The biodegradability of a polymer increases as its

degree of crystallinity decreases. The inclusion of ester or amide linkages in the polymer molecule enhances the biodegradation process due to their sensitivity to hydrolysis[14].

d) **Temperature characteristics of a polymer**: The extent to which a polymer may biodegrade is significantly influenced by its melting and softening points. Typically, the biodegradability of a polymer has a negative correlation with its melting point, indicating that as the melting point of a polymer increases, its biodegradability tends to decrease. The lipase derived from the species Rhizopus delemar has been shown to have hydrolytic activity towards low melting point polyesters, namely polycaprolactone[9].

I.2.4.2 Nature of Microorganism

Enzymes that are excreted by diverse bacteria possess distinctive active sites that facilitate the process of biodegradation for certain polymers. The straight-chain polyesters derived from dicarboxylic acids with carbon atom between 6 to 12 exhibit notable susceptibility to enzymatic biodegradation by the fungus *Aspergillus flavus* and *Aspergillus niger*. This stands in contrast to polyesters synthesized from alternative monomers. The processes used by depolymerases in the exoenzymatic degradation of polyhydroxybutyrate vary depending on the individual depolymerase involved[9].

I.2.4.3 Environmental Conditions

Environmental factors (temperature, moisture content in the liquid or gaseous phase, presence or absence of oxygen (aerobic or anaerobic decomposition)) should be selected so as to create optimum conditions for biodegradation.

a) **Moisture:** The presence of moisture is an essential condition for the proliferation and reproductive processes of microorganisms. Research has shown that the rate of polymer biodegradation is enhanced when an adequate level of moisture is present. Furthermore, increased atmospheric humidity facilitates the process of polymer hydrolysis[9] .

b) **Potential of hydrogen (pH):** The rate of polymer hydrolysis may be modified by manipulating the pH. An optimal rate of polylactide hydrolysis has been observed at a pH of 5, as reported in reference[9]. It is important to acknowledge that the byproducts resulting from the breakdown of different polymers have the ability to alter the pH level. Consequently, this pH alteration has an impact on the proliferation of microorganisms as well as the process of biodegradation.

c) **Availability or lack of access to oxygen:** In the presence of oxygen (aerobic conditions), oxygen serves as an electron acceptor within the respiratory electron transport chain. Consequently, the byproducts of biodegradation include carbon dioxide, water, hydrocarbon residues, hydrocarbon biomass, and salts. In the absence of oxygen, the resultant reaction products remain consistent with those seen in the presence of oxygen, with the additional release of methane as shown in Figure I.2. In the present scenario, the ultimate electron acceptor comprises sulfate and nitrate ions, carbon dioxide, and iron and manganese cations. In both forms of respiration, the liberation of free energy during the reaction is subsequently stored inside the electrochemical potential gradient[7].

The decomposition of polymers in the environment often occurs in the presence of oxygen. The process of biodegradation in sediments and landfills occurs in an oxygen-deprived environment. When polymer samples are placed in compost or soil, their exposure to oxygen is not completely restricted, but rather restricted to some extent. Consequently, the process of biodegradation takes place in circumstances that are partly aerobic, potentially leading to the emission of a little quantity of methane [7].

I.2.4.4 Other Factors

It is important to acknowledge that the degradation of polymers may be facilitated by abiotic hydrolysis, photo-induced oxidation, and physical disruption. These mechanisms contribute to an increase in the surface area of the polymer, as well as a reduction in its molecular weight and degree of crystallinity [15].

I.3. Classification of Bioplastics

Bioplastics, sometimes referred to as biodegradable polymers, are created from many sources such as biomass, microorganisms, petrochemicals, and biotechnological processes. Bioplastics may be broadly classified into two primary types, namely agro-polymers and bio-polyesters FigureI.4. Agro-based polymers are generated from natural and renewable sources, which include a variety of substances such as polysaccharides, starch, cellulose, lignin, pectin, animal and plant proteins, as well as oils. On the other hand, bio-polyesters are created via a combination of microorganisms, petrochemicals, and biotechnological processes. Agro-polymers mostly derive from biomass derived from plant and animal sources. Biopolymers generated from starch has many notable characteristics, including renewability, high

biodegradability, and a favorable oxygen barrier property. These attributes make them more suited for various applications compared to conventional plastics[16].

The majority of proteins derived from animal and plant sources are used as a primary resource in the manufacturing process of bioplastics. Proteins are well recognized as a prominent resource used within the plastic production sectors [17].

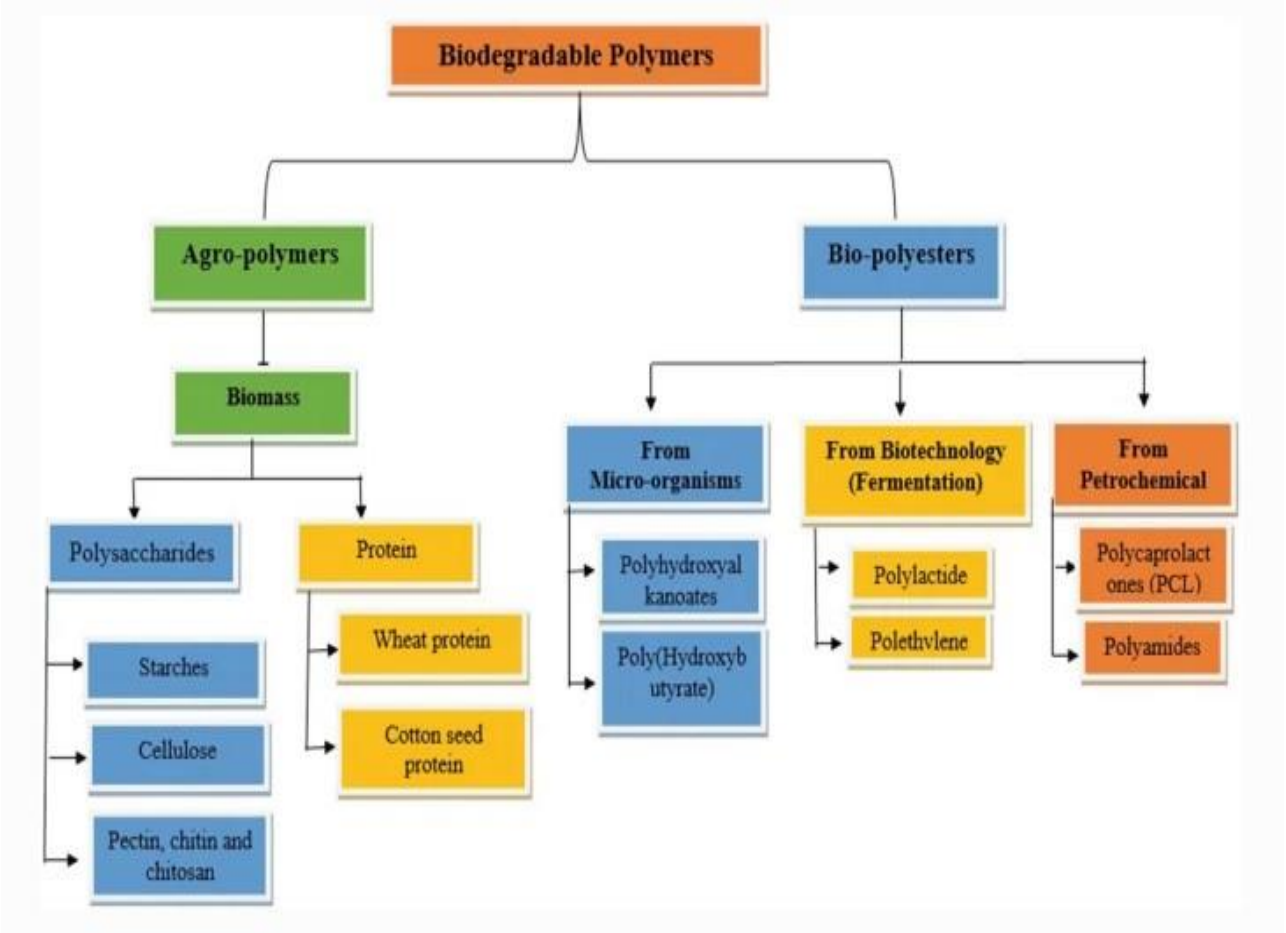

Figure I.4. Classification of biodegradable polymers[17].

I.4. Applications and state-of-the-art technologies for bioplastics innovation and production

Most traditional plastics processing methods may be used to process biodegradable polymers, however some changes to processing conditions and modifications to equipment may be necessary. Film extrusion, injection molding, blow molding, and thermoforming are among the processing processes often used in many industries. Biodegradable polymers have been implemented in three primary industries, including medical, packaging, and agriculture. The applications of biodegradable polymers include a wide range of areas, including

pharmacological devices such as matrices for enzyme immobilization and controlled-release devices [18]. Additionally, these polymers find use in therapeutic devices, serving as temporary prostheses and providing a porous structure for tissue engineering purposes.

The present bioplastic manufacturing model focuses on developing innovative protocols to valorize renewable resources from urban, agricultural, and food wastes. Chemical industry focused on biocatalytic transformation and synthetic chemistry to generate biomass feedstock monomers and biodegradable polymers [19,20]. Innovation in sustainable bioplastics involves creating novel polymers or drop-in alternatives from renewable resources. Modern industrial biotechnology offers chemo-enzymatic or bio-catalytic synthesis methods for turning biomass or renewable feedstocks into high-value monomers [21]. Additionally, creating consumer-grade bioplastics from waste residual monomers promotes a circular bioeconomy via sustainable manufacturing. Research to encourage and scale up bioplastic manufacturing was driven by worldwide demand for biobased and biodegradable polymers. Bio-based industries (BBI) consortia and EU are spending around 3.7 billion in flagship projects to promote novel bio-based monomer and polymer manufacturing technologies from waste biomass/renewable feedstocks [22]. Bioplastics manufacturing techniques may expand in the following decade as BBI aims to replace at least 30% of fossil-based raw materials with bio-based and biodegradable ones by 2030 [23].

The use of greenhouse gases, such as carbon dioxide, in the manufacturing of bioplastics is an increasingly prominent sustainable carbon upcycling method [24]. The Nova Institute's recent paper has brought attention to the expected projection of directly converting 70% of CO_2 to create bioplastics [25]. Significant advancements in the field of selective copolymerization processes have led to the successful industrial-scale manufacturing of polycarbonates, which account for around 30-50 weight percent of carbon dioxide waste [26]. Efforts in the upcycling of CO_2 are undergoing continuous development in order to satisfy the projected need of creating 450 million tonnes of plastic by the year 2050, all of which will be derived from renewable carbon sources [25] . The proposed CO_2 recycling method has the advantage of being readily adaptable to existing polymer production infrastructure reliant on fossil fuels, hence yielding economic and environmental advantages. The reduced reliance on agro-feedstocks, monomer extraction/transformations, and complicated pre-treatments is widely recognized as a significant benefit over polymers obtained from bio-resources [27].

I.5. Poly (lactic acid): synthesis, structure, properties, and applications

I.5. 1.Poly lactic acid (PLA)

Lactic acid (LA), a linear aliphatic thermoplastic polyester, is the starting point for the production of PLA[28]. It is usually produced from hydroxyl acids, and it is known as and categorized as one of the aliphatic polyesters. It is comparable to polyglycolic acid (PGA), which is another kind of aliphatic polyester[29]. L-LA and D-LA are the two different forms that LA may take, as seen in Figure I.5. This is because the molecule of LA contains an asymmetric carbon atom. Both of these forms are identical reflections of one another. When they are in their purest forms, their physical and chemical characteristics are identical. The only distinction that can be noticed is that plane-p The sign of (+) and (-) [2]. indicates the direction of rotation of the plane-polarized light that is created when a chemical reaction takes place. Polarized light spins in a manner that is comparable but in opposing directions. This indicates that other asymmetric (chiral) reagents, such as the majority of enzymes found in biological systems, have different responses. The plane-polarized light path or similar PETE polymer, but in term of temperature control condition, it has a significantly lower maximum continuous usage of temperature [30]. In addition, PLA may be re-polymerized by a chemical reaction when it is converted back into lactic acid[31] . The natural PLA cycle is shown in the following figure I.5

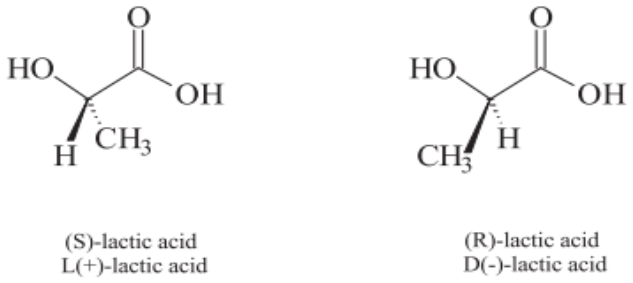

Figure I.5. Enantiomeric forms of lactic acid [30].

I.5. 2. PLA synthesis methods

There exist three fundamental procedures employed in the synthesis of PLA, namely the microbial fermentation process for lactic acid production, the subsequent purification of lactic acid and its conversion into a cyclic dimer, and the final step involving the ring-opening polymerization (ROP) of lactides or the polycondensation of the PLA monomer, specifically known as LA[32]. The ring-opening polymerization procedure is often used as the predominant technique for synthesizing high molecular weight polylactic acid (PLA)[33]. Controlling the

polymerization parameters is crucial due to the fact that the characteristics of PLA are influenced by isomer composition, temperature, and reaction time[34]. Figure I-6 illustrates the polymer chains generated by two distinct forms of lactic acid, namely L- and D- lactic acid. Three distinct stereo forms of poly have been manufactured, namely poly (l-lactide), poly (d-lactide), and poly (dl-lactide) [35]. Poly (dl-lactide), sometimes referred to as meso-dilactide, is synthesized by the combination of L- and D- lactic acid.

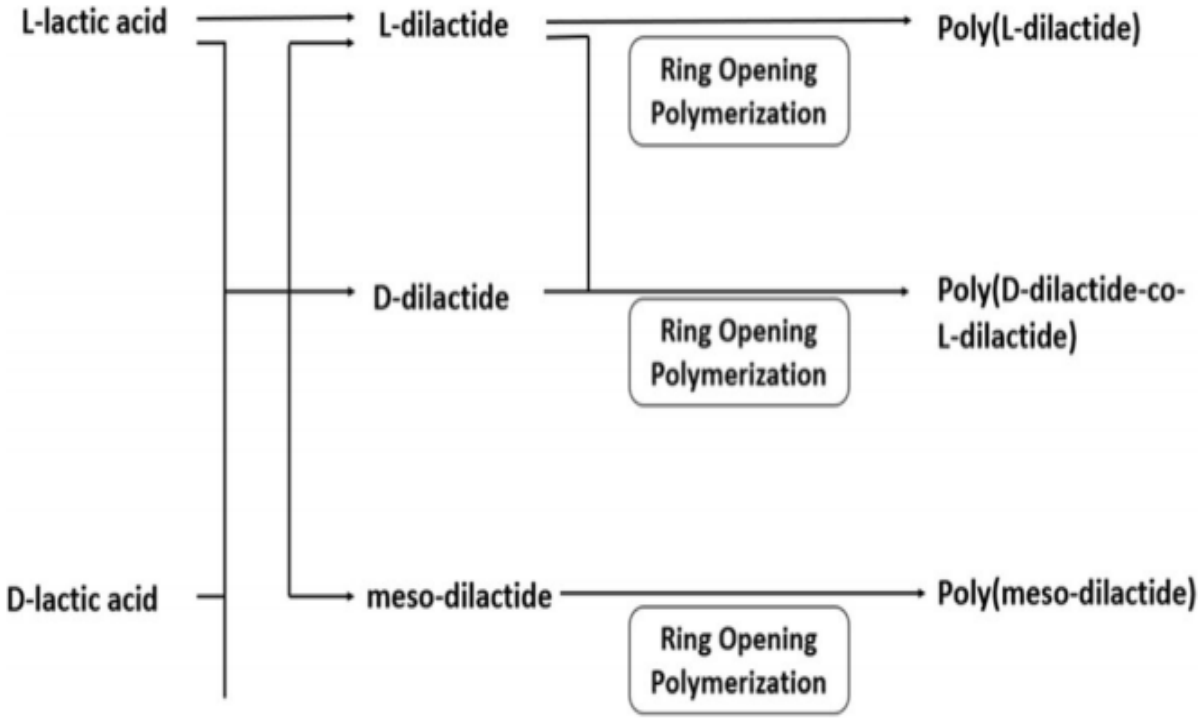

Figure I.6. Types of lactic acid and chains of polymers produced [3].

Initially, lactic acid (LA) is generated and created by fermentation or chemical synthesis. The production of isomers would vary based on the procedures used. When using chemical synthesis, a racemic mixture is generated, including equimolar concentrations of both L- (+)-lactic acid and D- (-)-lactic acid. In contrast, the use of the fermentation method results in a greater production of any variant of the LA isomer. In general, the use of microbial fermentation processes including renewable feedstock, such as sago and cassava starch, has the potential to create lactic acid that is either optically pure L (+)- or D (−)- isomer. This outcome may be achieved by carefully selecting suitable microbes for the fermentation process[36]. Following the formation of LA, it would undergo a process of purification. Various purification procedures may be used, such as nanofiltration and electrodialysis, ion exchange resin, hybrid

short path evaporation, and reactive distillation[3]. Subsequently, the purified lactic acid is used in the production of polylactic acid (PLA).

I.5.2.1. Ring-opening polymerization (ROP)

The first synthesis technique used is known as ring-opening polymerization (ROP). The conversion of lactide, which is the cyclic dimer of lactic acid, to polylactic acid (PLA) is facilitated by organometal catalysts, hence enhancing the efficiency of this approach. The majority of polylactic acid (PLA) manufacturing techniques use this particular technology. In this particular approach, the reactive core of the polymer chain is situated at its terminal end. Therefore, the length of the polymer chain may increase as more cyclic monomers undergo ring-opening reactions. Initially, the process involves subjecting lactic acid to high temperatures and vacuum conditions, resulting in its dehydration and subsequent poly-condensation into oligomers. Subsequently, by the process of internal transesterification, the substance would undergo catalytic depolymerization, resulting in the formation of lactide. The formation of polylactic acid (PLA) with a high molecular weight occurs via the opening of the lactide ring. The removal of residual moisture, lactic acid, and meso-lactide from optically pure D or L form lactide may be achieved by the processes of distillation or crystallization. Figure I-7 illustrates the cyclic dimers that are formed during the ring-opening polymerization (ROP) process [30].

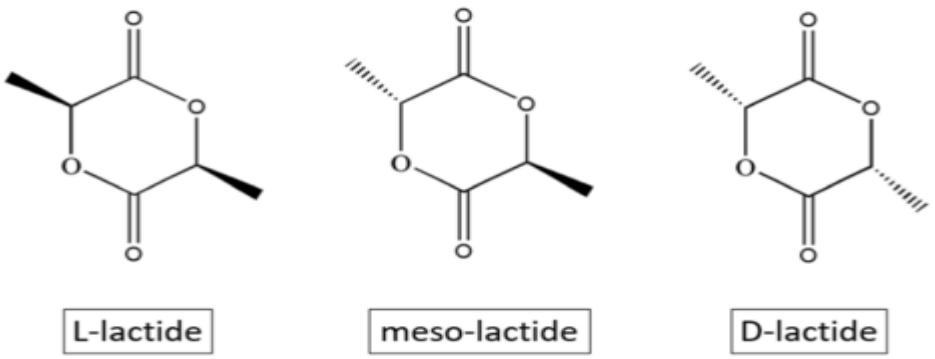

Figure I.7. Cyclic dimers for ROP process [30].

Furthermore, the molten PLA resin exhibits a little amount of moisture that has to be extracted [2,3]. The selection of ring-opening polymerization (ROP) as the ideal technique for industrial-scale manufacturing is justified by many factors, including short residence durations, benign process conditions, the absence of by-products, and high molecular weight[30]. Figure I-8 depicts the schematic diagram of a conventional ROP (Ring Opening Polymerization) process.

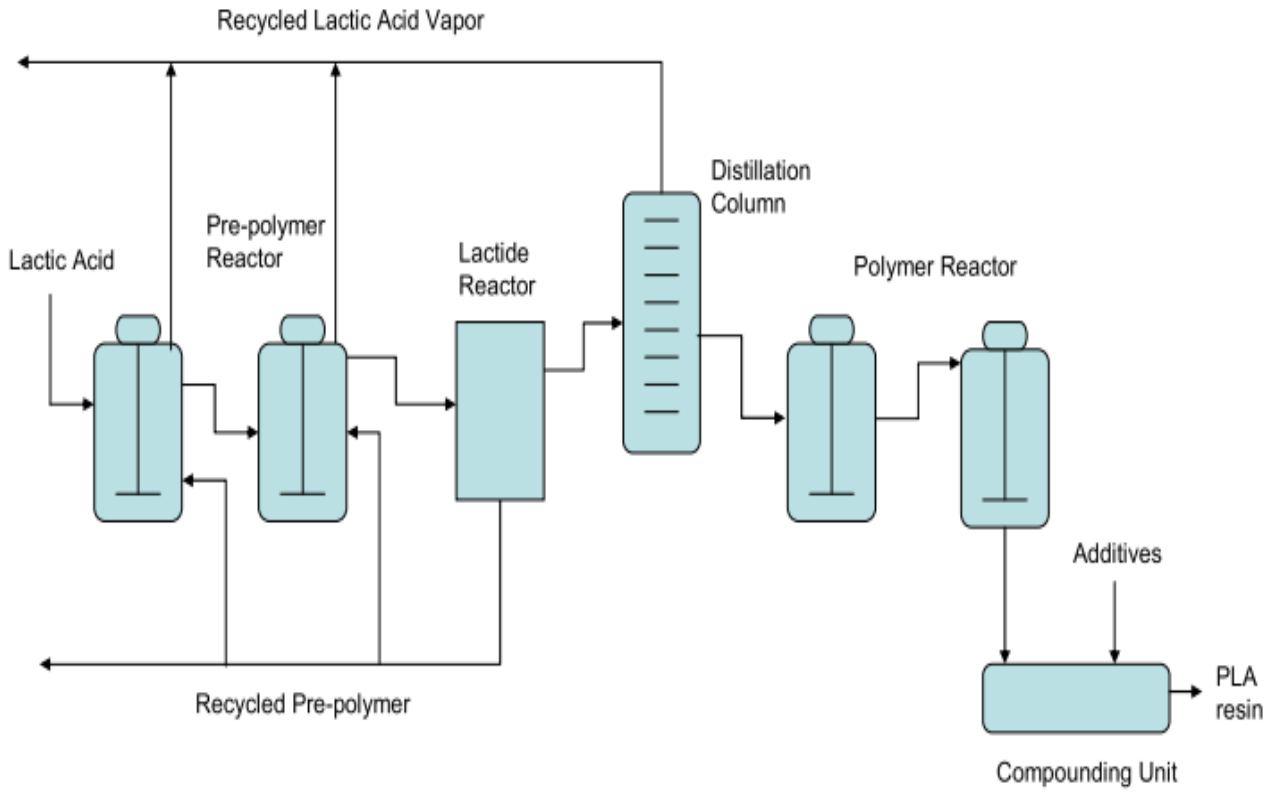

Figure I.8 Schematic diagram of a typical Ring-Opening Polymerization process [2].

For large-scale production of ROP, as shown in Figure I.9, a variety of polymerization methods are available, the most common of which is melt polymerization owing to its ease of use and repeatability. The catalyst and initiator concentration system governs the polymerization pathway. It might be cationic, anionic, or coordination-insertion type. Because of its reaction speed, high transformation rate, high molecular weight, and relatively moderate reaction conditions [37], stannous octoate is the most often utilized organometallic chemical for catalyzing polymerization. Many benign catalysts derived from magnesium, calcium, zinc, alkali metals, and aluminum have been developed for the ROP of lactides to overcome environmental concerns created by heavy metal catalysts [38].

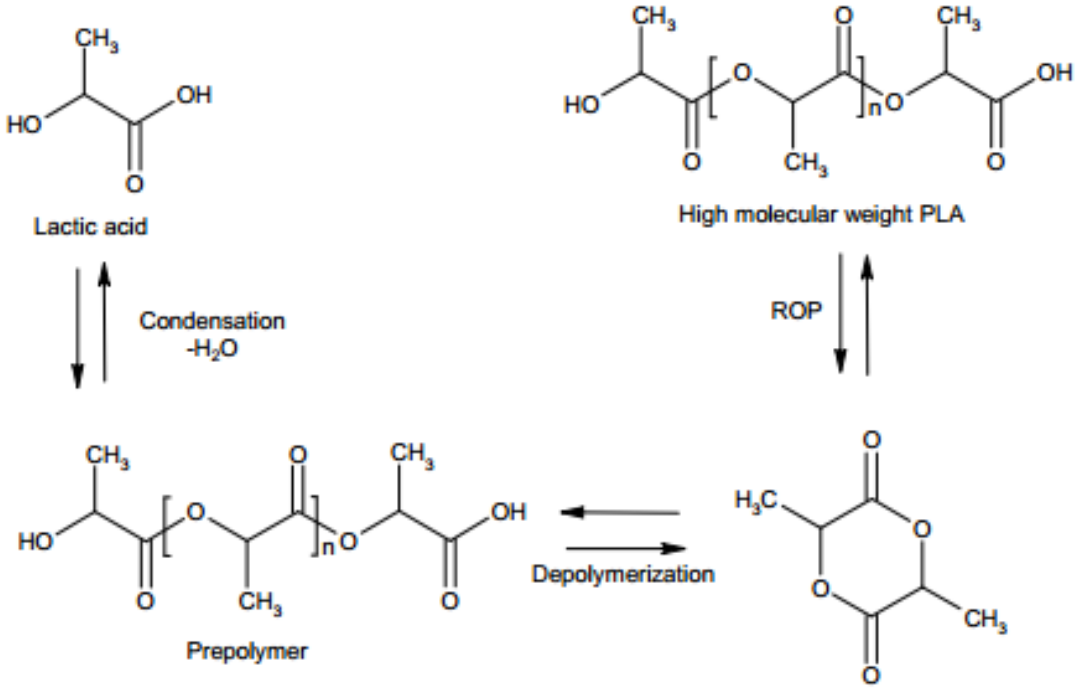

Figure I.9 PLA synthesis reaction via ring-opening polymerization using lactide monomer [39].

I.5.2.2. Direct polycondensation polymerization

The synthesis of PLA may be achieved by the polycondensation process involving the hydroxyl and carboxylic acid functional groups present in lactic acid. The reaction progresses towards the product side, PLA, by eliminating the water generated during this condensation process, as seen in Figure I.10. The polymer obtained by direct polycondensation often exhibits low molecular weight (<50,000 $g.mol^{-1}$) and low-quality due to the challenges associated with thorough removal of byproducts from the very viscous reaction fluid. Despite being the most cost-effective technique utilizing solvents in a high vacuum and high temperature environment, it is not widely employed in the industrial production of PLA. This is primarily due to the limitations in obtaining polymers with low to intermediate molecular weights (oligomers) caused by impurities, viscosity accumulation during polymerization, and the challenging removal of water from the condensation equilibrium reaction. These factors contribute to a decrease in conversion and potential depolymerization [40,41]. In order to enhance the molecular weight, esterification-promoting adjuvants such as bis(trichloromethyl) carbonate, dicyclohexylcarbodiimide, and carbonyl diimidazole, as well as chain extenders like butyl glycidyl ether or isocyanates, are employed. This inevitably leads to an increase in the number of steps and the intricacy of the production process, as well as the overall cost of the end

product[29,41]. Furthermore, it should be noted that the resulting polymer may potentially include impurities and residual chain extenders, which might consist of compounds that are nonbiodegradable or nonbioresorbable [41].

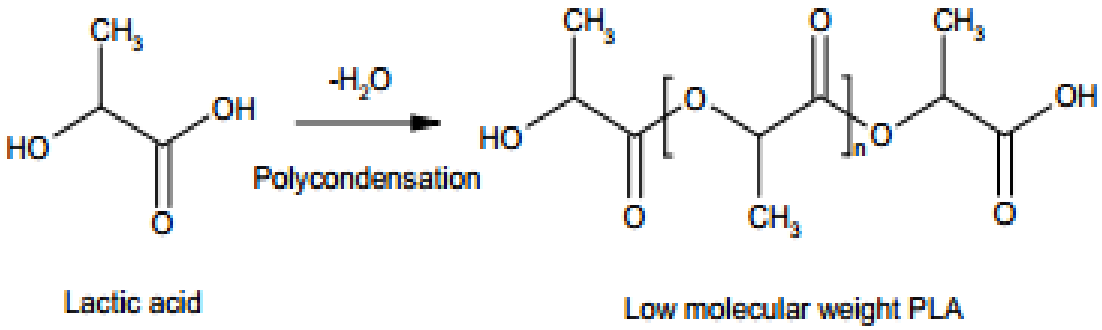

Figure I.10 Low-molecular-weight PLA synthesised by directly polycondensing the monomer of lactic acid [2].

I.5.2.3. Azeotropic condensation polymerization

Lastly, azeotropic condensation polymerization is also used. Using an organic solvent like toluene, xylene, or diphenyl ether, this technique enables the LA to have direct contact with the polycondensate, which then results in the formation of a polymer with a high molecular weight. The azeotropic removal of water is then accomplished by the use of distillations [36]. Nevertheless, this particular methodology yields significant amounts of catalyst residues owing to the need of a high concentration in order to achieve a satisfactory reaction rate. The aforementioned phenomenon might give rise to several disadvantages in the course of processing, including deterioration and hydrolysis. The problem of catalyst toxicity is of great sensitivity in the context of biomedical and packaging applications. The deactivation of the catalyst may be achieved by the introduction of phosphoric acid, or alternatively, it can be separated and removed from the reaction mixture by using strong acids like sulfuric acid, followed by precipitation and filtration. Therefore, it is possible to decrease the remaining catalyst levels to a few parts per million (ppm). Furthermore, the excessive use of solvents, both fresh and dehydrated, in the process of polymerization, as well as the usage of non-solvents for the collection of the resulting polymer, renders this technology environmentally unfavorable. Moreover, the involvement of several phases in this process contributes to its labor-intensive nature and high cost [39,42]. The many steps involved in the production of PLA are shown in Figure I.11.

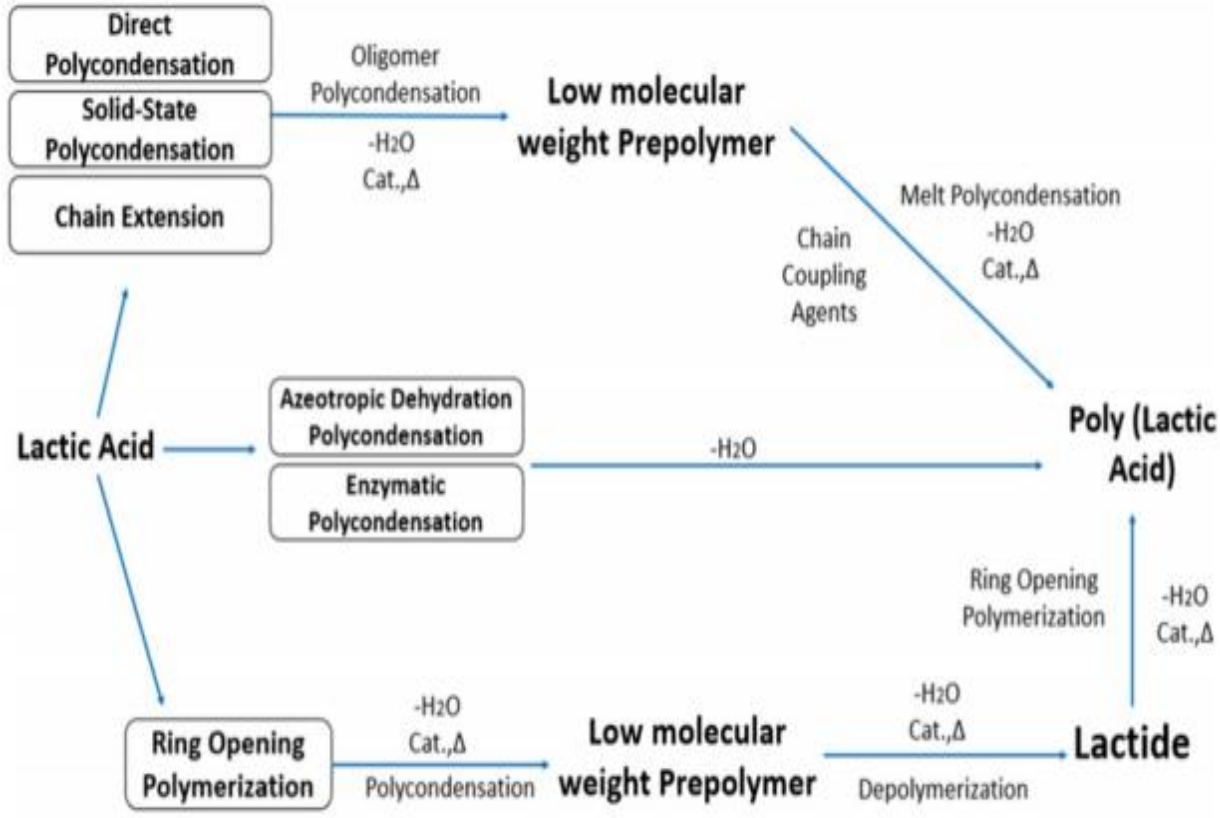

Figure I.11 Synthesis method for PLA [29].

I.5.3. Properties of PLA

The characteristics of polylactic acid (PLA), like other polymers, are significantly influenced by its stereochemical makeup. By manipulating the chemical composition in terms of L- and D-enantiomers during the synthesis process, it is possible to customize many significant characteristics of polylactic acid (PLA) to meet the specific performance demands of different applications. In addition, the characteristics of polylactic acid (PLA) are greatly influenced by several parameters, including molecular weight, annealing time, and processing temperature [1,43,44]. This section provides a comprehensive discussion on many features of PLA polymer, including thermal, behavior crystallinity, optical characteristics, rheological properties, processing attributes, solubility, barrier properties, physical properties, mechanical capabilities, and degrading qualities.

I.5.3.1 Thermal properties

The stability of PLA behavior may be achieved with a comprehensive knowledge of its amorphous and crystalline states. The glass transition temperature (Tg) has significant importance for amorphous PLA, since it governs the mobility of polymer chains at this temperature and beyond. Furthermore, both the glass transition temperature (Tg) and the melting temperature (Tm) are significant factors in the characterization of semi-crystalline polylactic acid (PLA)[45,46]. The Tg and Tm are significantly influenced by several factors such as the optical composition, fundamental structure, thermal history, and molecular weight [45,47].

PLA may be either semicrystalline or amorphous in the solid state, depending on the stereochemistry and thermal history[48] . PLA behaves like glass below Tg, but amorphous PLAs change from glassy to rubbery at Tg and will become more viscous fluid when heated further[48]. At room temperature, PLA is highly stiff , but its Tg is quite low[49], with a Tm of 160°C [50].

Table I-1 summarizes the thermal characteristics of PLA containing different amounts of isomer ratio [37]. Nevertheless, the Tg establishes the maximum usage temperature for the majority of amorphous PLA's commercial uses. Moreover, two other useful characteristics on Tg are orientation and physical aging. Physical aging may happen between 45 C and Tg by influencing the glass transition of PLA. Using the DSC technique,it was discovered that this endothermic event reduces the free volume, but that the volume expands instantly as a result of the enthalpy of relaxation after Tg. The pace and extent of PLA aging are also slowed by both crystallization and orientation. On the other hand, up to Tg, the rate of aging increases with temperature [48].

Table I.1. Thermal properties of PLA [37]

Polymer	Mw	Glass transition temperature[°C]	Melting temperature [°C]
L-PLA	50,000	54	170
L-PLA	1,00,000	58	159
L-PLA	3,00,000	59	178
D, L-PLA	20,000	50	-
D, L-PLA	1,07,000	51	-
D, L-PLA	5,50,000	53	-

The relationship between molecular weight and Tg is linear, meaning that as molecular weight increases, so does Tg. Furthermore, PLA morphologies may be altered by combining L and D differently. PLA with an L-content (more than or equal to 90%) tunes to be (semi) crystalline, while PLA with a higher D level tunes to be more amorphous, as Table I-2 illustrates [51,52]. At infinite molecular weight, the glass transition temperature rises with increasing L-stereoisomer concentration Figure I-12[53].

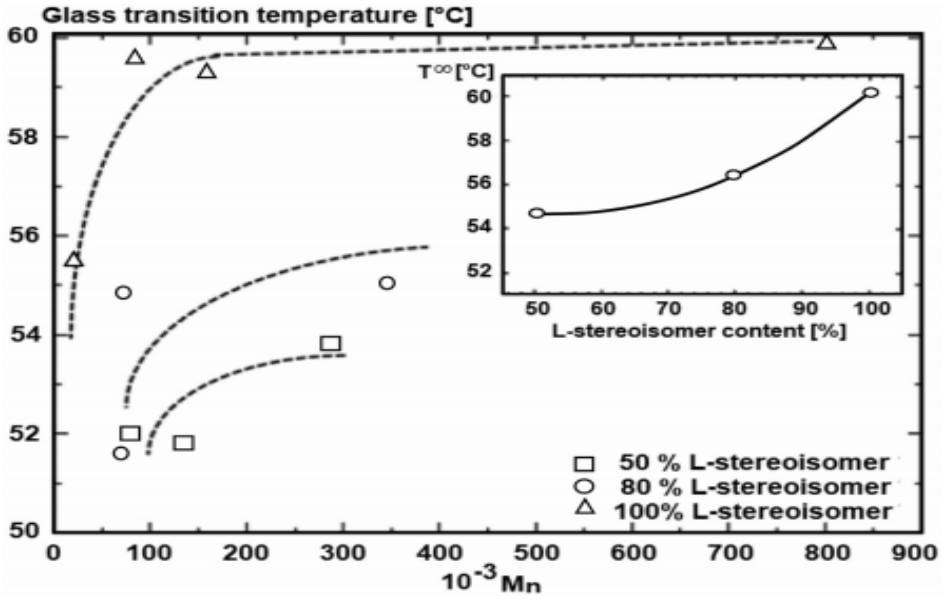

Figure I.12 Tg of PLA polymers with different L-Stereoisomers content as a function of number-average molecular weight (Mn) [54].

Table I.2. Melting temperature and Glass transition temperature of PLA with different L and D content [51].

Copolymer ratio	Glass transition temperature[°C]	Melting temperature [°C]
100/0 (L/D, L) -PLA	63	178
95/5 (L/D, L) -PLA	59	164
90/10 (L/D, L) -PLA	56	150
85/15 (L/D, L) -PLA	56	140
80/20 (L/D, L) -PLA	56	125

Tg may be significantly reduced by stopping Poly-L-lactide (PLLA) from shrinking. It is noteworthy that the melting point noticeably rises when PLLA and Poly-D-lactide (PDLA) are blended. Tg at infinite molecular weight was calculated to be 61, 46, and 53C for Poly (meso lactide), Poly-DL-lactide (PDLLA), and PLLA, respectively[48,55] .

Tg (onset and midway) of PLA over a wide composition range (0–50 mol% D-lactide) is shown in Figure I-13 Additionally, the figure shows that a higher D-lactide concentration reduces stereo-regularity, which in turn lowers the stereo-copolymers' midpoint Tg. For poly (L-lactide) and poly (50 L/50 D-lactide), this value shifts from 63 to 54 C, respectively [56].

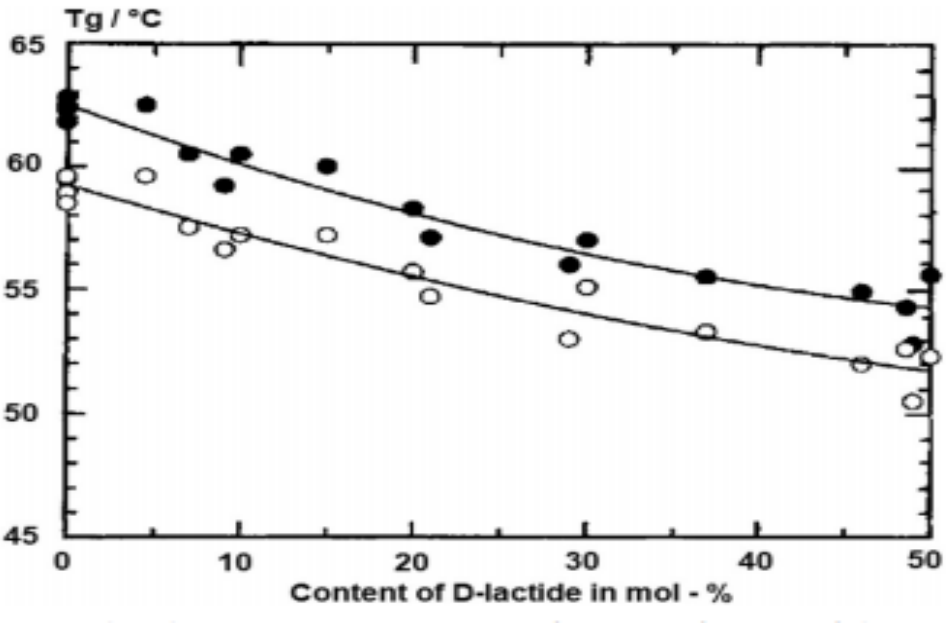

Figure I.13 The Glass transition temperature of PLA as a function of the stereocopolymer composition (o onset and ●midpoint Tg)[56].

I.5.3.2 Crystallization behavior

For polymers, the rate of crystallinity is an important characteristic. Respecting the amorphous content, the quantity of crystalline area in the polymer may be used to calculate this content[45] . PLA's composition and temperature history have an impact on the crystal shape of PLA[48]. The pace, extent, and melting point of crystallization are all influenced by the optical composition. Crystallinity affects a variety of polymer characteristics, such as stiffness, tensile strength, melting temperatures, and hardness [45].

Thermal and rheological characteristics may be influenced by chain architecture; branched polymers crystallize more quickly than their linear analog [45]. PLA crystals can grow in three structural positions: (I) α form that grows upon melt or cold crystallization; (II) β form which develops upon mechanical stretching of the more stable α -form; and (III) γ form that develops on hexamethylbenzene substance [57]. This is achieved by characterizing helix conformations and cell symmetries. If crystallization occurs at about 100 C, PLA has a practical melting point of 180 °C. PLA processing may be done at temperatures as low as 20 °C and as high as 200

°C[58]. PLA with more than 90% PLLA content is typically crystalline; in contrast, PLA with lower optical purity is in an amorphous phase [45].

The equilibrium temperature for PLLA has been established at 211-212°C [45,59]. The morphology of PLLA undergoes variations throughout the processes of nucleation and crystal development. At temperatures below 145°C, PLLA exhibits a spherulitic morphology during crystallization. However, with time and during isothermal growth, these spherulites transform into a linear morphology. The observation of hexagonal lamellar stacking crystal shape during PLLA crystallization was achieved by increasing the temperature above 150°C. The study conducted by reference[48] aimed to investigate the impact of incorporating D- and meso-lactides into L-rich polymers on the equilibrium melting temperature and optical purity (OP). Additionally, the degradation of PLA affects the overall crystallinity of the material as the hydrolytic chain cleavage progresses, leading to changes in the amorphous areas [60]. Therefore, in order to evaluate the extent of degradation, it is necessary to determine the crystallinity of the sample both before and after the degradation process.

I.5.3.3 Physical properties

The distinctive physical attributes of polylactic acid (PLA) render it well-suited for a wide range of applications. Polylactic acid (PLA) has favorable characteristics in terms of retention and crimp capabilities, displaying exceptional resistance to grease and oil. Additionally, it demonstrates ease of use at low temperatures, stability at high heat conditions, and an effective barrier against odors and fragrances. In terms of physical properties, PLA is sometimes compared to polystyrene [39]. Table I.3 presents the data overview of the physical parameters of PLA.

Table I.3. Physical properties of PLA [61] .

Characteristics	Unit	Amount
Tg	°C	57-60
Tm	°C	160
Specific gravity	$g.cm^{-3}$	1.25
Melt density	$g.cm^{-3}$	1.073
Enthalpy of cold crystallization (ΔH_c)	$J.g^{-1}$	24
Enthalpy of fusion (ΔH_m)	$J.g^{-1}$	28
Melt flow index	g/10 min	10
Percent crystallinity (*Xc*)	-	29.0 ± 0.5
Rockwall hardness	-	82–88

I.5.3.4 Solubility and miscibility

The main determinants of PLA solubility are molar mass, degree of crystallinity, and the presence of comonomer units, as stated in reference [62]. Dioxane, acetonitrile, chloroform, methylene chloride, 1,1,2-trichloroethane, and dichloroacetic acid are considered effective solvents for PLA products. PLA exhibits partial dissolution in cold solvents such as ethylbenzene, toluene, acetone, and tetrahydrofuran. However, complete solubility of PLA may be achieved by elevating the temperature of these solvents to their boiling points. Water and alcohols, such as methanol, ethanol, and propylene glycol, as well as unsubstituted hydrocarbons like hexane and heptane, are examples of nonsolvents for lactic acid-based polymers. The solubility of crystalline PLLA has been investigated and it has been shown to be insoluble in acetone, ethyl acetate, and tetrahydrofuran, as reported in references [45,62]. Table I.4 presents the solubility characteristics of the lactic acid-based polymer in several organic solvents commonly used.

Table I.4. The solubility of lactic acid polymers in an organic solvent [62].

Polymer	Soluble	Swelling	Nonsoluble
P(LLA)	Chloroform Furan 1,4-Dioxane 1,3-Dioxolane Pyridine	Xylene Ethyl acetate Tetrahydrofuran Methyl ethyl ketone Acetone Dimethyl sulfoxide	sopropyl ether Cyclohexane Ethano
P(LLA-co-GA)	Chloroform		Cyclohexane Acetone
P(LLA-co-CL)	Chloroform Tetrahydrofuran		Isopropyl Ether Ethano

PLA exhibits brittleness, which is attributed to its sluggish crystallization rate, thereby impeding its processability [63]. The incorporation of PLA with other polymers has the potential to modify several characteristics such as degradation rate, drug release profile, as well as thermal and mechanical properties [64,65]. Several blends using PLA have been reported in the literature. These include PLA/poly(ε-caprolactone) (PCL) [66,67], PCL/PLA/montmorillonite (MMT) [68], PLA/thermoplastic polyurethane (TPU) [69], poly (butylene terephthalate) The approval of poly(lactic-co-glycolic acid) PLGA and polylactic-co-caprolactone (PLA-CL) synthetic polymers was documented by Liao et al. in their study [70]. According to prior studies, the incorporation of chitosan (CS) into PLA blends has been shown to broaden its potential applications in several fields such as medicine, edible packaging or coatings, food additives, cosmetics, water treatment, and antifungal agents [60]. The incorporation of microcellular cellulose or glass fiber into PLA has been shown to have practical implications in the field of 3D printing manufacturing, as evidenced by studies [71–73]. The Blending PLA/microcellular cellulose has been shown to enhance the toughness and bending capability of the material via an increase in hardness. The incorporation of glass fiber into PLA has been seen to enhance its hardness while concurrently reducing its toughness and somewhat increasing its brittleness [74].

I.5.3.5 Degradation properties

Polymer decomposition occurs via heat activation, hydrolysis, biological activity, oxidation, photolysis, or radiolysis [45]. Processing options for degrading PLA include thermal degradation and biodegradation. Due to oxidative deterioration, polymers may become embrittled and lose strength. This procedure affects the chain scission and crosslinking

processes. PLA, a type of polymer that contains tertiary hydrogen atoms, has the potential for oxidative degradation

The impact of the factor on reactivity is influenced by a wide variety of parameters, including but not limited to particle size and shape, temperature, moisture, crystallinity, % isomer, residual lactic acid concentration, physical aging, article dimensions, blends, Mw, water diffusion, and metal impurities from the catalyst. As a result, they will have an impact on the rate at which polymers degrade [39,46,75]. Degradation rates may be slowed by raising the Mw, which in turn raises the Tg. In addition, glassy polymers, deteriorate less quickly than rubbery polymers. The rate of polymer degradation may be calculated by observing the polymer's reaction to water and catalysts. Li [64] noted that PLA degradation may be sped up more than ten times by preparing the material with ferric chloride (FeCl3). It is more difficult for the whole structure to degrade with higher crystallinity [18]. Additionally, the polymer crystallinity increases during the hydrolytic breakdown of amorph PLA as a result of the cleavage process [60]. Because it offers a quicker rate of disintegration and reduces inflammation and infection, low Mw PLAs is preferred for medicinal applications [3]. When comparing PLA to its monomer, lactic acid, it can be shown that PLA degrades more safely in the environment, making it a viable option for application in a variety of biological sectors [60,76,77].

I.5.4. Applications of PLA as biodegradable polymers

PLA has numerous desirable qualities, including high mechanical strength and modulus, biodegradability, biocompatibility, and simple manufacturing, that set it apart from other aliphatic polyesters. Improvements in heat resistance, copolymerization, and blending have all contributed to PLA's expanding use [78]. Here are some examples of sectors where the PLA has been used:

I.5.4.1. Medical/biomedical industry

PLA bioplastic is used in a variety of applications, including those in the biomedical sphere. Due to its unique set of characteristics, PLA has emerged as a promising material for usage in the healthcare industry. One of them is hydrolysis, a natural process by which PLA breaks down in the environment. Thus, subsequent procedures are not required to take out the planted gadget. Hence the patient's recovery rate may be enhanced, and the health system expenses are also lowered. Because of its inherent biocompatibility, PLA also helps to delay the development of a detrimental immune response. Degradation products are easily digested by

the body because they consist of recognizable components such lactic acids and short oligomers [30]. However, pure PLA may struggle to meet all required parameters in this field. Thus, PLA nanocomposites have been intensively studied as alternative materials. Matrix-based PLA-based nanocomposites include copolymers [79]. Nanomedicine is a developing medical field due to nanomaterials improvement and suitable use. According to the 2017 FDA recommendation, these nanomaterials, ranging from 1 to 1000 nm, resemble proteins and viruses. Polymer nanoparticles may be absorbed by cells, opening up novel biomedical applications such diagnostic image contrast agents, tailored drug delivery medium, and vaccination delivery systems [79].

The surface and small-scale effects of nanoparticles are anticipated to enhance PLA's characteristics. For this reason, PLA-based nanocomposites are better than materials composed entirely of PLA in biomedical applications such tissue engineering, drug delivery systems, and the replacement and repair of synthetic bone. When it comes to therapeutic applications, poly (lactic-glycolic acid) (PLGA) has garnered the greatest interest among other PLA-based copolymers. Polymer-based plates, screws, and pins have been utilized in orthopedic, dental, and craniofacial operations to replace and repair synthetic bone. The two materials that have been thoroughly researched and utilized to create porosity scaffolds and restore broken bones are PLA and PLGA. since of the PLA material's better degradation, the patient will have less discomfort since fewer procedures and implant removal are required. Aside from this, employing PLA may lower operational risk and prevent stress blocks. Furthermore, pure PLA materials do not exhibit bone-bonding force in contrast to PLA-based nanocomposites. When compared to PLA-based nanocomposites, they are less effective in regenerating and exhibiting deterioration behavior [79].

Tissue engineering, which is concerned with the creation and regeneration of tissue and organs, is a rapidly developing field in human health care. Scafolds are essential in tissue engineering because they serve as growth and cell adhesion factors. Scafolds are used in the treatment of blood vessels, bone regeneration, and the nervous system, among other biomedical fields. PLA materials have a high degree of biocompatibility and are often employed as scaffolds. Because of their broad melting and glass transition temperatures, PDLLA and PLGA are two of the most often utilized biopolymers in tissue engineering. Furthermore, the aligned nanofbrous PLLA scaffold has remarkable potential in the field of brain tissue engineering. PLLA has shown to be very helpful in promoting favorable outcomes in osteogenesis. By adhering a tripeptide

moiety that promoted cell adhesion, Gutierrez- Sanchez and associates functionalized PLA scafolds [79,80]. Table I-5 provides a summary of PLA's biomedical uses.

Table I.5. The biomedical applications of PLA [30].

Field	Application
Orthopedic	Peripheral nerve and spinal cord injury regeneration
	Bioabsorbable screws
	Meniscus repair
	Guided bone regeneration
Cardiac	Chest wall reconstruction
	Stent
Dentistry	Guided tissue regeneration
	Biocompatibility space fllers
Plastic surgery	Suture
	Reconstructive surgery
	Dermal fllers
	Skin draft
General surgery	Hemia mesh
Gynecology	Stress incontinence mesh
Radiology	Theranostic imaging
Oncology	Nanoparticles for drug delivery

I.5.4.2. Packaging/food packaging

The packaging industry is the next industrial application. Lactic acid is the source of PLA, a thermoplastic aliphatic polyester that degrades biodegradably and has a wide range of packaging applications. The ratio between the two optical isomers of the lactic acid monomer determines the properties of PLA as a packaging material. For example, using 100% L-PLA monomers would result in high melting and crystallinity points. Using 90/10% D/L copolymers, on the other hand, will result in a polymerizable melt that is above its Tg and meets the requirements for bulk packing. PLA is an excellent substitute for traditional plastics like PS, PET, high-density polyethylene (HDPE), LDPE in packaging [53].

High molecular weight, good processability, biodegradability, and superior water solubility resistance are desirable qualities that make PLA a great choice for packaging. PLA has characteristics with PET or flexible PVC, such as tensile strength modulus, flavor, and odor barrier. In addition, PLA possesses the polyethylene's printability and grease resistance, as well as the PS's processability and temperature stability. PLA is also one of the first bio-based polymers to be commercialized on a wide scale; it can be molded into coatings, films, and injection-molded products. Among the applications for processed PLA are films, containers,

and coatings for paper and paperboard. Prior to repolymerization, PLA may be recycled back to LA [31,81].

The Technological University of Denmark found that PLA containers for butter, yoghurt, cheeses, and margarine have outstanding moisture barrier, mechanical protection, and fat, light, and gas protection. Lactic acid migration to products during biodegradation is negligible. Since bakeries, fruits, and vegetables have a short shelf life or high breathing, PLA-based food packaging is perfect [3]. PLA has also been utilized in juice and water bottles, although the market is smaller. PLA's low CO2 barrier and inefficient creep behavior restrict its employment in bottle manufacture to non-carbonated drinks [82] .

Due to limitations in barrier and mechanical performance, using PLA for commercial packaging presents issues. PLA is stiff and brittle compared to petroleum-based PET. It has low gas barrier and heat deformation sensitivity. It's hard to heat seal this material. These issues may be solved by adjusting polymer processing, mixing, and adding nucleating agents and plasticizers. Nano and micro-composites and PLA coating with high barrier materials may also help. Coating PLA films with a thin coating of poly (ethylene oxide) or poly (ε-caprolactone) (PCL) improves gas and water vapor barrier characteristics without altering their visual appearance [3,80] . Table I-6 lists PLA packaging uses and companies

Table I.6. PLA as packaging materials and its applications [81].

Packaging application	Biopolymer	Company
Coffee and tea	Cardboard cups coated with PLA	KLM
Beverages	PLA cups	Mosburger (Japan)
Fresh salad	PLA bowls	McDonald's
Fresh cut fruits and vegetables	Rigid PLA trays and packs	Asda (retailer)
Potato chips	PLA bags	PepsiCo's Frito-Lay
Yoghurt	PLA jars	Stonyfeld (Danone)
Bread	Paper bags with PLA window	Delhaize (retailer)

I.5.4.3. Agriculture

PLA has been utilized in agriculture. Plasticulture was introduced in the 1950s to boost agricultural yield. Soil erosion and plant protection from insects, birds, and weeds using mulch, drip irrigation tubing, and greenhouse tunnel shielding are all strong reasons to utilize plastic in agriculture.This industry once relied on non-renewable polymers. Biodegradable polymers like PLA, PHAs, and PBAT replaced them as environmental effects persisted. The plasticulture industry has limited use of homopolymer PLA because to its weak mechanical and thermal

characteristics. Thus, PLA is blended with biodegradable polyesters to make commercial mulch films. Commercial PLA-based mulch films employ LA derivates or oligomers as plasticizers, which are biodegradable. The field of plasticulture is continually evolving. Due to the high cost of polymers and the relative youth of bioplastics in agriculture, several areas require improvement [82].

I.5.4.4. Automotive industry

Over time, the automobile industry has showed interest in using natural materials in its components. These materials not only function well but also improve fuel efficiency by reducing vehicle weight. Also, greenhouse gas (GHG) emissions are reduced [83]. 23% of global carbon emissions and 80% of environmental pollutants come from vehicular exhaust. Every 10% decrease in vehicle weight may increase fuel efficiency by 7%, and every 1 kg saved reduces CO_2 emissions by 20 kg. Biocomposite materials in this business improve fuel efficiency by reducing vehicle weight and CO_2 emissions [84]. Nanocomposite materials may reduce car auto-body weight by 40–55% compared to steel and aluminum. Mass reduction in automotive applications is vital for future electrical cars to maximize weight-to-battery capacity [3]. Bioplastics like PLLA and composites are being considered for automotive usage. PLLA is a great alternative for this business because to its biodegradability, recyclability, and favorable mechanical and physical qualities. Brittleness and thermal stability remain issues for PLA. However, correct modifers and additives may solve such issues. Ford, Mazda, Toyota, and Hyundai Motors used bio-based PLLA mixes to make parts. PLLA might be utilized in car interiors. Doors, tread plates, and automotive dashboards may be made by BIOFRONT utilizing PLA [83].

REFERENCES

[1] G. E. Luckachan and C. K. S. Pillai, “Biodegradable Polymers- A Review on Recent Trends and Emerging Perspectives,” J. Polym. Environ., vol. 19, no. 3, pp. 637–676, 2011.

[2] K. J. Jem and B. Tan, “The development and challenges of poly (lactic acid) and poly (glycolic acid),” Adv. Ind. Eng. Polym. Res., vol. 3, no. 2, pp. 60–70, 2020.

[3] N. A. A. B. Taib et al., A review on poly lactic acid (PLA) as a biodegradable polymer, vol. 80, no. 2. Springer Berlin Heidelberg, 2023.

[4] J. M. Raquez, Y. Habibi, M. Murariu, and P. Dubois, “Polylactide (PLA)-based nanocomposites,” Prog. Polym. Sci., vol. 38, no. 10–11, pp. 1504–1542, 2013.

[5] H. Balakrishnan, A. Hassan, M. Imran, and M. U. Wahit, “Toughening of Polylactic Acid Nanocomposites: A Short Review,” Polym. - Plast. Technol. Eng., vol. 51, no. 2, pp. 175–192, 2012.

[6] K. Hamad, M. Kaseem, Y. G. Ko, and F. Deri, “Biodegradable polymer blends and composites: An overview,” Polym. Sci. - Ser. A, vol. 56, no. 6, pp. 812–829, 2014.

[7] D. V. Sevast’yanov et al., “Biodegradation of Synthetic Thermoplastic Polymers and Plastics Based on Them (Review),” Polym. Sci. Ser. D, vol. 14, no. 1, pp. 119–128,2021.

[8] E. Castro-Aguirre, R. Auras, S. Selke, M. Rubino, and T. Marsh, “Insights on the aerobic biodegradation of polymers by analysis of evolved carbon dioxide in simulated composting conditions,” Polym. Degrad. Stab., vol. 137, pp. 251–271, 2017.

[9] T. Ahmed et al., “Biodegradation of plastics: current scenario and future prospects for environmental safety,” Environ. Sci. Pollut. Res., vol. 25, no. 8, pp. 7287–7298, 2018.

[10] A. A. Shah, F. Hasan, A. Hameed, and S. Ahmed, “Biological degradation of plastics: A comprehensive review,” Biotechnol. Adv., vol. 26, no. 3, pp. 246–265, 2008.

[11] M. C. Krueger, H. Harms, and D. Schlosser, “Prospects for microbiological solutions to environmental pollution with plastics,” Appl. Microbiol. Biotechnol., vol. 99, no. 21, pp. 8857–8874, 2015.

[12] G. A. M. Ali and A. S. H. Makhlouf, Handbook of Biodegradable Materials. 2023.

[13] ASTM, D. 6400-04 Standard specification for compostable plastics. J ASTM Int, West Conshohocken, PA, 2004.

[14] F. Alshehrei, “Biodegradation of Synthetic and Natural Plastic by Microorganism. Journal of Applied & Environmental Microbiology.,” J. Appl. Environ. Microbiol., vol. 5, 8–1, no. 1, pp. 8–19, 2017.

[15] S. Veerappapillai and A. Muthukumar, “Biodegradation of Plastics-A Brief Review,” Int. J. Pharm. Sci. Rev. Res., vol. 31, no. 2, pp. 204–209, 2015.

[16] M. Thuwall, A. Boldizar, and M. Rigdahl, “Extrusion processing of high amylose potato starch materials,” Carbohydr. Polym., vol. 65, no. 4, pp. 441–446, 2006.

[17] M. Kuddus and R. Roohi, Bioplastics for Sustainable Development. Springer Singapore, 2021.

[18] V. Siracusa, P. Rocculi, S. Romani, and M. D. Rosa, “Biodegradable polymers for food packaging: a review,” Trends Food Sci. Technol., vol. 19, no. 12, pp. 634–643, 2008.

[19] D. K. Schneiderman and M. A. Hillmyer, “50th Anniversary Perspective: There Is a Great Future in Sustainable Polymers,” Macromolecules, vol. 50, no. 10, pp. 3733–3749, 2017.

[20] S. T. Ahmed, N. G. H. Leferink, and N. S. Scrutton, “Chemo-enzymatic routes towards the synthesis of bio-based monomers and polymers,” Mol. Catal., vol. 467, no. November 2018, pp. 95–110, 2019.

[21] X. Zhang, M. Fevre, G. O. Jones, and R. M. Waymouth, “Catalysis as an Enabling Science for Sustainable Polymers,” Chem. Rev., vol. 118, no. 2, pp. 839–885, 2018.

[22] Bio-based Industries - https://www.bbi-europe.eu/projects. consult :12/01/2024.

[23] Bio-Based Industries Joint Undertaking Investing in the European bioeconomy - https://www.bbi-europe.eu/sites/default/files/media/bbi_article_may_2016.pdf.consult ,12/01/2024

[24] R. Muthuraj and T. Mekonnen, “Recent progress in carbon dioxide (CO2) as feedstock for sustainable materials development: Co-polymers and polymer blends,” Polymer (Guildf)., vol. 145, pp. 348–373, 2018.

[25] S. RameshKumar, P. Shaiju, K. E. O’Connor, and R. B. P, “Bio-based and biodegradable polymers - State-of-the-art, challenges and emerging trends,” Curr. Opin. Green Sustain. Chem., vol. 21, pp. 75–81, 2020.

[26] P. Markewitz et al., “Worldwide innovations in the development of carbon capture technologies and the utilization of CO2,” Energy Environ. Sci., vol. 5, no. 6, pp. 7281–7305, 2012.

[27] Y. Zhu, C. Romain, and C. K. Williams, “Sustainable polymers from renewable resources,” Nature, vol. 540, no. 7633, pp. 354–362, 2016.

[28] J. Muller, C. González-Martínez, and A. Chiralt, “Combination Of Poly(lactic) acid and starch for biodegradable food packaging,” Materials (Basel)., vol. 10, no. 8, pp. 1–22, 2017.

[29] A. J. R. Lasprilla, G. A. R. Martinez, B. H. Lunelli, A. L. Jardini, and R. M. Filho, “Poly-lactic acid synthesis for application in biomedical devices - A review,” Biotechnol. Adv., vol. 30, no. 1, pp. 321–328, 2012.

[30] T. Casalini, F. Rossi, A. Castrovinci, and G. Perale, “A Perspective on Polylactic Acid-Based Polymers Use for Nanoparticles Synthesis and Applications,” Front. Bioeng.

Biotechnol., vol. 7, no. October, pp. 1–16, 2019.

[31] S. Mangaraj, A. Yadav, L. M. Bal, S. K. Dash, and N. K. Mahanti, "Application of Biodegradable Polymers in Food Packaging Industry: A Comprehensive Review," J. Packag. Technol. Res., vol. 3, no. 1, pp. 77–96, 2019.

[32] M. Singhvi and D. Gokhale, "Biomass to biodegradable polymer (PLA)," RSC Adv., vol. 3, no. 33, pp. 13558–13568, 2013.

[33] S. Bin Park, E. Lih, K. S. Park, Y. K. Joung, and D. K. Han, "Biopolymer-based functional composites for medical applications," Prog. Polym. Sci., vol. 68, pp. 77–105, 2017.

[34] C. Gonçalves, I. C. Gonçalves, F. D. Magalhães, and A. M. Pinto, "Poly(lactic acid) composites containing carbon-based nanomaterials: A review," Polymers (Basel)., vol. 9, no. 7, pp. 1–37, 2017.

[35] A. B. Nair, P. Sivasubramanian, P. Balakrishnan, K. A. N. A. Kumar, and M. S. Sreekala, "Environmental Effects, Biodegradation, and Life Cycle Analysis of Fully Biodegradable 'Green' Composites," Polym. Compos. Biocomposites, vol. 3, pp. 515–568, 2013.

[36] A. Komesu, J. A. R. de Oliveira, L. H. da Silva Martins, M. R. W. Maciel, and R. M. Filho, "Lactic Acid Production to Purification: A Review," BioResources, vol. 12, no. 2, pp. 4364–4383, 2017.

[37] R. Mehta, V. Kumar, H. Bhunia, and S. N. Upadhyay, "Synthesis of poly(lactic acid): A review," J. Macromol. Sci. - Polym. Rev., vol. 45, no. 4, pp. 325–349, 2005.

[38] S. Jacobsen, H. G. Fritz, and R. Jerome, "Polylactide (PLA)-A New Way of Production " pp. 1311–1319,1999.

[39] R. E. Drumright, P. R. Gruber, and D. E. Henton, "Polylactic acid technology," Adv. Mater., vol. 12, no. 23, pp. 1841–1846, 2000.

[40] Y. Hu, W. A. Daoud, K. K. L. Cheuk, and C. S. K. Lin, "Newly developed techniques on polycondensation, ring-opening polymerization and polymer modification: Focus on poly(lactic acid)," Materials (Basel)., vol. 9, no. 3, 2016.

[41] D. Garlotta, "A Literature Review of Poly (Lactic Acid) A Literature Review of Poly (Lactic Acid)," J. Polym. Environ., vol. 9, no. 2, pp. 63–84, 2019.

[42] L. Avérous, "Polylactic acid: Synthesis, properties and applications," Monomers, Polym. Compos. from Renew. Resour.chapter 21, pp. 433–450, 2008.

[43] D. Cohn and A. Hotovely Salomon, "Designing biodegradable multiblock PCL/PLA thermoplastic elastomers," Biomaterials, vol. 26, no. 15, pp. 2297–2305, 2005.

[44] T. Tanaka, T. Tsuchiya, H. Takahashi, M. Taniguchi, and D. R. Lloyd, "Microfiltration membrane of polymer blend of poly(l-lactic acid) and poly(ε-caprolactone),"

Desalination, vol. 193, no. 1–3, pp. 367–374, 2006.

[45] S. Farah, D. G. Anderson, and R. Langer, "Physical and mechanical properties of PLA, and their functions in widespread applications — A comprehensive review," Adv. Drug Deliv. Rev., vol. 107, pp. 367–392, 2016.

[46] R. Auras, B. Harte, and S. Selke, "An overview of polylactides as packaging materials," Macromol. Biosci., vol. 4, no. 9, pp. 835–864, 2004.

[47] A. N. Malathi, K. S. Santhosh, and U. Nidoni, "Recent trends of Biodegradable polymer: Biodegradable films for food packaging and application of nanotechnology in biodegradable food Packaging," Curr. Trends Technol. Sci., vol. 3, no. 2, pp. 73–79, 2014.

[48] A. K. Agrawal, Spinning of Poly(Lactic Acid) Fibers. pp,323-341,2010.

[49] V. Vilay, M. Mustapha, Z. Ahmad, and T. Mitsugu, "Characterization of the Microstructure and Mode I Fracture Property of Biodegradable Poly(L-lactic acid) and Poly(ε-caprolactone) Polymer Blends with the Additive Lysine Triisocyanate," Polym. - Plast. Technol. Eng., vol. 52, no. 8, pp. 768–773, 2013.

[50] O. Avinc and A. Khoddami, "Overview of poly lactid acid (PLA) fibre part I : Production , properties , performance , environmental impact , and end-use applications of poly (lactic acid) Fibres," Fibre Chem., vol. 41, no. 6, pp. 16–25, 2009.

[51] L. T. Lim, R. Auras, and M. Rubino, "Processing technologies for poly(lactic acid)," Prog. Polym. Sci., vol. 33, no. 8, pp. 820–852, 2008.

[52] M. Murariu and P. Dubois, "PLA composites: From production to properties," Adv. Drug Deliv. Rev., vol. 107, pp. 17–46, 2016.

[53] K. Hamad, M. Kaseem, H. W. Yang, F. Deri, and Y. G. Ko, "Properties and medical applications of polylactic acid: A review," Express Polym. Lett., vol. 9, no. 5, pp. 435–455, 2015.

[54] J. R. Dorgan, J. Janzen, M. P. Clayton, S. B. Hait, and D. M. Knauss, " Melt rheology of variable L -content poly(lactic acid) ," J. Rheol. (N. Y. N. Y)., vol. 49, no. 3, pp. 607–619, 2005.

[55] B. D. Fitz, D. D. Jamiolkowski, and S. Andjelić, "Tg depression in poly(L(-)-lactide) crystallized under partially constrained conditions," Macromolecules, vol. 35, no. 15, pp. 5869–5872, 2002.

[56] C. A. P. Joziasse, H. Veenstra, D. W. Grijpma, and A. J. Pennings, "On the chain stiffness of poly(lactide)s," Macromol. Chem. Phys., vol. 197, no. 7, pp. 2219–2229, 1996.

[57] M. L. Di Lorenzo, "Crystallization behavior of poly(l-lactic acid)," Eur. Polym. J., vol. 41, no. 3, pp. 569–575, 2005.

[58] J. J. Kolstad, "Crystallization kinetics of poly(L-lactide-co-meso-lactide)," J. Appl. Polym. Sci., vol. 62, no. 7, pp. 1079–1091, 1996.

[59] H. Tsuji and Y. Ikada, "Properties and morphology of poly(L-lactide) 4. Effects of structural parameters on long-term hydrolysis of poly(L-lactide) in phosphate-buffered solution," Polym. Degrad. Stab., vol. 67, no. 1, pp. 179–189, 2000.

[60] M. A. Elsawy, K. H. Kim, J. W. Park, and A. Deep, "Hydrolytic degradation of polylactic acid (PLA) and its composites," Renew. Sustain. Energy Rev., vol. 79, no. June 2016, pp. 1346–1352, 2017.

[61] F. Ebrahimi and H. Ramezani Dana, "Poly lactic acid (PLA) polymers: from properties to biomedical applications," Int. J. Polym. Mater. Polym. Biomater., vol. 71, no. 15, pp. 1117–1130, 2022.

[62] K. Madhavan Nampoothiri, N. R. Nair, and R. P. John, "An overview of the recent developments in polylactide (PLA) research," Bioresour. Technol., vol. 101, no. 22, pp. 8493–8501, 2010.

[63] L. R. Antunes, G. L. Breitenbach, M. C. G. Pellá, J. Caetano, and D. C. Dragunski, "Electrospun poly(lactic acid) (PLA)/poly(butylene adipate-co-terephthalate) (PBAT) nanofibers for the controlled release of cilostazol," Int. J. Biol. Macromol., vol. 182, pp. 333–342, 2021.

[64] X. Li et al., "Study on the degradation behavior and mechanism of Poly(lactic acid) modification by ferric chloride," Polymer (Guildf)., vol. 188, pp 121991,2020.

[65] M. Okamoto and B. John, "Synthetic biopolymer nanocomposites for tissue engineering scaffolds," Prog. Polym. Sci., vol. 38, no. 10–11, pp. 1487–1503, 2013.

[66] A. C. Vieira, J. C. Vieira, J. M. Ferra, F. D. Magalhães, R. M. Guedes, and A. T. Marques, "Mechanical study of PLA-PCL fibers during in vitro degradation," J. Mech. Behav. Biomed. Mater., vol. 4, no. 3, pp. 451–460, 2011.

[67] J. P. Mofokeng and A. S. Luyt, "Dynamic mechanical properties of PLA/PHBV, PLA/PCL, PHBV/PCL blends and their nanocomposites with TiO_2 as nanofiller," Thermochim. Acta, vol. 613, pp. 41–53, 2015.

[68] B. Zhu, Y. Wang, H. Liu, J. Ying, C. Liu, and C. Shen, "Effects of interface interaction and microphase dispersion on the mechanical properties of PCL/PLA/MMT nanocomposites visualized by nanomechanical mapping," Compos. Sci. Technol., vol. 190, no. February, p. 108048, 2020.

[69] S. M. Lai and Y. C. Lan, "Shape memory properties of melt-blended polylactic acid (PLA)/thermoplastic polyurethane (TPU) bio-based blends," J. Polym. Res., vol. 20, no. 5, pp. 2–9, 2013.

[70] S. Liao, C. K. Chan, and S. Ramakrishna, "Stem cells and biomimetic materials strategies for tissue engineering," Mater. Sci. Eng. C, vol. 28, no. 8, pp. 1189–1202, 2008.

[71] M. Yang, J. Hu, N. Xiong, B. Xu, Y. Weng, and Y. Liu,"Preparation and properties of PLA/PHBV/PBAT blends 3D printing filament," Mater. Res. Express, vol. 6, no. 6,2019.

[72] A. Ji, S. Zhang, S. Bhagia, C. G. Yoo, and A. J. Ragauskas, "3D printing of biomass-derived composites: Application and characterization approaches," RSC Adv., vol. 10, no. 37, pp. 21698–21723, 2020.

[73] L. Solorio, A. Vega, "applied sciences Filament Extrusion and Its 3D Printing of Poly (Lactic Acid) / Poly (Styrene- co -Methyl Methacrylate) Blends," Appl. Sci., vol. 9, pp. 1–17, 2019.

[74] P. A. Gunatillake, R. Adhikari, and N. Gadegaard, "Biodegradable synthetic polymers for tissue engineering," Eur. Cells Mater., vol. 5, pp. 1–16, 2003.

[75] E. Jabbari and X. He, "Synthesis and characterization of bioresorbable in situ crosslinkable ultra low molecular weight poly(lactide) macromer," J. Mater. Sci. Mater. Med., vol. 19, no. 1, pp. 311–318, 2008.

[76] R. Sarvari et al., "Shape-memory materials and their clinical applications," Int. J. Polym. Mater. Polym. Biomater., vol. 71, no. 5, pp. 315–335, 2022.

[77] B. Massoumi, R. Sarvari, and S. Agbolaghi, "Biodegradable and conductive hyperbranched terpolymers based on aliphatic polyester, poly(D,L-lactide), and polyaniline used as scaffold in tissue engineering," Int. J. Polym. Mater. Polym. Biomater., vol. 67, no. 13, pp. 808–821, 2018.

[78] X. Qi, Y. Ren, and X. Wang, "New advances in the biodegradation of Poly(lactic) acid," Int. Biodeterior. Biodegrad., vol. 117, pp. 215–223, 2017.

[79] L. Sha, Z. Chen, Z. Chen, A. Zhang, and Z. Yang, "Polylactic acid based nanocomposites: Promising safe and biodegradable materials in biomedical field," Int. J. Polym. Sci., vol. 2016, 2016.

[80] T. Narancic, F. Cerrone, N. Beagan, and K. E. O'Connor, "Recent advances in bioplastics: Application and biodegradation," Polymers (Basel)., vol. 12, no. 4, 2020.

[81] N. Jabeen, I. Majid, and G. A. Nayik, "Bioplastics and food packaging: A review," Cogent Food Agric., vol. 1, no. 1, pp. 1–6, 2015.

[82] E. Castro-Aguirre, F. Iñiguez-Franco, H. Samsudin, X. Fang, and R. Auras, "Poly(lactic acid)—Mass production, processing, industrial applications, and end of life," Adv. Drug Deliv. Rev., vol. 107, pp. 333–366, 2016.

[83] A. Bouzouita, D. Notta-Cuvier, J. M. Raquez, F. Lauro, and P. Dubois, "Poly(lactic acid)-based materials for automotive applications," Adv. Polym. Sci., vol. 282, pp. 177–219, 2018.

[84] O. Akampumuza, P. M. Wambua, A. Ahmed, W. Li, and X. Qin, "Review of the applications of biocomposites in the automotive industry," Polym. Compos., vol. 38, no. 11, pp. 2553–2569, 2017.

Chapter II. Polymer Blends Based on PLA

Chapter II. polymer blends based on PLA

II.1. Introduction

PLA-based polymer blends have advanced rapidly, achieving incredible feats, particularly in high toughness performance. Numerous studies covering a range of topics related to PLA materials have been published in the last 20 years, including compatibilization techniques and tactics, phase morphologies, behavior, and the link between the structural performances [1–4]. The fundamental ideas, limitations, and successes of the several bulk and surface modification techniques used to date were detailed by researchers[5]. Other investigations have also described a few methods for controlling crystallization to produce high-performance PLA materials [4]. Researchers methodically outlined several techniques for compatibilizing PLA blends with various polymers [6].

II.2.PLA modifications

The most popular techniques for altering polymer characteristics include polymer blending, chemical copolymerization, and nanocomposite technology. Chemical copolymerization is a crucial technique for changing the characteristics of homopolymers. Several commercially significant copolymers have been produced through chemical copolymerization and macromolecular design. By carefully choosing co-monomers and varying copolymer proportions, novel materials with adjustable characteristics may be created regarding structure-properties interactions. Physical blending is a practical method for creating novel polymeric materials that combine the benefits of many current polymers. By altering the blend composition and selecting different blending components, one may further control the performance of the resulting polymer blends. The process of dispersing nanosized particles into a polymer matrix at the nanoscale is known as nanocomposite technology. The nanoparticles' surface areas are quite large. Their large surface area may, in the case of excellent dispersion, result in strengthened nanocomposites. For the same number of fillers, the reinforcing efficiency is often higher than that of traditional micro- and macro-composites. Although this technology offers an effective means to reinforce physical properties without sacrificing the benefits of the polymer matrix. Comprehensive details about the modification of PLA properties using nanocomposite technology are available in a recent study by Raquez et al. [7]. Nonetheless, the study covers the usage of nanoparticles as compatibilizers for blends based on PLA.

II.2.1. Chemical copolymerization

Several polymerization processes, including condensation polymerization [8,9], ROP [10,11], and the chain-extension reaction [12,13], have been used to copolymerize PLA with other polymers, including polyesters, polyolefins, and natural polymers, to modify PLA's properties or create new materials. In a recent review work, Rasal et al. detailed the process of chemical copolymerization for changing the properties of PLA [5]. The potential number of materials with different characteristics that may be chosen to copolymerize with PLA to create a range of novel materials with variable qualities and various uses should confirm the most significant benefit of chemical copolymerization. Crystalline to amorphous, petroleum-based to biobased, biodegradable to non-degradable, and biobased to petroleum-based may be copolymerized with PLA to create new materials with various characteristics. Nevertheless, there are also apparent drawbacks to using chemical copolymerization for PLA modification. Every time a polymer undergoes chemical copolymerization, its qualities increase, while other properties invariably deteriorate in tandem. When poly(3-caprolactone) (PCL) is used to copolymerize PLA, it can toughen the PLA. Depending on the composition, the elongation at break of the PLA–PCL multiblock copolymer can reach 600%; however, the tensile strength and Young's modulus drop dramatically to 32 MPa and 30 MPa, respectively, and the degree of crystallinity and melting temperature also appear to be decreased [14]. The main drawbacks of modifying PLA by chemical copolymerization, particularly by ROP, are the extended reaction time, strict copolymerization conditions, and high cost. Simply put, chemical copolymerization is an effective process for creating new materials with unique qualities and uses. However, it is not a practical or cost-effective way to change PLA's features without significantly sacrificing other qualities.

II.2.2. Polymer blending

Physical blending with a well-chosen component is a practical and cost-effective alternative to chemical copolymerization for changing the characteristics of homopolymers [8,15]. Blends of PLA with other plasticizers and polymers have been used to create novel materials with specific characteristics [5,16]. Due to the plasticization effect, PLA's toughness, particularly its elongation at break, might be significantly enhanced by adding tiny molecular or macromolecular plasticizers. This, in turn, could lower the glass transition temperature and boost PLA's ductility [16]. More crucially, physical blending with other polymers is the most promising method for changing PLA's characteristics. Since many polymers with different characteristics may be chosen to mix with PLA, theoretically, PLA-based products with

various properties can be produced via blending. This does not imply, however, that combining essential PLA mixtures may provide blends with high characteristics. Instead, since most of the current polymers are incompatible with PLA, it is challenging to generate high-performance PLA mixes via simple mixing in most situations [17–19]. Compatibility is often necessary for incompatible polymer mixes to have exceptional characteristics.

II.3. Generalities of compatibilization

It is essential to discuss miscibility before describing compatibilization. Thermodynamically, "miscibility" explains how two polymer pairs behave when mixed, including the number and composition of phases produced [20]. Regarding miscibility, blends may be classified as (1) completely miscible, (2) partly miscible, or (3) immiscible. A polymer blend's morphology and glass transition temperature (Tg) may be used to determine its miscibility. Polymer blends may have one of two morphologies: homogeneous or heterogeneous. With a single Tg that fluctuates depending on composition and is between the Tg values of both components, a perfectly miscible mix has a homogenous morphology. A suitable blend is a partly miscible mixture that often exhibits a one phase morphology with enhanced characteristics [20]. A partly miscible blend consists of two homogenous phases, each containing some of one polymer dissolved in the other.

Each of the two Tg values of the blend, representing the two phases, moves from one component's value to another. Whatever the blend composition, a completely immiscible blend often has a macrophase-separated morphology with a coarse interface boundary, a sizeable dispersed phase size, low phase adhesion, and two Tg values. The state of miscibility of two polymers is governed by the free energy of mixing, ΔG_{mix}, which is defined as follows:

$$\Delta G_{mix}=\Delta H_{mix}-T\Delta S_{mix}$$

where ΔH_{mix} and ΔS_{mix} are the enthalpy change and entropy change by mixing, respectively

If the ΔG_{mix} is negative, the two polymers are miscible; if not, they are immiscible. It is known that blending two high molecular weight polymers results in little ΔS_{mix}. Therefore, only when ΔH_{mix} is negative can ΔG_{mix} be negative. In other words, exothermic mixing necessitates unique interactions between the blend's constituent parts. These particular interactions might be donor and acceptor interactions, ion-dipole, dipole-dipole, or relatively weak hydrogen bonding. However, most of the polymers now in use are immiscible because

Vander Waals interactions between them are often rather weak. Unless they are compatible, their mixtures are often worthless.

Compatibility is a technical word that describes a blend's phase morphology and property profile concerning a specific application [21]. Suppose the blending of two partially miscible or immiscible polymers produces a delicate phase structure and combines the beneficial characteristics of both polymers. In that case, it indicates good compatibility between them. Conversely, if blending results in a coarse phase structure and inferior properties, it suggests that the two polymers are incompatible. Compatibilization is often used to enhance the compatibility of incompatible polymer mixtures. Suppose the phase morphology of an incompatible blend transitions from coarse to fine, and the characteristics improve from bad to excellent following compatibilization. In that case, we consider the blend to have transitioned from incompatible to compatible.

Compatibilization is a method used to increase compatibility and improve the qualities of polymer blends that are not naturally compatible. The primary functions of compatibilization are to decrease the size of the dispersed phase by reducing interfacial tension and preventing the dispersed phase from coalescing, stabilizing the resulting delicate phase morphology [20]. Furthermore, using compatibilizers, typically macromolecular species with interfacial activities, may enhance the interfacial contacts between the dispersed phase and matrix in heterogeneous blends [21]. By achieving a refined phase structure and enhancing the interaction between different components, it is possible to transform incompatible mixes into compatible materials that exhibit the superior qualities of each component. Using the immiscible poly-(lactic acid)/low-density polyethylene (PLLA/LDPE) blend as a case study, Figure II.1 displays the cryofractured surface structures of the blend before and after being made compatible by the addition of block copolymer PLLA-b-LDPE, as documented by Wang and Hillmyre [22]. The blend without compatibilizer exhibited a coarse morphology characterized by large dispersed LDPE particles and a visible phase boundary, indicating a lack of compatibility and interfacial adhesion. However, as the content of the compatibilizer increased, the size of the dispersed LDPE particles gradually decreased and the phase boundary became less distinct. The mixes that were made compatible exhibited significantly enhanced mechanical qualities compared to the original mixture. Furthermore, apart from using block copolymers, there exist other alternative methods to achieve compatibility in PLA-based blends, which will be further upon in the subsequent section.

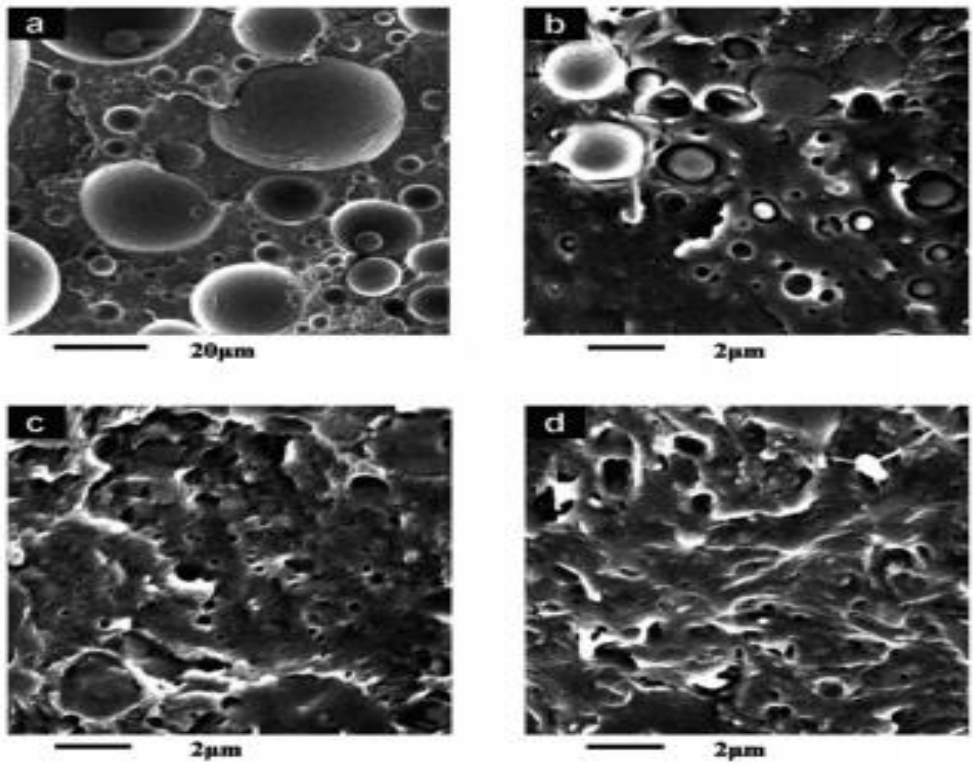

Figure II.1 Morphologies for cryofractured surfaces of (a) 80: 20 PLLA/LDPE, and (b) 80 :20: 2, (c) 80: 20: 5, and (d) 80: 20: 10 PLLA/LDPE/PE-b-PLLA blends [22].

II.4. PLA blend preparation methods

Two distinct techniques for preparing PLA blends are solution blending and melt blending. Nevertheless, choosing a particular technique for preparing PLA blends depends on two distinct factors: the compatibility of the blend components and the final product's physical structure and mechanical characteristics [23].

II.4.1 Solution blending

The solution blending process generally consists of three stages: dissolving the polymer mixture in a suitable solvent, physically mixing the blend components, and evaporating the solvent. Due to the challenges associated with solvent evaporation and the exorbitant cost of solvents, this technique is considered impractical on an industrial scale. The solution blending process is regarded as a favourable approach, especially for biomedical applications[24] , as it helps prevent degradation and interchain chemical interactions that may arise during the melt mixing of PLA with specific natural polymers. Various solvents, including chloroform, dichloromethane, dimethylformamide, tetrahydrofuran, and 1,4-dioxan, are often used to manufacture PLA mixes using the solution blending technique[25–28]. The choice of solvent

significantly influences the ultimate shape of the PLA blend produced with this technique. The morphology of PLA/chitosan blends was strongly influenced by the choice of solvent utilized in the production process, such as chloroform, dichloromethane, and tetrahydrofuran [27]. It was discovered that when the solvent used was chloroform, blend solutions containing no less than 50% (w/w) chitosan generated smooth fibres without any bead-like structures. However, polymer beads were effectively produced when using dichloromethane, but tetrahydrofuran resulted in substantially fewer fibres.

II.4.2 Melt blending

compared to the solution blending approach, the melt blending process for preparing PLA blends does not include any solvent contamination or the necessity for solvent removal [29]. The blend components mix at a temperature higher than the melting points of the components using a heated mixer, such as an internal blender, single-screw extruder, or twin-screw extruder. This process results in the creation of PLA blends that are fully miscible. From an industrial perspective, a twin-screw extruder is preferable due to its enhanced blending efficiency, reduced blending times, and increased production. Hence, this technology is notably intriguing owing to its many advantages, including simplicity, cost-effective processing, and industrial-level accessibility, enabling the acquisition of materials with the appropriate performance by altering the blend composition.

Additionally, it is crucial to note that the blend components must be dried before melting. This is because a high moisture content may result in bubbles, delamination, and striations on the product's surface, which can negatively impact the final output quality [30] . Furthermore, it is essential to tune the processing parameters, including screw speed, mixing time, and temperature profile, to get optimal results during the extrusion phase.

As previously mentioned, solution blending is recommended for biomedical applications with PLA mixes due to the challenges that may develop when melt blending certain natural polymers, which tend to deteriorate during or before the melting process. The melt blending process is considered more successful than solution blending due to its ability to achieve improved miscibility. For example, the ability of PLA/ Polyhydroxybutyrate (PHB) blends to mix well when generated by melting them together was higher than those made using the solution approach in chloroform [31]. Additionally, it should be noted that PLA blends produced using solution blending or melt blending techniques may undergo multiple

procedures to achieve diverse morphologies, including films, fibres, and porous structures, according to specific end-use demands [29].

II.5. Compatibilization agents of PLA blends

II.5.1 Copolymers (PLA-co-polymer)

Copolymerization is a viable option to control the characteristics of PLA blends. When a copolymer is introduced to a PLA blend, the appropriate component acts as a compatibilizer, ensuring all of the blend's components are miscible. Therefore, adding copolymers that may be localized at the interface between the blend components tends to lower the interfacial tension between the PLA mix's components [6] . Therefore, while the addition of copolymers may prevent the aggregation of the scattered particles. Various copolymers were used as compatibilizers in PLA blends, including PLA-co-PE [32], PLA-co-glycolic acid (PLA-co-GA) [33], PLA-co-PCL [34], and PLA-co-NR [35]. An instance of effective compatibilization was achieved by finding a PLA-co-PE copolymer at the interface of a PLA/PE blend, as documented by Wang and Hillmyer [22]. The addition of 2 wt.% PLA-co-PE to the PLA/PE blend resulted in a significant drop in the particle size of the PE, from 25.7 to 3.5 μm. This decrease in particle size improved the performance of the characteristics of the PLA/PE blend. Alternatively, several copolymers, such as poly (LA-co-CL)[36], PLAco-PCL [60], and PLA-PCL-PLA [61], were used to enhance the compatibility of the PLA/PCL blend. For instance, when 5 wt.% of P(LA-co-CL) was added to the PLLA/PCL blend, the size of the PCL decreased by up to 70%, resulting in a notable improvement in the compatibility of the PLLA/PCL blend.

II.5.2 Functionalized polymers

Functionalized polymers used as compatibilizers for PLA blends must mix well with one component of the blend and chemically react with the functional groups in the other. Therefore, it is possible to significantly decrease the interfacial tension and enhance the adhesion between the parts of the PLA blends [20]. Nevertheless, this approach may be categorized into two distinct forms depending on whether the PLA is combined with a polyolefin. A polyolefin-based compatibilizer achieves compatibility between the PLA and polyolefin blend. Maleic anhydride (MA)-grafted-polyolefins have been widely used to enhance the compatibility of PLA/polyolefin blends [22,26,28,36–38]. For example, Singh et al. [38] investigated the impact of adding 4 wt.% PE-g-MA to a composition containing 20 wt.% PLA and 80 wt.% low density polyethylene (LDPE). The researchers discovered that

the addition of PE-g-MA facilitated a homogeneous dispersion of the PLA phase inside the LDPE matrix, resulting in the superior performance of the PLA/LDPE blends. Lee et al. [39]found that the compatibility between the components of a PLA/PP blend was much improved by using a hybrid compatibilizer consisting of PE-g-MA and PP-g-MA, compared to using separate compatibilizers like PP-g-MA or PE-g-MA. In addition, studies have shown that the compatibility of PLA/PP, PLA/ABS, and PLA/NR blends can be significantly enhanced by incorporating compatibilizers. These compatibilizers include PP-grafted glycidyl methacrylate (PP-g-GMA) [38], ABS-grafted glycidyl methacrylate (ABS-g-GMA) [40], and natural rubber-grafted glycidyl methacrylate (NR-g-GMA) [41]. Conversely, when combining PLA with polymers that possess functional groups, such as thermoplastic starch (TPS) and poly (butylene adipate-co-terephthalate) (PBAT), it is common to enhance compatibility by employing PLA-based compatibilizers. These include polylactic acid-g-maleic anhydride (PLA-g-MA), PLA-grafted modified TPS (PLA-g-MTPS), PLA-grafted acrylic acid (PLA-g-AA), and polylactic acid-g-glycidyl methacrylate (PLA-g-GMA) [37,42,43]. For instance, Huneault and Li. [42] proposed that PLA-g-MA may be a successful compatibilizer for PLA/TPS blends. This is because the compatibilized blend revealed TPS particles with a smaller size range of 1-3 μm, in contrast to the non-compatibilized blend with bigger particles ranging from 5-30 μm.In addition, Teamsinsungvon et al. [44] discovered that the compatibility of PLA/PBAT blends may be improved by adding PLA-g-MA. This resulted in a significant reduction in the size of the PBAT domain, compared to blends without PLA-g-MA. Liu and colleagues [43] found that incorporating PLA-g-GMA enhanced the dispersion of starch particles and increased the interfacial interaction between starch and PLA.

II.6.PLA/polyolefins blends

II.6.1. Polyethylene

Similar to other polymer blends, PLA and PEs do not mix well, and their characteristics are greatly influenced by the arrangement of their phases, composition, mixing circumstances, type of PE, and the quality of interface between the components. The incompatibility between the two parts (PLA and PE) in this system was identified by the analysis of rheological, mechanical, thermal, and morphological test results. Recently, Djellali et al.[45] used a twin-screw extruder to make PLA/LDPE blends and studied their rheological characteristics. The melt flow behavior observed using a parallel-plate rotating rheometer provided significant evidence of immiscibility for the blends under investigation. Specifically, the flow behavior of the blend varied irrespective of the composition. The findings agreed with those of Hamad

et al. [46,47], who used a capillary rheometer to examine the rheological characteristics of PLA/LDPE polymer blends. They discovered that the PLA/LDPE blends were immiscible as their melt viscosities were lower than the miscible blend line.

Additionally, it was found that the performance and morphology of PLA/LLDPE polymer blends were affected by the proportion of linear low-density polyethylene (LLDPE) [48]. Based on the results of this study, adding more LLDPE to the blend reduced its tensile qualities, including modulus, strength, and elongation. However, up to 10 wt.% LLDPE, the blend's impact strength was higher and subsequently dropped.

A lack of compatibility between the two components in this blend leads to reduced malleability, worse resilience, and restricted use. Furthermore, several investigations have shown the enhancement of compatibility and improved interfacial adhesion via different compatibilizers [32,38,49,50]. Research was conducted to enhance the durability of PLA by studying the compatibility of PLA/LDPE polymer blends that do not mix well [49]. Blends with varying proportions of PLA were created by a melt mixing technique, with the addition of GMA and PE-GMA as reactive compatibilizers, to achieve this objective. These compatibilizers decrease the interfacial tension and improve the adhesion between the various components of the blend. The chemical reactivity of the included compatibilizers may be readily characterized in the following manner. Firstly, the compatibilizer must possess some degree of miscibility with PE.

Conversely, the material must react with PLA's -COOH end groups. Therefore, the compatibilizers help decrease the size of the dispersed phase particles and facilitate the effective transmission of mechanical stresses at the interface. Both effects are crucial for achieving a favorable equilibrium of the mechanical characteristics. The use of PE-GMA as a compatibilizer undeniably enhanced the blend's performance. The PLA and compatibilizer (PE-GMA) reaction products were analyzed using nuclear magnetic resonance spectroscopy (NMRS). Anderson et al. conducted a comparative study [32,50] to analyze the impact of various kinds of polyethylene (PE) on the characteristics of PLA/PE polymer blends. The study included the use of two specific types of PE, namely linear low-density polyethylene (LLDPE) and high-density polyethylene (HDPE). The study used a range of PLA-PE block copolymers with varying molecular weights to create compatible mixes using PLA and PE. These copolymers acted as compatibilizers. The study revealed that LLDPE exhibited lower toughness, while HDPE demonstrated the most significant improvement.

In a recent study, Singh et al. [38] examined using LDPE-g-MA as a compatibilizer in a blend of PLA and LLDPE (20/80). The mechanical characteristics of the created mixtures demonstrated that adding LDPE-g-MA improved the compatibility between PLA and LLDPE. The scanning electron microscopy (SEM) analysis of the blends, both with and without the compatibilizer, showed that the blend with the compatibilizer had a higher level of miscibility.

Compared to pure PLA, a simple method may be used to manufacture cost-effective plastic materials with superior toughness, flexibility, and thermal stability. The alteration degree of PLA characteristics is contingent upon both the sort of PE and the impact of the used compatibilizer. For instance, the mixture's durability is much enhanced when rigid PE (HDPE) is added. On the other hand, because to the non-degradable properties of PEs, the biodegradability of this system is often poorer compared to clean PLA. Several studies have shown the biodegradation of the PLA/PE blends [51,52]. Nevertheless, there is little understanding of the biodegradation characteristics of PLA/non-degradable polymer blends and the underlying processes that drive the biodegradation process in these blends.

II.6.2. Polypropylene

Polypropylene (PP) is a commonly used plastic with the least density among all thermoplastic polymers, about 0.9 g/cm^3. Furthermore, PP has exceptional strength and exhibits excellent resistance to chemicals. Hamad et al. [53] investigated the compatibility of PLA/PP polymer blends made by a single-screw extruder technique by examining their flow behavior and tensile characteristics. The rheological analysis indicated that the blend exhibited pseudo-plastic behavior, and the viscosity of the melt was found to be intermediate between that of the individual components, namely polypropylene (PP) and polylactic acid (PLA). The tensile tests demonstrated a decrease in the blend's strength and elongation-at-break when the PLA content reached 50 wt.%. However, above this threshold, both properties showed a noticeable improvement. Reddy et al. [54] provided more information on the compatibility of this system by producing a mix (PLA/PP) to enhance both the hydrolysis resistance and dye-ability of PLA fibers, scanning electron microscopy (SEM) examinations of a blend consisting of 50 wt.% polylactic acid (PLA) and 50 wt.% polypropylene (PP) indicated that the PP phase had indistinct spherical forms (white phase in Figure II.2 (a). This suggests that the blend demonstrated a high level of compatibility, similar to what was seen in the PLA/polyethylene (PE) blend that was made compatible by adding a compatibilizer [32]. In addition, the study revealed that the blend fibers had a higher ability to be dyed than the pure PLA fibers. This was due to the incorporation of PP in the fibers, which created a more porous structure. As a

result, more dye molecules could be absorbed by the PLA fibers Figure II.2 (b). Furthermore, tests on biodegradation and hydrolysis demonstrated that the PLA in the blends had significantly less degradation and hydrolysis compared to the pure PLA fibers. This suggests that the presence of PP in the blend provided protection against biodegradation and hydrolysis for the PLA.In their study, Yoo et al.[55] examined the impact of two compatibilizers on the characteristics and structures of PLA/PP polymer blends including a small amount of PLA (20 wt.%). PP-g-MA was determined to be a suitable enhancer for increasing the strength of the PLA/PP blend. On the other hand, SEBS-g-MA was discovered to be an effective agent for enhancing the impact strength of the blend. A study was conducted where PLA/PP blends with varying amounts of PLA (from 0 to 100 wt.%) were created. An ethylene-butyl acrylate-glycidyl methacrylate terpolymer (EBA-GMA) was used to improve the characteristics of the blends [56]. Figure II.2 (c) and (d) summarize the cryo-fractured surface morphology and the impact tests conducted on the manufactured blends. Blends with 30,50, and 70 wt.% PLA displayed co-continuous phase morphologies, according to the findings. When compared to the neat polymers (PLA and PP) and the blend with the co-continuous phase morphology, the blends with small quantities of the second phase (10 wt.% PLA or 10 wt.% PP) exhibited a sea-island type morphology and enhanced impact strength. The blend with 70 wt.% PLA had a co-continuous phase morphology, but it was altered to a sea-island type morphology to increase the impact strength. This morphology involves evenly scattered tiny PP particles (~2 μm) in a PLA matrix. Figure II.2 (d) shows this was accomplished by lowering the interfacial tension between the PLA and PP using EBA-GMA. Considering the strong compatibility between PP and EBA-GMA and the chemical interactions between the functional groups in PLA and EBA-GMA, the impact modifying role of EBA-GMA was elucidated. So, the mechanical characteristics were improved because EBA-GMA facilitated the creation of stress transfer bridges between the two phases.

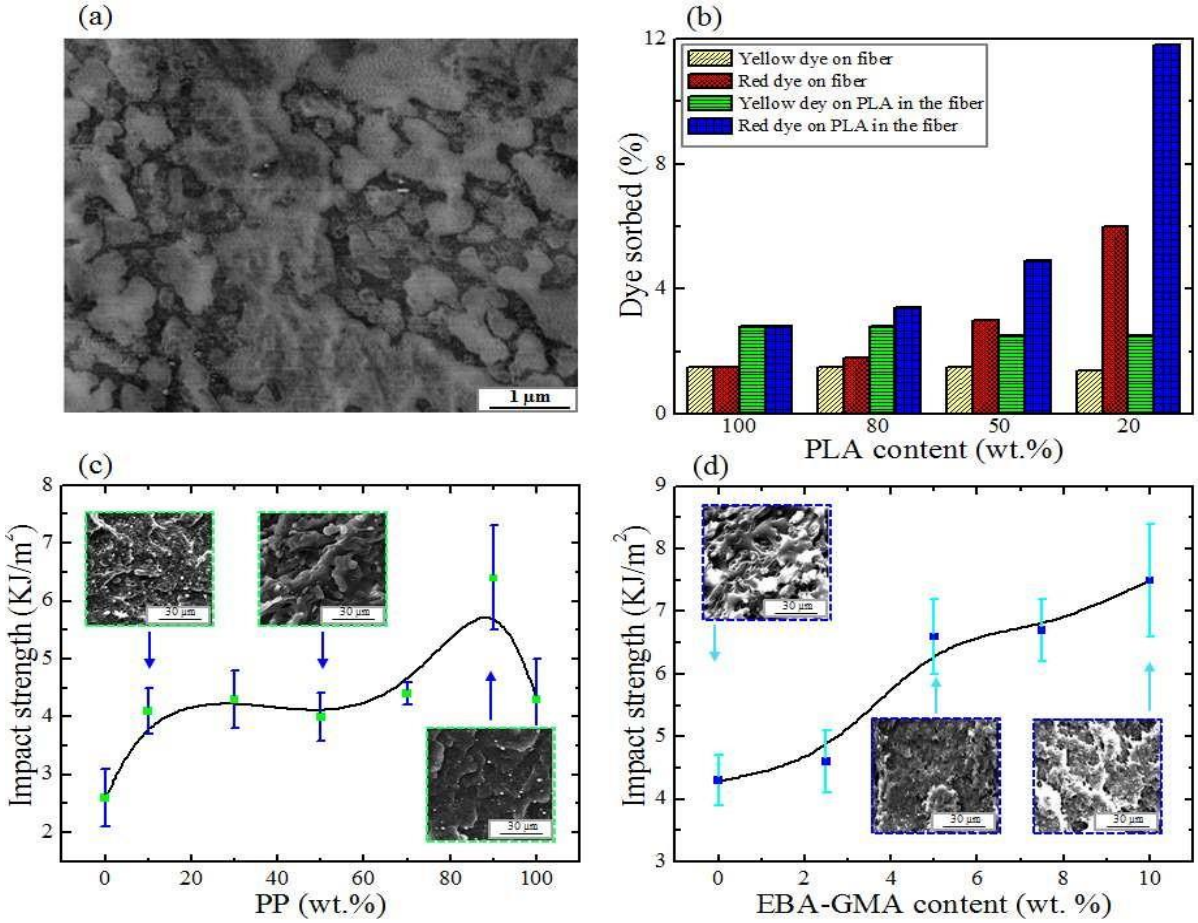

Figure II.2 The morphology of (a) PLA/PP polymer blend. (b) The dye-ability of PLA/PP blend fibers as a function of PLA content [54]. (c and d) Impact strength and morphology of PLA/PP/EBA-GMA blends [56].

Based on the results mentioned above, it is evident that combining PLA with PP not only enhances toughness but also provides a cost-effective and simple approach to producing materials with enhanced resistance to hydrolysis and favorable dyeability, surpassing those of pure PLA. The improved performance of this mix may increase its potential for use in fiber production for textile applications. Furthermore, the limited compatibility between PLA and PP may catalyze further investigation into using this blend to produce bi-component medical fibers. The limited solubility in this blend might result in total separation during the production of fibers, leading to the formation of a two-component structure in PLA/PP blends.

II.7.PLA/Styrenic polymers blends

II.7.1. Polystyrene

The main objective of using the PLA/PS system is to manufacture environmentally-friendly and affordable products. The combination of PLA/PS blends intending to achieve this

objective has been documented in many studies [57–62]. The system's compatibility was evaluated using the embedded fiber retraction (IFR) technique at temperatures ranging from 170 to 200 °C [57]. This approach allows for the simple determination of interfacial tension in multiphase systems. The findings from the IFR analysis indicated that the PLA/PS blends demonstrated a certain level of compatibility, as measured by the interaction between the unshared electrons (n electrons) of the C=O groups in PLA and the π-electrons of the aromatic rings in PS, forming a (n-π) bond. The existence of intermolecular contacts in the PLA/PS blend was verified using FT-IR spectroscopy. This was shown by a change in the peak attributed to the carbonyl groups of PLA from 1767 to 1759 cm^{-1}, indicating the occurrence of the interaction [58] . The addition of PS to PLA resulted in an enhancement in the thermal stability of PLA/PS blends. The current author, who earlier conducted a study on the mechanical recyclability of a blend consisting of 50% PLA and 50% PS, also reported this enhancement [61]. The blend was forced through a small opening to create small particles then inserted into molds to produce samples such as dog bones. The samples undergo numerous rounds of the same cycle (extrusion-injection). The PLA/PS blend samples exhibited superior mechanical and rheological capabilities compared to pure PLA, indicating enhanced stability. Nevertheless, the specific impact of these polymers (PLA and PS) on the degrading characteristics of one another remained unclear in the absence of evidence about phase separation.

Biresaw and Carriere. [60] conducted a study where they prepared blends of polystyrene (PS) with three different biodegradable polyesters (PCL, PLA, and Eastar Bio Ultra (EBU)). The tensile properties of these blends were then analyzed to assess their compatibility. In general, the strength of EBU/PS and PCL/PS blends increased but the elongation-at-break dropped with an increase in the percentage of PS. This work focused on preparing and characterizing a single ratio (75/25, wt.%) of the PLA/PS blend. The findings indicated that this blend's strength and yield strain were lower than neat PLA. Additionally, it was discovered that the PS/PCL blend exhibited superior compatibility compared to the PS/EBU blend. However, the compatibility of the PS/PLA blend could not be confirmed. This was since just one specific blend, consisting of 25 wt.% PS was prepared and examined. Therefore, more data was required to evaluate the suitability of the PLA/PS blend based on its tensile characteristics. The authors of this study created several ratios of this blend [59,62]. It was observed that the strength of the blends dropped until a concentration of 40 wt.% PLA, after which it rose slightly.

Regarding the mechanical performance of this system, it is observed that it exhibited inadequate compatibility. Imre et al. [21] recently provided more evidence for this finding by examining the interfacial interaction and morphology of the PLA/PS blends. Their findings indicated that the PLA/PS blends resulted in the formation of large particles. The particle size reached its peak at about 50 wt.% PS content, suggesting a lack of compatibility and weak interactions between the PLA and PS phases. Based on the above results, it can be inferred that the addition of PS is a successful technique for reducing costs and improving the thermal stability of PLA.

Consequently, the processability of this blend is superior to that of pure PLA [61]. Nevertheless, the mechanical characteristics of the combination, such as toughness, ductility, and strength, tend to be inferior to those of pure PLA. This may be related to the poor mechanical performance of PS, characterized by low strength and weak toughness. Conversely, this blend created porous PLA substances utilized in medicinal applications [63]. In an earlier study [64], the pore size was decreased from around 2 to less than 1 μm using a block copolymer (PLA-b-PS). In this kind, the compatibilizer must undergo diffusion and be located at the interface. Due to functional groups (-OH and -COOH), PLA may undergo reactive compatibilization during processing, forming copolymers at the interface. This method stabilizes the morphology more successfully than just adding pre-made copolymers. For instance, the presence of PS-g-MA in PLA/PS may augment the natural formation of PLA-co-PS at the interface, thus lower the interfacial tension. Furthermore, the co-continuous morphology may be stabilized by the preferential deposition of nanoparticles at the interface, in addition to using compatibilizers [65]. Hence, to expand the potential of PLA/PS blends in porous PLA materials, future study should consider the impacts of various kinds of interfacial modifiers. Furthermore, it is necessary to consider the broader effects of in order porous PLA materials that are created using PLA/PS blends [66].

II.7.2. Acrylonitrile-butadiene-styrene

ABS is a copolymer with a composition consisting of a rubbery phase (polybutadiene PB) dispersed in a rigid matrix (styrene-acrylonitrile copolymer (SAN)). The blending of PLA with ABS has been investigated in recent years, and most studies have focused on improving the properties of the PLA/ABS blends by increasing the compatibility between the components. The enhanced morphology attained for the PLA/ABS blends also yielded elevated toughness and improved ductility, but retained the strength of the pure PLA. PLA/ABS blends, which were compatibilized by SAN-GMA in the presence of ETPB,

exhibited an elongation about six times greater than clean PLA. Furthermore, the compatibilized blend showed an impact strength of 124 kJ/m^2, about double the value of the pure PLA's impact strength (69 kJ/m2). Sun et al. conducted a study on the impact of GMA as a compatibilizer, which further enhanced this blend [40,67]. The findings indicated that GMA shown a superior capacity for toughening compared to the previously published results for SAN-GMA. Sun et al. attributed this enhancement to the elevated rubber content (60 wt.%) in the used ABS, increasing toughening capability. Furthermore, based on the FT-IR findings, it was shown that GMA was predominantly incorporated into the shell layer of ABS (SAN), specifically at the interface between PLA and ABS. This resulted in enhanced interfacial interactions between the two phases. In conclusion, ABS is a viable option for improving PLA's resilience. Nature Works Co. (a company specializing in PLA production) has just introduced Blendex™ 338, a highly efficient ABS-based toughening agent for PLA. Several factors need to be considered to enhance the durability via the incorporation of ABS, including the blending ratio, composition of ABS, compatibilizers, and processing conditions. Of all the characteristics, the ABS composition is the most important. For instance, ABS with a high rubber component (about 60 wt.%) may significantly improve toughness. Moreover, the effective compatibilizers used for PLA/ABS blends may augment the dispersion of rubber particles in both PLA and SAN. Consistent with prior research, it may be inferred that, besides its limited biodegradability, this blend can demonstrate a diverse array of enhanced characteristics compared to pure PLA.

REFERENCES

[1] L. T. Lim, R. Auras, and M. Rubino, “Processing technologies for poly(lactic acid),” Prog. Polym. Sci., vol. 33, no. 8, pp. 820–852, 2008.

[2] S. Farah, D. G. Anderson, and R. Langer, “Physical and mechanical properties of PLA, and their functions in widespread applications — A comprehensive review,” Adv. Drug Deliv. Rev., vol. 107, pp. 367–392, 2016.

[3] M. Nofar, D. Sacligil, P. J. Carreau, M. R. Kamal, and M. C. Heuzey, “Poly (lactic acid) blends: Processing, properties and applications,” Int. J. Biol. Macromol., vol. 125, pp. 307–360, 2019.

[4] G. Liu, X. Zhang, and D. Wang, “Tailoring crystallization: Towards high-performance poly (lactic acid),” Adv. Mater., vol. 26, no. 40, pp. 6905–6911, 2014.

[5] R. M. Rasal, A. V. Janorkar, and D. E. Hirt, “Poly(lactic acid) modifications,” Prog. Polym. Sci., vol. 35, no. 3, pp. 338–356, 2010.

[6] J. B. Zeng, K. A. Li, and A. K. Du, “Compatibilization strategies in poly(lactic acid)-based blends,” RSC Adv., vol. 5, no. 41, pp. 32546–32565, 2015.

[7] J. M. Raquez, Y. Habibi, M. Murariu, and P. Dubois, “Polylactide (PLA)-based nanocomposites,” Prog. Polym. Sci., vol. 38, no. 10–11, pp. 1504–1542, 2013.

[8] Y. S. He, J. B. Zeng, S. L. Li, and Y. Z. Wang, “Crystallization behavior of partially miscible biodegradable poly(butylene succinate)/poly(ethylene succinate) blends,” Thermochim. Acta, vol. 529, pp. 80–86, 2012.

[9] R. Slivniak and A. J. Domb, “Lactic acid and ricinoleic acid based copolyesters,” Macromolecules, vol. 38, no. 13, pp. 5545–5553, 2005.

[10] D. Haynes, N. K. Abayasinghe, G. M. Harrison, K. J. Burg, and D. W. Smith, “ In Situ Copolyesters Containing Poly(l -lactide) and Poly(hydroxyalkanoate) Units ,” Biomacromolecules, vol. 8, no. 4, pp. 1131–1137, 2007.

[11] A. Meduri, T. Fuoco, M. Lamberti, C. Pellecchia, and D. Pappalardo, “Versatile copolymerization of glycolide and rac-lactide by dimethyl(salicylaldiminato)aluminum compounds,” Macromolecules, vol. 47, no. 2, pp. 534–543, 2014.

[12] J. B. Zeng, Y. D. Li, W. Da Li, K. K. Yang, X. L. Wang, and Y. Z. Wang, “Synthesis and properties of poly(ester urethane)s consisting of poly(l-lactic acid) and poly(ethylene succinate) segments,” Ind. Eng. Chem. Res., vol. 48, no. 4, pp. 1706–1711, 2009.

[13] J. B. Zeng, Y. D. Li, Q. Y. Zhu, K. K. Yang, X. L. Wang, and Y. Z. Wang, “A novel biodegradable multiblock poly(ester urethane) containing poly(l-lactic acid) and poly(butylene succinate) blocks,” Polymer (Guildf)., vol. 50, no. 5, pp. 1178–1186, 2009.

[14] D. Cohn and A. Hotovely Salomon, “Designing biodegradable multiblock PCL/PLA thermoplastic elastomers,” Biomaterials, vol. 26, no. 15, pp. 2297–2305, 2005.

[15] J. B. Zeng, Y. D. Li, Y. S. He, S. L. Li, and Y. Z. Wang, “Improving flexibility of Poly(l -lactide) by blending with poly(l -lactic acid) based poly(ester-urethane): Morphology, mechanical properties, and crystallization behaviors,” Ind. Eng. Chem. Res., vol. 50, no. 10, pp. 6124–6131, 2011.

[16] K. S. Anderson, K. M. Schreck, and M. A. Hillmyer, “Toughening polylactide,” Polym. Rev., vol. 48, no. 1, pp. 85–108, 2008.

[17] Y. Li and H. Shimizu, “Improvement in toughness of poly(l-lactide) (PLLA) through reactive blending with acrylonitrile-butadiene-styrene copolymer (ABS): Morphology and properties,” Eur. Polym. J., vol. 45, no. 3, pp. 738–746, 2009.

[18] E. Zuza, A. Lejardi, J. M. Ugartemendia, N. Monasterio, E. Meaurio, and J. R. Sarasua, “Compatibilization through specific interactions and dynamic fragility in poly-(D,L-lactide)/Polystyrene blends,” Macromol. Chem. Phys., vol. 209, no. 23, pp. 2423–2433, 2008.

[19] J. Qiu et al., “Miscibility and double glass transition temperature depression of poly(L-lactic acid) (PLLA)/poly(oxymethylene) (POM) blends,” Macromolecules, vol. 46, no. 14, pp. 5806–5814, 2013.

[20] C. Koning, M. Van Duin, C. Pagnoulle, and R. Jerome, “Strategies for compatibilization of polymer blends,” Prog. Polym. Sci., vol. 23, no. 4, pp. 707–757, 1998.

[21] B. Imre and B. Pukánszky, “Compatibilization in bio-based and biodegradable polymer blends,” Eur. Polym. J., vol. 49, no. 6, pp. 1215–1233, 2013.

[22] Y. Wang and M. A. Hillmyer, “Polyethylene-poly(L-lactide) diblock copolymers: Synthesis and compatibilization of poly(L-lactide)/polyethylene blends,” J. Polym. Sci. Part A Polym. Chem., vol. 39, no. 16, pp. 2755–2766, 2001.

[23] P. Saini, M. Arora, and M. N. V. R. Kumar, “Poly(lactic acid) blends in biomedical applications,” Adv. Drug Deliv. Rev., vol. 107, pp. 47–59, 2016.

[24] L. Yu, K. Dean, and L. Li, “Polymer blends and composites from renewable resources,” Prog. Polym. Sci., vol. 31, no. 6, pp. 576–602, 2006.

[25] C. Vogel, G. G. Hoffmann, and H. W. Siesler, “Rheo-optical FT-IR spectroscopy of poly(3-hydroxybutyrate)/poly(lactic acid) blend films,” Vib. Spectrosc., vol. 49, no. 2, pp. 284–287, 2009.

[26] Z. Bartczak, A. Galeski, M. Kowalczuk, M. Sobota, and R. Malinowski, “Tough blends of poly(lactide) and amorphous poly([R,S]-3-hydroxy butyrate) - Morphology and properties,” Eur. Polym. J., vol. 49, no. 11, pp. 3630–3641, 2013.

[27] M. Peesan, R. Rujiravanit, and P. Supaphol, "Journal of Biomaterials Science , Electrospinning of hexanoyl chitosan / polylactide blends," no 1, pp. 37–41, 2012.

[28] X. Jing et al., "Morphology, mechanical properties, and shape memory effects of poly(lactic acid)/ thermoplastic polyurethane blend scaffolds prepared by thermally induced phase separation," J. Cell. Plast., vol. 50, no. 4, pp. 361–379, 2014.

[29] M. P. Arrieta, M. D. Samper, M. Aldas, and J. López, "On the use of PLA-PHB blends for sustainable food packaging applications," Materials (Basel)., vol. 10, no. 9, pp. 1–26, 2017.

[30] J. Urquijo, G. Guerrica-Echevarría, and J. I. Eguiazábal, "Melt processed PLA/PCL blends: Effect of processing method on phase structure, morphology, and mechanical properties," J. Appl. Polym. Sci., vol. 132, no. 41, pp. 1–9, 2015.

[31] L. Zhang, C. Xiong, and X. Deng, "Miscibility, crystallization and morphology of poly(β-hydroxybutyrate)/poly(d,l-lactide) blends," Polymer (Guildf)., vol. 37, no. 2, pp. 235–241, 1996.

[32] K. S. Anderson and M. A. Hillmyer, "The influence of block copolymer microstructure on the toughness of compatibilized polylactide/polyethylene blends," Polymer (Guildf)., vol. 45, no. 26, pp. 8809–8823, 2004.

[33] Z. Ma, N. Zhao, and C. Xiong, "Degradation and miscibility of poly(DL-lactic acid)/poly(glycolic acid) composite films: Effect of poly(DL-lactic-co-glycolic acid)," Bull. Mater. Sci., vol. 35, no. 4, pp. 575–578, 2012.

[34] H. Tsuji, T. Yamada, M. Suzuki, and S. Itsuno, "Blends of aliphatic polyesters. Part 7. Effects of poly(L-lactide-co-ε-caprolactone) on morphology, structure, crystallization, and physical properties of blends of poly(L-lactide) and poly(ε-caprolactone)," Polym. Int., vol. 52, no. 2, pp. 269–275, 2003.

[35] V. Nagarajan, A. K. Mohanty, and M. Misra, "Perspective on Polylactic Acid (PLA) based Sustainable Materials for Durable Applications: Focus on Toughness and Heat Resistance," ACS Sustain. Chem. Eng., vol. 4, no. 6, pp. 2899–2916, 2016.

[36] C. Kim, K. U. K. Y. Cho, E. Choi, and J. Park, "Effect of P (lLA-co- PCL) on the Compatibility and Crystallization Behavior of PCL / PLLA Blends," pp. 13–15, 1999.

[37] D. Wu, Y. Zhang, L. Yuan, M. Zhang, and W. Zhou, "Viscoelastic interfacial properties of compatibilized poly(ε- caprolactone)/polylactide blend," J. Polym. Sci. Part B Polym. Phys., vol. 48, no. 7, pp. 756–765, 2010.

[38] G. Singh, H. Bhunia, A. Rajor, R. N. Jana, and V. Choudhary, "Mechanical properties and morphology of polylactide, linear low-density polyethylene, and their blends," J. Appl. Polym. Sci., vol. 118, no. 1, pp. 496–502, 2010.

[39] H. S. Lee and J. D. Kim, "Effect of a hybrid compatibilizer on the mechanical

properties and interfacial tension of a ternary blend with polypropylene, poly(lactic acid), and a toughening modifier," Polym. Compos., vol. 33, no. 7, pp. 1154–1161,2012.

[40] S. Sun, M. Zhang, H. Zhang, and X. Zhang, "Polylactide toughening with epoxy-functionalized grafted acrylonitrile–butadiene–styrene particles," J. Appl. Polym. Sci., vol. 122, no. 5, pp. 2992–2999, 2011.

[41] P. Juntuek, C. Ruksakulpiwat, P. Chumsamrong, and Y. Ruksakulpiwat, "Effect of glycidyl methacrylate-grafted natural rubber on physical properties of polylactic acid and natural rubber blends," J. Appl. Polym. Sci., vol. 125, no. 1, pp. 745–754, 2012.

[42] M. A. Huneault and H. Li, "Morphology and properties of compatibilized polylactide/thermoplastic starch blends," Polymer (Guildf)., vol. 48, no. 1, pp. 270–280, 2007.

[43] J. Liu, H. Jiang, and L. Chen, "Grafting of Glycidyl Methacrylate onto Poly(lactide) and Properties of PLA/Starch Blends Compatibilized by the Grafted Copolymer," J. Polym. Environ., vol. 20, no. 3, pp. 810–816, 2012.

[44] A. Teamsinsungvon, Y. Ruksakulpiwat, and K. Jarukumjorn, "Preparation and Characterization of Poly(lactic acid)/Poly(butylene adipate-co-terepthalate) Blends and Their Composite," Polym. - Plast. Technol. Eng., vol. 52, no. 13, pp. 1362–1367, 2013.

[45] S. Djellali, T. Sadoun, N. Haddaoui, and A. Bergeret, "Viscosity and viscoelasticity measurements of low density polyethylene/poly(lactic acid) blends," Polym. Bull., vol. 72, no. 5, pp. 1177–1195, 2015.

[46] K. Hamad, M. Kaseem, and F. Deri, "Poly(lactic acid)/low density polyethylene polymer blends: preparation and characterization," Asia-Pacific J. Chem. Eng., vol. 7, no. pp.310-316, 2012.

[47] K. Hamad, M. Kaseem, and F. Deri, "Melt Rheology of Poly(Lactic Acid)/Low Density Polyethylene Polymer Blends," Adv. Chem. Eng. Sci., vol. 01, no. 04, pp. 208–214, 2011.

[48] H. Balakrishnan, A. Hassan, and M. U. Wahit, "Mechanical, thermal, and morphological properties of polylactic acid/linear low density polyethylene blends," J. Elastomers Plast., vol. 42, no. 3, pp. 223–239, 2010.

[49] Y. F. Kim, C. N. Choi, Y. D. Kim, K. Y. Lee, and M. S. Lee, "Compatibilization of immiscible poly(l-lactide) and low density polyethylene blends," Fibers Polym., vol. 5, no. 4, pp. 270–274, 2004.

[50] K. S. Anderson, S. H. Lim, and M. A. Hillmyer, "Toughening of polylactide by melt blending with linear low-density polyethylene," J. Appl. Polym. Sci., vol. 89, no. 14, pp. 3757–3768, 2003.

[51] L. As'habi, S. H. Jafari, H. A. Khonakdar, R. Boldt, U. Wagenknecht, and G. Heinrich, "Tuning the processability, morphology and biodegradability of clay incorporated

PLA/LLDPE blends via selective localization of nanoclay induced by melt mixing sequence," Express Polym. Lett., vol. 7, no. 1, pp. 21–39, 2013.

[52] H. T. Oyama, "Super-tough poly(lactic acid) materials: Reactive blending with ethylene copolymer," Polymer (Guildf)., vol. 50, no. 3, pp. 747–751, 2009.

[53] K. Hamad, M. Kaseem, and F. Deri, "Rheological and mechanical characterization of poly(lactic acid)/polypropylene polymer blends," J. Polym. Res., vol. 18, no. 6, pp. 1799–1806, 2011.

[54] N. Reddy, D. Nama, and Y. Yang, "Polylactic acid/polypropylene polyblend fibers for better resistance to degradation," Polym. Degrad. Stab., vol. 93, no. 1, pp. 233–241, 2008.

[55] T. W. Yoo, H. G. Yoon, S. J. Choi, M. S. Kim, Y. H. Kim, and W. N. Kim, "Effects of compatibilizers on the mechanical properties and interfacial tension of polypropylene and poly(lactic acid) blends," Macromol. Res., vol. 18, no. 6, pp. 583–588, 2010.

[56] H. Kang, X. Lu, and Y. Xu, "Properties of immiscible and ethylene-butyl acrylate-glycidyl methacrylate terpolymer compatibilized poly (lactic acid) and polypropylene blends," Polym. Test., vol. 43, pp. 173–181, 2015.

[57] G. Biresaw and C. J. Carriere, "Interfacial tension of poly(lactic acid)/polystyrene blends," J. Polym. Sci. Part B Polym. Phys., vol. 40, no. 19, pp. 2248–2258, 2002.

[58] A. Mohamed, S. H. Gordon, and G. Biresaw, "Poly(lactic acid)/polystyrene bioblends characterized by thermogravimetric analysis, differential scanning calorimetry, and photoacoustic infrared spectroscopy," J. Appl. Polym. Sci., vol. 106, no. 3, pp. 1689–1696, 2007.

[59] K. Hamad, M. Kaseem, and F. Deri, "Effect of recycling on rheological and mechanical properties of poly(lactic acid)/polystyrene polymer blend," J. Mater. Sci., vol. 46, no. 9, pp. 3013–3019, 2011.

[60] G. Biresaw and C. J. Carriere, "Compatibility and mechanical properties of blends of polystyrene with biodegradable polyesters," Compos. Part A Appl. Sci. Manuf., vol. 35, no. 3, pp. 313–320, 2004.

[61] K. Hamad, M. Kaseem, and F. Deri, "Rheological and mechanical properties of poly(lactic acid)/polystyrene polymer blend," Polym. Bull., vol. 65, no. 5, pp. 509–519, 2010.

[62] K. Hamad, M. Kaseem, F. Deri, and Y. G. Ko, "Mechanical properties and compatibility of polylactic acid/polystyrene polymer blend," Mater. Lett., vol. 164, pp. 409–412, 2016.

[63] S. Mangaraj, A. Yadav, L. M. Bal, S. K. Dash, and N. K. Mahanti, "Application of Biodegradable Polymers in Food Packaging Industry: A Comprehensive Review," J.

Packag. Technol. Res., vol. 3, no. 1, pp. 77–96, 2019.

[64] P. Sarazin and B. D. Favis, “Morphology control in co-continuous poly(L-lactide)/polystyrene blends: A route towards highly structured and interconnected porosity in poly(L-lactide) materials,” Biomacromolecules, vol. 4, no. 6, pp. 1669–1679, 2003.

[65] S. Huang, L. Bai, M. Trifkovic, X. Cheng, and C. W. Macosko, “Controlling the morphology of immiscible cocontinuous polymer blends via silica nanoparticles jammed at the interface,” Macromolecules, vol. 49, no. 10, pp. 3911–3918, 2016.

[66] X. Liao, H. Zhang, Y. Wang, L. Wu, and G. Li, “Unique interfacial and confined porous morphology of PLA/PS blends in supercritical carbon dioxide,” RSC Adv., vol. 4, no. 85, pp. 45109–45117, 2014.

[67] Z. Y. Tan et al., “Influence of rubber content in ABS in wide range on the mechanical properties and morphology of PC/ABS blends with different composition,” Polym. Eng. Sci., vol. 46, no. 10, pp. 1476–1484, 2006.

Chapter III. Materials and Methodology

Chapter III. Materials and Methodology

III.1 Introduction

This chapter describes all the materials used in our study and summarises the formulation components. There is also an in-depth explanation of the methods used to characterize experimental and Computational study, melt mixing, and compounding.

III.2. Materials

The materials used in this study are summarized below and consist of the main components available on the market.

- **Poly (lactic acid) (PLA)**

PLA resin (PLI 005), an injection-grade resin with a density of 1.25 g/cm^3 (ISO 1183) and a melting temperature (Tm) ranging from 145-155 °C, was obtained from Nature Plast (Caen, France).

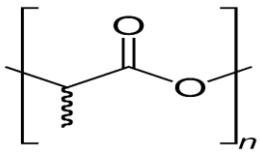

PLA

- **Polystyrene (PS)**

Total Petrochemicals, a French chemical company, supplied polystyrene (PS Crystal 1540) for various applications. It has a density of 1.05 g/cm^3 (ISO 1183) and a melt flow index (MFI) of 12 g/10 min (200 °C/5Kg), making it suitable for extrusion or injection processes (ISO 1133H).

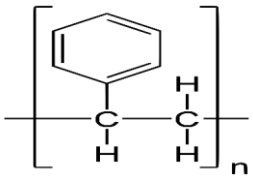

PS

- **Low-density polyethylene (LDPE)**

The LDPE (Lotrène®FD0274), supplied by Qatar Petrochemical Company, has a melt flow rate of 2.4 g/10 min (190 °C, 2.16 kg).

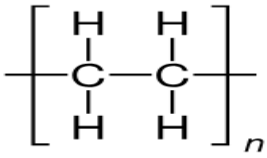

LDPE

- **Maleic anhydride grafted styrene-ethylene-butylene-styrene (SEBS-g-MAH)**

The maleated styrene-ethylene-butylene triblock copolymer (SEBS-g-MAH) was purchased from Shell Chemical Company, specifically KratonTM FG-1924X. The MFI and density are 22 g/10 min (ASTM D 1238, 230 °C/5 kg) and 0.90 g/cm^3.

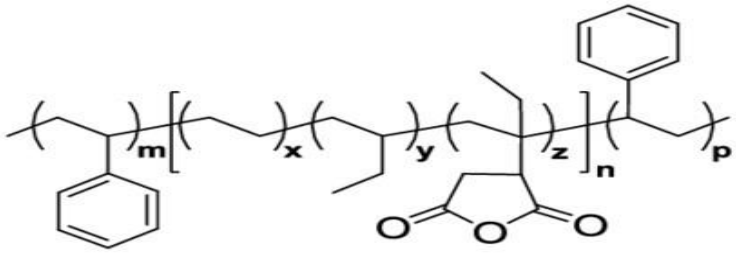

SEBS-g-MAH

III.3. Preparation of the blends

This study aims to develop PLA-based blends with polyolefins to examine and improve the compatibility and characteristics of these blends. The first part of the investigation involves the combination of PLA and PS, followed by introducing SEBS-g-MAH with different concentrations to enhance the system's compatibility. The compositions were chosen based on an initial literature assessment [1]. Based on the acquired findings, the ideal mixture ratio for PLA/PS blends was established (75/25). The second part of the study focuses on another bioblend, PLA/LDPE, compatibilized with SEBS-g-MAH. Based on the study's findings, it was established that the best mixing ratio between PLA and LDPE is (20/80) [2].

The ingredients were vacuum oven dried at recommended temperatures overnight before blending. PLA, LDPE, and SEBS-g-MAH were dried at 40°C, while PS had to be dried at

80°C. Melt compounding was used to produce the blends following the encoded formulations. Table III.1 summarises the compositions of PLA/PS blends, whereas Table III.2 summarises the compositions of PLA/LDPE blends. After drying, the different formulations (Table III.1 and 2) were mixed for 8 minutes at 200°C using a PlastographTM PL2100 internal mixer (Brabender®, Duisburg, Germany) with a rotor speed of 50 rpm. After being removed from the mixing chamber, the blend was left to cool at room temperature for 24 hours and then granulated and dried at 40°C. The dried pellets were subjected to compression in a hydraulic press heated to 200°C using a POLYLAB. Preheating and degassing steps were included, and optimal results were obtained with 5 minutes of compression at 180 Kg/cm^2. This enabled samples to be used for subsequent characterizations.

Table III.1. Composition and codes of PLA/PS

Codes	PLA	PS	PLA/PS	2.5%	5%	7.5%	10%
Sample (wt%)	PLA	PS	PLA/PS	SEBS-g-MAH (2.5%)	SEBS-g-MAH (5%)	SEBS-g-MAH (7.5%)	SEBS-g-MAH (10%)
PLA	100	-	75	73.75	72.5	71.25	70
PS	-	100	25	23.75	22.5	21.25	20
SEBS-g-MAH	-	-	-	2.5	5	7.5	10

Table III.2. Sample codes and compositions of PLA/LDPE.

Samples (wt%)	Codes	PLA	LDPE	PLA/LDPE	SEBS-g-MAH
PLA	S1	100	-	-	-
LDPE	S2	-	100	-	-
LDPE/PLA (80/20)	S3	20	80	100	0
LDPE/PLA/SEBS-g-MAH (2.5%)	S4	20	80	97.5	2.5
LDPE/PLA/SEBS-g-MAH (5%)	S5	20	80	95	5
LDPE/PLA/SEBS-g-MAH (7.5%)	S6	20	80	92.5	7.5
LDPE/PLA/SEBS-g-MAH (10%)	S7	20	80	90	10

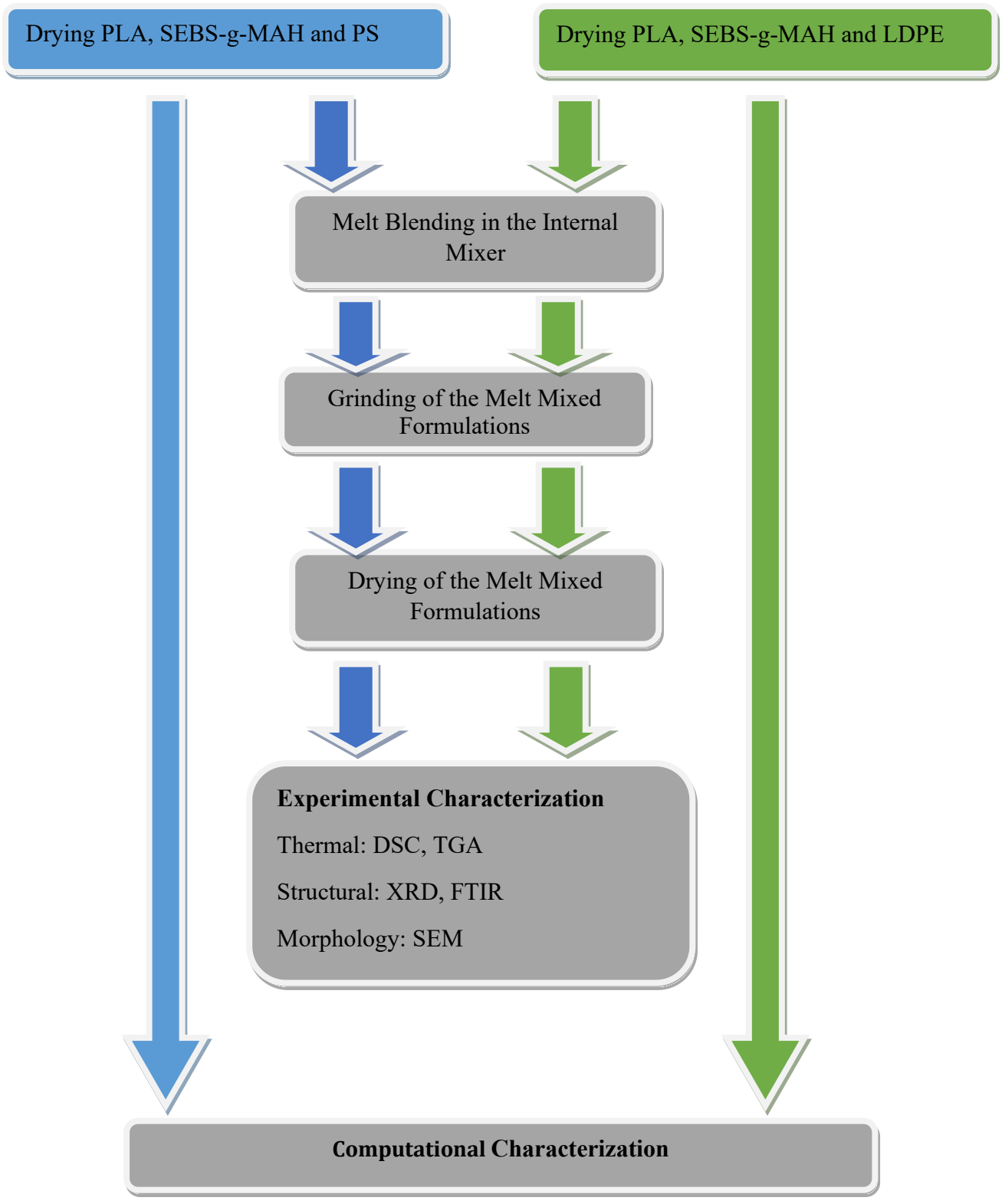

Figure III.1. Work Flowchart.

III.4. Characterization techniques

To examine the impact of incorporating SEBS-g-MAH as a compatibilizing agent on the microstructure enhancement in distinct blends (PLA/PS and PLA/LDPE). The formulated blends were subjected to several analytical procedures to assess their specific characteristics. Each of the following strategies is discussed in more detail in the subsequent section:

- Fourier transform infrared (FTIR) spectroscopy to observe the functional groups and the C-H environment along the backbone;
- Thermogravimetric analysis (TGA) for observing the thermal stability;
- Differential scanning calorimetry (DSC) is used to monitor the thermal characteristics;
- Tensile and hardness tests for evaluating the mechanical properties of plastics;
- X-ray diffraction (XRD) for calculating the extent of crystallinity;
- Scanning electron microscopy (SEM) for observing morphologies;

III.4. 1. Fourier transform infrared spectroscopy (FTIR)

Fourier transforms infrared (FTIR) spectroscopy is a non-destructive technique commonly employed to analyze the molecular composition of materials and investigate the physicochemical interactions between different chemical species. This study used FTIR spectroscopy to examine potential interactions between the compatibilizer SEBS-g-MAH and the PLA and PS components of the PLA/PS blend. SEBS-g-MAH compatibilizer and the PLA and PS components of the PLA/PS blend. The FTIR spectra and PLA, PS, SEBS-g-MAH, as well as their binary blend (PLA/PS) and ternary blend (PLA/PS/SEBS-g-MAH), were obtained using a SHIMADZU IR Sprit spectrometer. The spectra were recorded in the wavenumber range of 4000 to 400 cm^{-1}, employing 64 scans and a resolution of 4 cm^{-1}. This allowed for the analysis of molecular vibrations and provided insights into the chemical bonds and functional groups present in the samples. By comparing the spectra of the individual components and the blends, it was possible to assess any changes or interactions that occurred due to incorporating the SEBS-g-MAH compatibilizer.

III.4.2. Thermogravimetric analysis (TGA)

The thermal degradation behavior of the PLA/PS and PLA/LDPE blends was investigated using a Netzsch STA 449C TG-DSC Jupiter Thermo analyzer device (Netzsch, Germany). The analysis was conducted under a nitrogen atmosphere, and the temperature was increased

from room temperature to 580 °C with a heating rate of 10 °C/min. This enabled the thermal stability and decomposition characteristics. Observing the changes in weight and heat flow during the heating process, valuable information about the thermal degradation properties of the PLA/PS blends and their constituents could be obtained.

III.4.3. Differential Scanning Calorimetry (DSC)

The thermal properties of the blend were analyzed using a differential scanning calorimeter DSC (Q20, TA). 5-10 mg samples were thermally analyzed under a nitrogen atmosphere within a 20-200°C range and 10 °C/min heating rate. The reported values represent the mean values of two replicates. The glass transition temperature (T*g*), crystallization temperature (T*c*), fusion temperature (T_m), and fusion enthalpy (ΔH_m) calorimetric events were determined from the heating scan. The relative crystallinity (*X*c) of each component in the PLA/LDPE and PLA in PLA/PS blends was calculated by the following equations [3]:

$$Xc(PLA)(\%) = \frac{\Delta Hm - \Delta Hcc}{\Delta H_m^0(PLA) \times W(PLA)} \times 100\% \quad (1)$$

$$Xc(\%)(LDPE) = \frac{\Delta Hm(LDPE)}{\Delta H_m^0(LDPE) \times W(LDPE)} \times 100\% \quad (2)$$

where $\Delta H_{m\ (PLA)}$ was the melting enthalpy of PLA, $\Delta H_{cc\ (PLA)}$ was the cold crystallization enthalpy of PLA, and $\Delta H_{m\ (PLA)}$ was the melting enthalpy of 100% crystalline PLA that was 93 J/g [4], $\Delta H_{m\ (LDPE)}$was the melting enthalpy of LDPE, $\Delta H^0_{m(LDPE)}$was the melting enthalpy of 100% crystalline LDPE that was considered to be 293 J/g [5], W was the weight fraction of each component in the PLA/LDPE blends.

III.4.4. Tensile and hardness tests

Tensile testing was conducted using an ASTM D882 universal MTS 500 instrument, a standard method for evaluating the mechanical properties of plastics. The tests were performed at room temperature and pressure, with a 10 mm/min cross-head speed. At least five samples were tested for each set to determine Young's modulus, tensile strength, and elongation at break.

A Qnes Q30 instrument designed for rigid polymers was used for the hardness test, following the ISO 869 standard. The specimens had dimensions of (63 x 12.7 x 2) mm^3. The sample was placed under the needle of the durometer, and a load of 5 kg was applied. Five measurements were taken on each sample at points approximately 3 mm apart and 12 mm from the borders. The average of the five test values was used to express the hardness results.

III.4.5 X-ray diffraction (XRD)

The blends ' X-ray diffraction (XRD) was carried out using the Rigaku miniflex Benchtop. The wavelengths of Cu kα1 and kα2 radiations (λ) were 1.54056 nm, respectively. The samples were characterized in the data angle range between 5° and 50°. The generator voltage was 40 kV, and the tube current was 15 mA.

III.4.6. Scanning electron microscopy (SEM) analysis.

The microstructure of the samples was analyzed using a JEOL JSM-7001F scanning electron microscope (JEOL Ltd., Tokyo, Japan) operating at an acceleration voltage of 10 kV. Cryogenic fracturing was performed by immersing the samples in liquid nitrogen to prepare the sample surfaces for observation. This freezing method was employed to prevent any plastic deformation during sample preparation.

III.5. Computational part

Theoretical computation, specifically molecular modeling, offers an alternative approach to obtaining results regarding structural and spectroscopic properties [6,7]. These results can be compared to experimental findings. Exploring the intermolecular bonding within blends through practical techniques is generally challenging. However, molecular dynamics simulations provide a reliable, cost-effective, and efficient tool to overcome this limitation. Atomic-level simulations have frequently been employed to predict the physical properties and interaction mechanisms of polymer blend compatibilization. We will present the types of theoretical calculations;

III.5.1. Molecular dynamic simulation (MDS)

This study performed molecular dynamics (MD) simulations using Materials Studio software (Accelrys Inc.). The PLA, PS and LDPE molecular chains, consisting of 50 repeated units, were constructed for the simulations. The COMPASS force field was employed to model the inter- and intra-molecular interactions within the system. For the simulation dynamics, a Verlet algorithm with a time integration step of 1 fs was utilized to govern the motion of the atoms. The van der Waals (VdW) interactions beyond a cutoff distance of 8.5 Å were truncated to account for the non-bonded interactions. The atomic and Ewald summation methods were employed to calculate the VdW and Coulomb interactions. During the NPT (isothermal-isobaric

thermodynamic ensemble) simulations, the temperature and pressure were controlled using the Anderson and Berendsen barostats [7].

III.5.2. Quantum Computational calculation

In the Density Functional Theory (DFT) investigation using the DMol3 module in Material Studio Software 7.0, the density of states (DOS) and the exchange-correlation function were estimated. The DOS calculation provided a graphical representation that illustrated the quantity of available electronic states at different energy levels, giving insights into the band gap of the materials. The band gap, which is the energy difference between the highest occupied molecular orbital (HOMO) and the lowest unoccupied molecular orbital (LUMO), is a critical parameter influencing the electrical conductivity and optical properties of a material [8].

Additionally, the investigation examined the frontier molecular orbitals (FMO) of PLA, PS, and their blends to analyze the effect of interactions on the electronic charge properties of the materials [8,9]. According to the frontier orbital hypothesis, the lowest unoccupied orbital is favourable for electrophilic activity.

III.5.3. COSMO-RS implementation

The conductor-like Screening Model COSMO was employed in the investigation after the geometry optimization and energy calculations. This model allows for the consideration of the reaction's specific environment. In this case, water was chosen as the solvating medium to replicate the appropriate reaction environment. The dielectric constant of water, which is 78.54, was utilized to compute sigma profiles [6].

REFERENCES

[1] K. Hamad, M. Kaseem, F. Deri, and Y. G. Ko, "Mechanical properties and compatibility of polylactic acid/polystyrene polymer blend," Mater. Lett., vol. 164, pp. 409–412, 2016.

[2] A. H. Setiawan and F. Aulia, "Blending of Low-Density Polyethylene and Poly-Lactic Acid with Maleic Anhydride as A Compatibilizer for Better Environmentally Food-Packaging Material," IOP Conf. Ser. Mater. Sci. Eng., vol. 202, no. 1, 2017.

[3] S. Pilla, S. G. Kim, G. K. Auer, S. Gong, and C. B. Park, "Microcellular extrusion foaming of poly(lactide)/poly(butylene adipate-co-terephthalate) blends," Mater. Sci. Eng. C, vol. 30, no. 2, pp. 255–262, 2010.

[4] X. Lu et al., "Morphology and properties of bio-based poly (lactic acid)/high-density polyethylene blends and their glass fiber reinforced composites," Polym. Test., vol. 54, pp. 90–97, 2016..

[5] S. Saikrishnan, D. Jubinville, C. Tzoganakis, and T. H. Mekonnen, "Thermo-mechanical degradation of polypropylene (PP) and low-density polyethylene (LDPE) blends exposed to simulated recycling," Polym. Degrad. Stab., vol. 182, pp. 109390, 2020.

[6] A. Zerriouh, A. Deghiche, W. Bououden, D. Cavallo, A. Erto, and N. Haddaoui, "A computational and experimental investigation of TEOS-treated graphene oxide-PVA interaction: molecular dynamics simulation and COSMO-RS insights," J. Mol. Liq., vol. 382, pp. 121914, 2023.

[7] L. Otmani, R. Doufnoune, Y. Benguerba, and A. Erto, "Experimental and theoretical investigation of the interaction of sulfonated graphene oxide with polyvinylalcohol/poly (4-styrenesulfonic) complex," J. Mol. Liq., vol. 284, pp. 599–606, 2019.

[8] J. M. Smith, S. P. Jones, and L. D. White, "Rapid Communication," Gastroenterology, vol. 72, no. 1, pp. 193, 1977.

[9] W. Bououden et al., "Surface adsorption of Crizotinib on carbon and boron nitride nanotubes as Anti-Cancer drug Carriers: COSMO-RS and DFT molecular insights," J. Mol. Liq., vol. 338, pp. 116666, 2021.

Chapter IV. Compatibility Enhancement of (PLA/PS) Blends by Incorporating SEBS-g-MAH as a Compatibilizer Agent: experimental and simulation study

Chapter IV. Compatibility Enhancement of (PLA/PS) Blends by Incorporating SEBS-g-MAH as a Compatibilizer Agent: Experimental and Simulation study

IV.1. Introduction

This study investigated the impact of incorporating maleic anhydride grafted styrene-ethylene-butylene-styrene (SEBS-g-MAH) at varying concentrations (2.5, 5.0, 7.5, and 10.0 wt %) into binary blends of polylactic acid (PLA) and polystyrene (PS) with a weight ratio of 75/25. Various characterization techniques, including Fourier transform infrared spectroscopy (FTIR), thermogravimetric analysis (TGA), differential scanning calorimetry (DSC), tensile testing, surface hardness measurements, and scanning electron microscopy (SEM) were employed to evaluate the structural, thermo-mechanical, surface, and morphological properties of the blends. Finally, study the simulation approaches.

IV.2. Results and discussion

IV.2.1. Fourier transform infrared spectroscopy

The Fourier transform infrared (FTIR) spectroscopy analysis was conducted on pure PLA, PS, and their blends with and without a compatibilizer. Figure IV.1 shows the FTIR spectra of PLA, PS, PLA/PS (75:25) (wt/wt), and PLA/PS with SEBS-g-MAH.

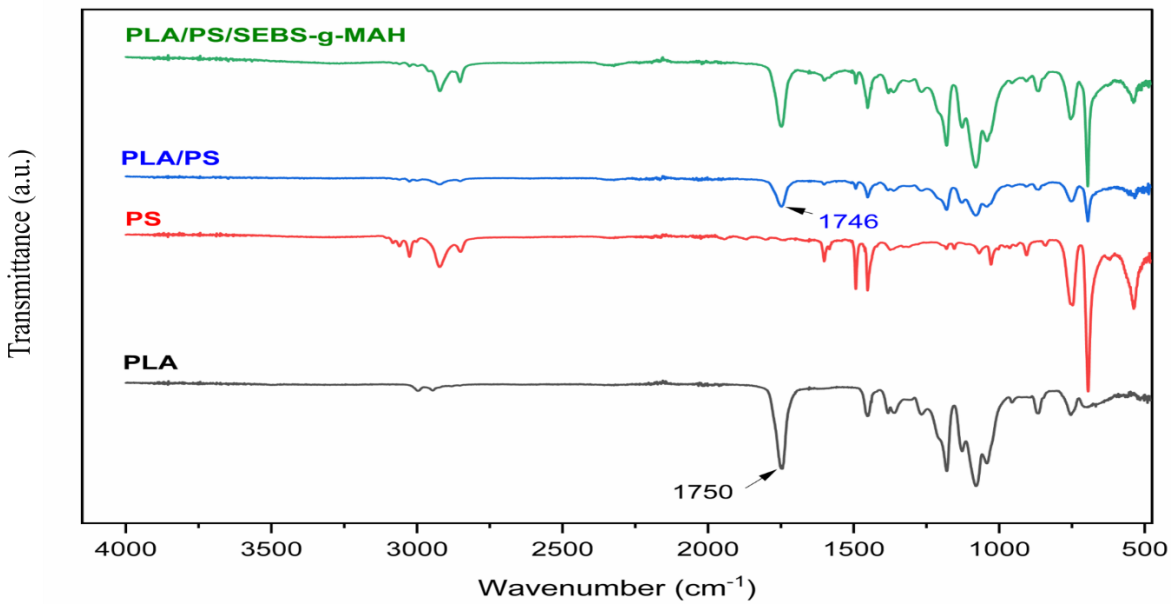

Figure IV.1. FTIR spectra of the PLA, PS, PLA/PS, and PLA/PS/SEBS-g-MAH blends

Table IV.1 provides the assignment of FTIR bands specific to PLA. The bands observed in the spectra correspond to various functional groups and bonds present in PLA compared with previous studies [1,2].

Table IV.1.PLA FTIR bands.

Wavenumber (cm^{-1})	Band assignment
1758-1802	Elongation vibration of the carbonyl group
2950-2994	Elongation vibration of the -CH bond of the CH_3 group
1037-1200	Elongation vibration of the C-O bond of the ester group
3505	Elongation vibration of the hydroxyl (OH) group

Similarly, FTIR analysis was performed on pure PS, and Table IV.2 presents the assignment of FTIR bands in PS. The peaks observed in the PS spectrum correspond to the vibrational modes of different bonds and groups present in PS. The data obtained for PS are compared with previous studies [3].

No new bands were observed in the PLA/PS blends that could compete with the characteristic bands of PLA and PS.The FTIR spectra of compatibilized and non-compatibilized PLA/PS blends showed similar patterns, slightly shifting the carbonyl group from 1767 to 1759 cm^{-1} (Figure 2).

Table IV.2. Assignment of FTIR bands in PS.

Wavenumber (cm^{-1})	Band assignment
3105	Valence vibration of the bond (=C-H) of the aromatic ring
2997 and 2964	Asymmetric valence vibration of the aliphatic bond (-CH_2-).
1597	Valence vibration of the aromatic ring bond (-C=C-).
1437	Deformation vibration of the bond (=C-H) of the aromatic ring.
780	Deformation vibration outside the plane of the aromatic ring's bond (-C=C-).

Figure IV.2 displays the FTIR spectra of PLA and PLA/SEBS-g-MAH (20/80 wt/wt). The observed frequency shifts are typically evidence of intermolecular interactions in polymer blends. In the case of PLA and PS blends, the n-π interaction can occur between the nucleophilic atoms in PLA (such as oxygen atoms in ester groups) and the π-electron systems in the aromatic rings of PS [4,5]. When the concentration of the compatibilizing agent (SEBS-g-MAH) was high, the peaks at 2945 and 2996 cm^{-1} shifted to 2851 and 2922 cm^{-1},

respectively Figure IV.2 [6]. This shift indicates possible interactions between PLA and SEBS-g-MAH in the blend.

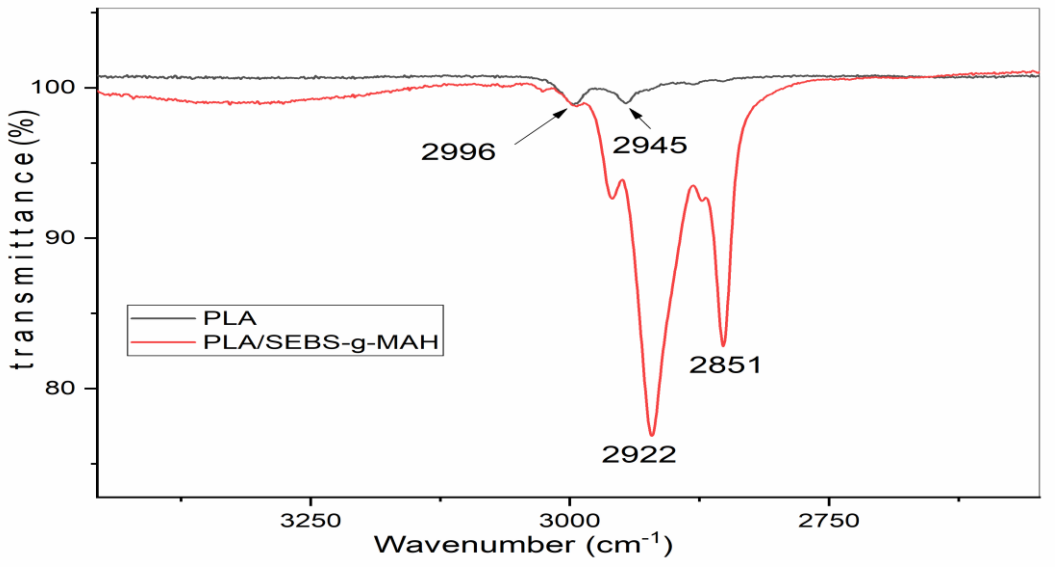

Figure IV.2. FTIR spectra of PLA and PLA/SEBS-g-MAH (20/80).

IV.2.2. Thermogravimetric Analysis (TGA)

The thermal stability of pure PLA, PS, and their blends with and without the addition of SEBS-g-MAH compatibilizer was analyzed using thermogravimetric analysis (TGA). Figure IV.3(a) presents the TGA curves obtained under an inert atmosphere. The TGA curves illustrate the changes in weight of PLA and PS as a function of temperature, as well as the effect of the SEBS-g-MAH compatibilizer on the PLA/PS (75/25 wt/wt) blend. The thermal stability profiles of the neat polymers reveal that PLA is less stable than PS. The PS starts to degrade at 342.31°C and undergoes complete decomposition at 372.82°C. On the PS thermogram, two distinct peaks can be observed, one at 384.88°C indicating the onset of degradation and another at 419.99°C indicating complete decomposition. At 300°C, both PLA and PS exhibit similar weight loss. However, when heated to 350°C, PLA demonstrates a significantly higher mass loss (30.70 wt.%) than PS (5.09 wt.%). This difference in mass loss can be attributed to the distinct structures of the two polymers. PLA is semi-crystalline, while PS is entirely amorphous [5,7].

The addition of the SEBS-g-MAH compatibilizer may affect the thermal stability of the PLA/PS blend, but the specific details of its impact are not mentioned in the provided information.

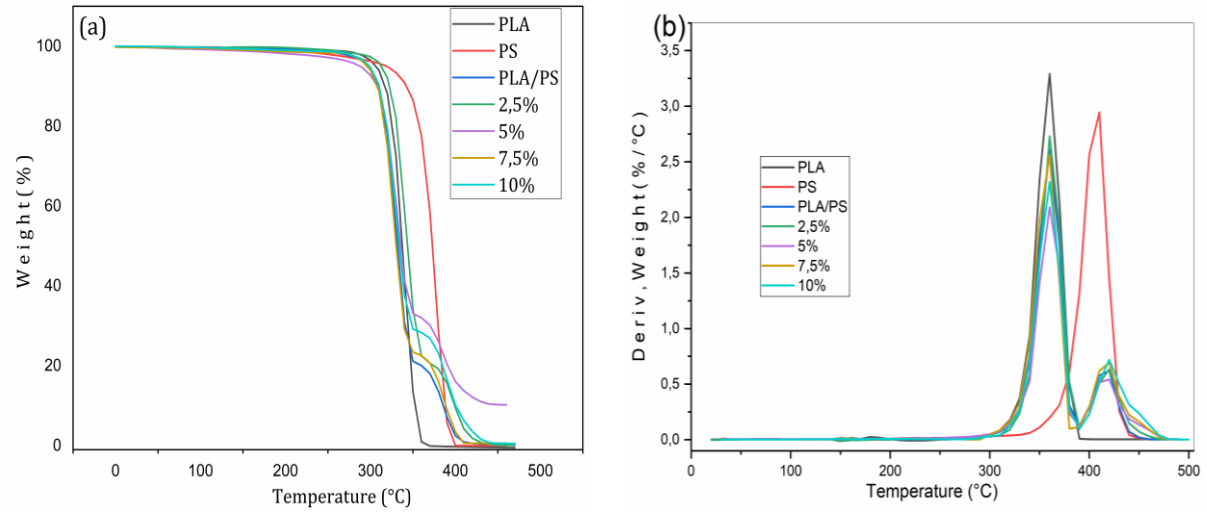

Figure IV.3 curves of PLA, PS, and their blends, (a) TGA (b) DTGA.

The degradation profiles of the blend mixtures exhibited two distinct transitions, with each transition corresponding to one of the blend's constituents. The first transition was observed in the vicinity of PLA at a lower temperature, whereas the second transition was identified in the PS region. This characteristic was clearly illustrated in the DTGA graph, as shown in Figure IV.3(b).Table IV.3.

Table IV.3. Thermogravimetric Analysis Data.

	Profile 1		Profile 2	
Samples	T_{onset}(°C)	T_f (°C)	T_{onset}(°C)	T_f (°C)
PLA	342	373	-	-
PS	-	-	385	420
PLA/PS	343	373	403	429
2.5%	345	373	406	432
5.0%	342	373	402	436
7.5%	340	370	403	436
10%	341	372	406	442

The PLA/PS (75:25) blend exhibited two distinct phases during thermal analysis. The first phase showed a breakdown temperature of 342.31 °C, which was identical to the pure PLA component. The second phase appeared simultaneously at the same temperature as pure PS (384.88 °C). With the addition of the compatibilizing agent, minor improvements in thermal stability were observed at the 7.5% and 10% weight percentages. The thermal stability of the blend without the SEBS-g-MAH compatibilizer was reduced due to the presence of PLA, which is semi-crystalline, and its interaction with the fully amorphous PS component. The

significant difference in glass transition temperature (Tg) between the two polymers also contributed to the degradation mechanism. However, the thermal stability of the overall PLA/PS/SEBS-g-MAH blends was greatly enhanced by the addition of SEBS-g-MAH, as evidenced by a noticeable increase in the intensity of the second degradation peak [5,6].

IV.2.3. Differential Calorimetric Analysis (DSC)

The thermal behavior of PLA, PS, and PLA/PS blends (75/25 wt/wt) with different concentrations of SEBS-g-MAH compatibilizer (2.5%, 5%, 7.5%, and 10% by weight) was investigated using DSC. A single heating scan from 0 to 190 °C was performed to obtain the DSC thermograms. The degree of crystallinity (Xc) of PLA was calculated using equation (1) (ChapterIII) to establish a relationship between the change in crystallinity and the mechanical properties of PLA. Figure IV.4 shows the DSC thermograms of PLA, PS, and PLA/PS blends with and without the SEBS-g-MAH compatibilizer.

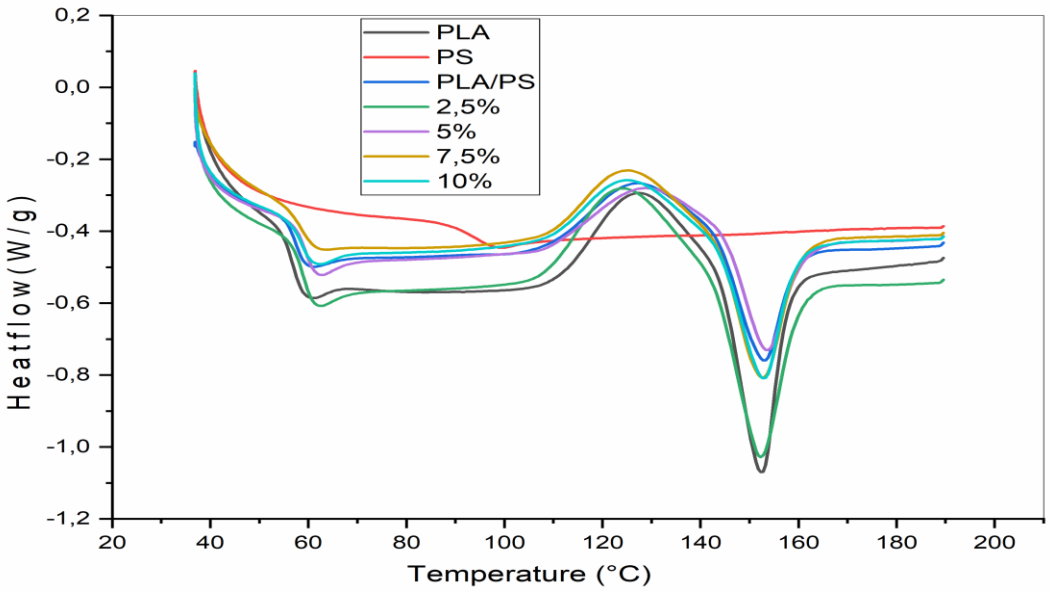

Figure IV.4 DSC thermograms of PLA, PS, and their blends.

PLA exhibited a glass transition temperature (Tg) of approximately 57 °C, a maximum cold crystallization temperature (Tcc) of around 127 °C, and a melting point of 152 °C. On the other hand, amorphous PS showed a Tg of about 88 °C [8]. The addition of PS to PLA resulted in slight increases in the Tg and melting peaks of PLA in both un-compatibilized and compatibilized blends, as observed in Table IV.4. The Tcc, representing the maximum temperature for crystallization initiation, remained unchanged. However, the presence of the dispersed SEBS phase led to an enlarged peak. As expected, the incorporation of PS in PLA

led to a slight decrease in the degree of crystallinity, from 15.4% to 13.7%. A further reduction to 10.3% was observed upon adding the SEBS-g-MAH compatibilizer to the PLA/PS blend. Similar findings were reported by Lima et al. in their study on bioblends containing PLA and SEBS [9]. The decrease in PLA crystallinity with increasing SEBS content indicates that SEBS inhibits the crystallization of PLA and does not act as a nucleating agent.

TableIV.4. DSC data of PLA, PS, and their blends.

Samples	Tg (°C)	Tcc (°C)	Tm(°C)	ΔHm (J/g)	Xc (%)
PLA	57	127	152	14.4	15.4
PS	88	-	-	-	-
PLA/PS	57	127.4	153	9.6	13.7
2.50%	59	123.9	153	7.9	11.7
5.00%	59	128.9	154	7.8	11.9
7.50%	59	125.4	153	7.3	11.6
10.00%	58	125.1	153	6.2	10.3

IV.2.4. Mechanical characterization

The interfacial adhesion between the polymers and the individual properties of each polymer influences the mechanical properties of polymer blends. In this study, the tensile properties of PLA/PS blends (75/25) were investigated to assess the effect of the compatibilizer quantity. Figure IV.5 illustrates the impact of the SEBS-g-MAH compatibilizer on the tensile and hardness characteristics of the PLA/PS blends. The results showed that both PLA and PS are rigid and brittle polymers [5,10,11]. with high Young's modulus values, approximately 3943.9 MPa and 3646.8 MPa, respectively. The Young's modulus of the PLA/PS (75/25) blend remained at 3899.97 MPa . However, the addition of the SEBS-g-MAH compatibilizer significantly reduced the stiffness of the PLA/PS blend. This was evidenced by a 50% decrease in hardness and a 45% decrease in Young's modulus.

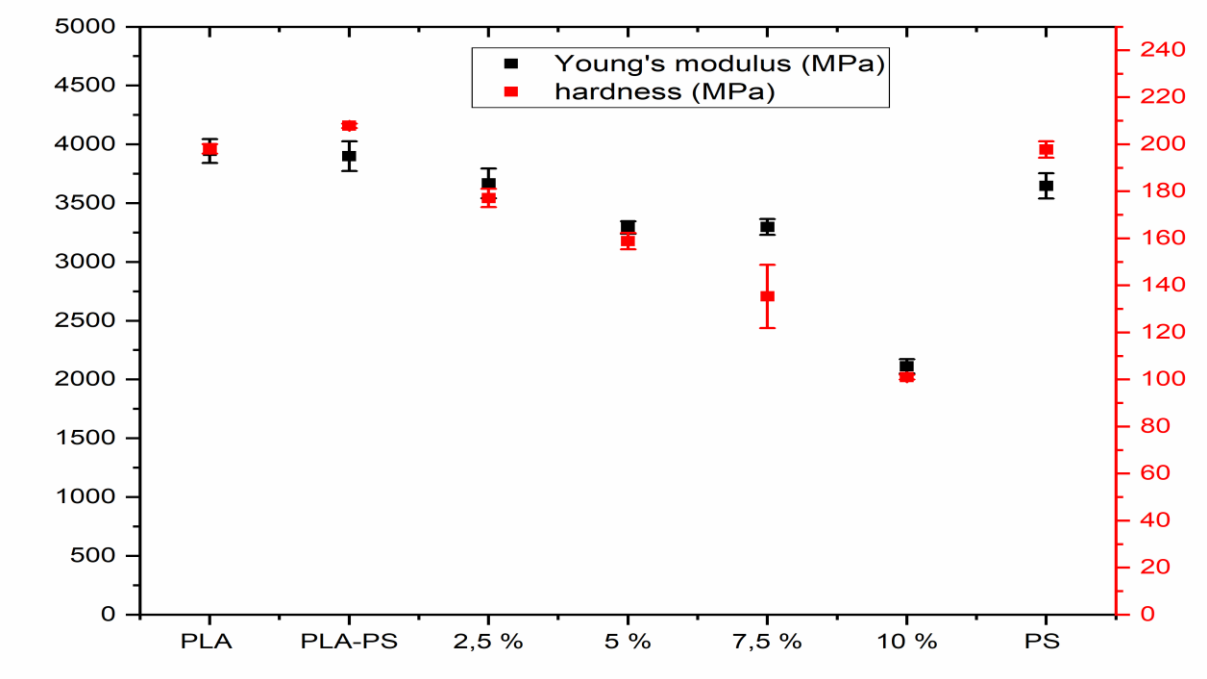

Figure IV.5. Young's modulus and hardness of PLA, PS, PLA/PS, and their blends with SEBS-g-MAH.

The results of tensile strength and elongation at break tests conducted on PLA, PS, and PLA/PS blends with and without SEBS-g-MAH compatibilization are presented in Figure IV.6. As expected, the rigid materials PLA and PS exhibited high tensile strength and low elongation at break values (21.3 MPa and 1% for PLA and 20.7 MPa and 0.96% for PS) due to their inherent stiffness. The PLA/PS blend showed a decrease of 38% in tensile strength and 40% in elongation at break compared to the pure polymers. For the PLA/PS blends with 2.5, 5.0, and 7.5 wt% SEBS-g-MAH, the obtained values for elongation at break and tensile strength were similar and not far from those of the un-compatibilized blends. However, the blend with a 10 wt% compatibilizer ratio exhibited significantly higher tensile strength and elongation at break.

A correlation between the concentration of SEBS-g-MAH and the tensile properties was observed in the blends. The compatibilized and un-compatibilized blends of PLA and PS showed less interaction between the two materials than the blend with 10 wt% SEBS-g-MAH. The weak interaction between the polymers could explain the decrease in tensile properties observed in the un-compatibilized blends. However, with the addition of 10 wt% SEBS-g-MAH as a compatibilizing agent, a significant improvement in tensile characteristics was observed, making the material more pliable. This improvement may be attributed to the compatibilizing agent's function as a binder with minimal impact on the intermolecular forces between the polymers [6]. The addition of SEBS-g-MAH to the PLA/PS blend decreased

Young's modulus and tensile strength this is due to the rubbery nature of the compatibilizer agent.

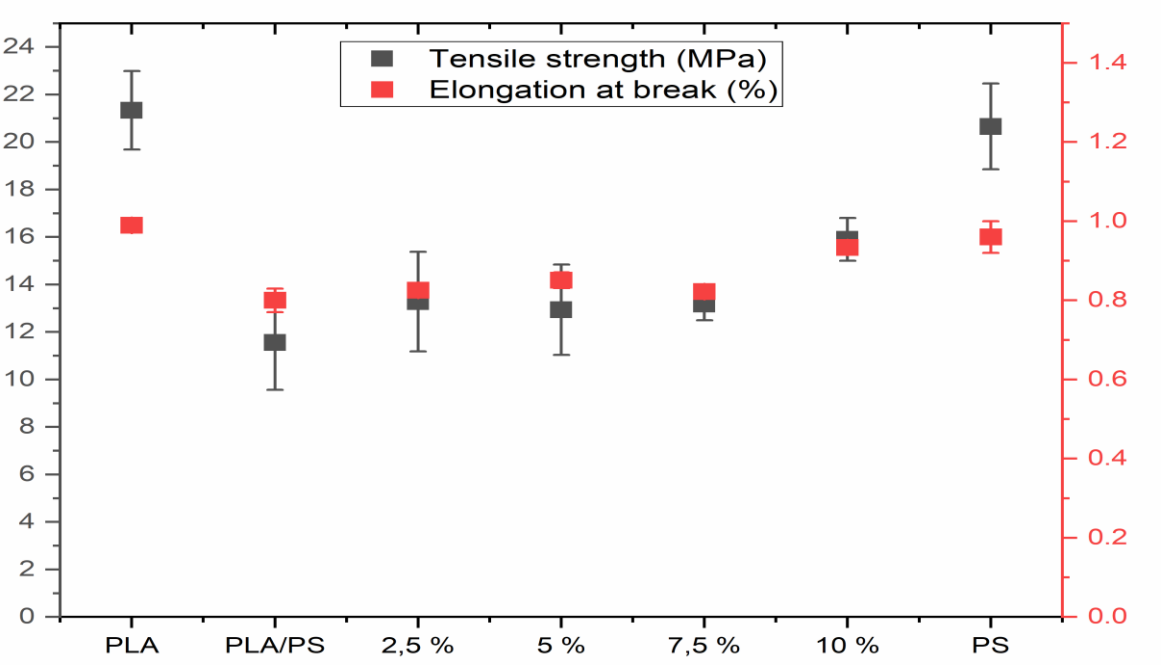

Figure IV.6 Tensile strength and elongation at break of PLA, PS, PLA/PS, and their blends SEBS-g-MAH.

IV.2.5. Scanning electron microscopy (SEM) analysis

FigureIV.7 depicts scanning electron microscopy (SEM) images of PLA, PS, and PLA/PS blends with and without the SEBS-g-MAH compatibilizer. The fracture surfaces of pure PLA and PS, as shown in Figures IV.7(a) and 7(b), appear smooth with sharp edges, indicating their brittleness [12,13]. The morphology of the PLA/PS blend exhibits a sea-island design, where discrete PS spheres are dispersed throughout the PLA matrix. Figure IV.7(c) highlights the biphasic nature of the blend, with evenly distributed PS domains within the PLA matrix. This morphology can be attributed to the differences in melt viscosity between PS and PLA, with PS having a higher viscosity [18]. These findings align with the observations made by Liao et al. [14].

The addition of the SEBS-g-MAH compatibilizer affects the morphology of the PLA/PS blend. Figure IV.7(e) demonstrates that the PS spheres shrink after exposure to the compatibilizing agent. Even with only 2.5% by weight of SEBS-g-MAH, the size of the PS phase is significantly reduced Figure IV.7(d). Furthermore, as the concentration of the compatibilizer increases from 5 to 10 wt%, the PS particle size continues to decrease (Figures

IV.7(f) and 8(g)) [15]. These observations highlight the beneficial compatibilizing activity of SEBS-g-MAH in promoting better dispersion and reducing the size of the PS domains within the PLA matrix.

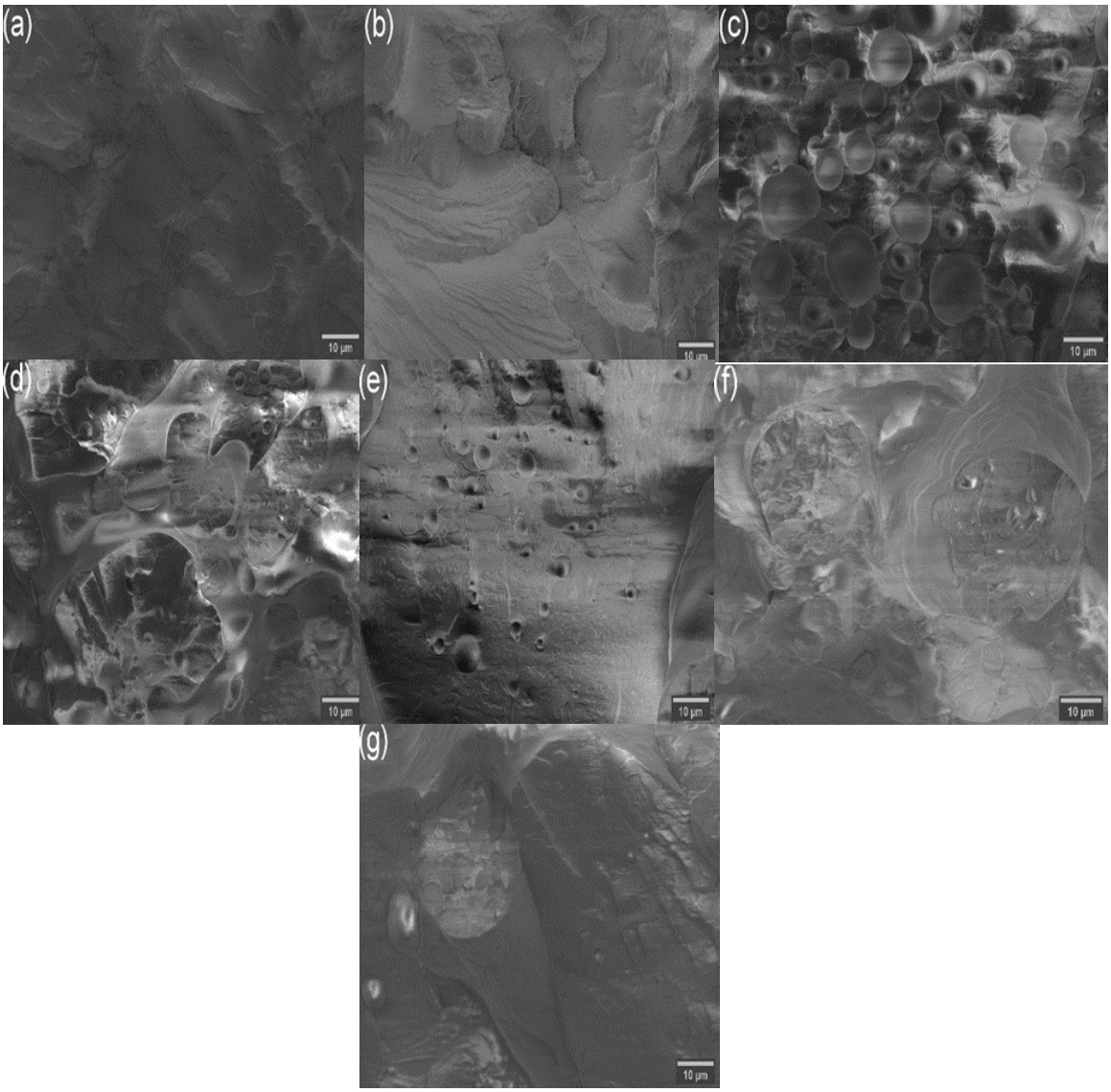

Figure IV.7. SEM micrographs of (a) PLA, (b) PS, (c) PLA/PS, and (d)PLA/PS/SEBS-g-MAH 2.5%, (e) PLA/PS/SEBS-g-MAH 5%, (f) PLA/PS/SEBS-g MAH 7.5%, (g)PLA/PS/SEBS-g-MAH 10%.

IV.3. Computational results

IV.3.1. Molecular dynamic simulation analysis

MD simulations were employed to investigate the binding energy and interaction mechanisms within the bioblends. The resulting structures obtained after equilibration and density stabilization are illustrated in Figure IV.8.

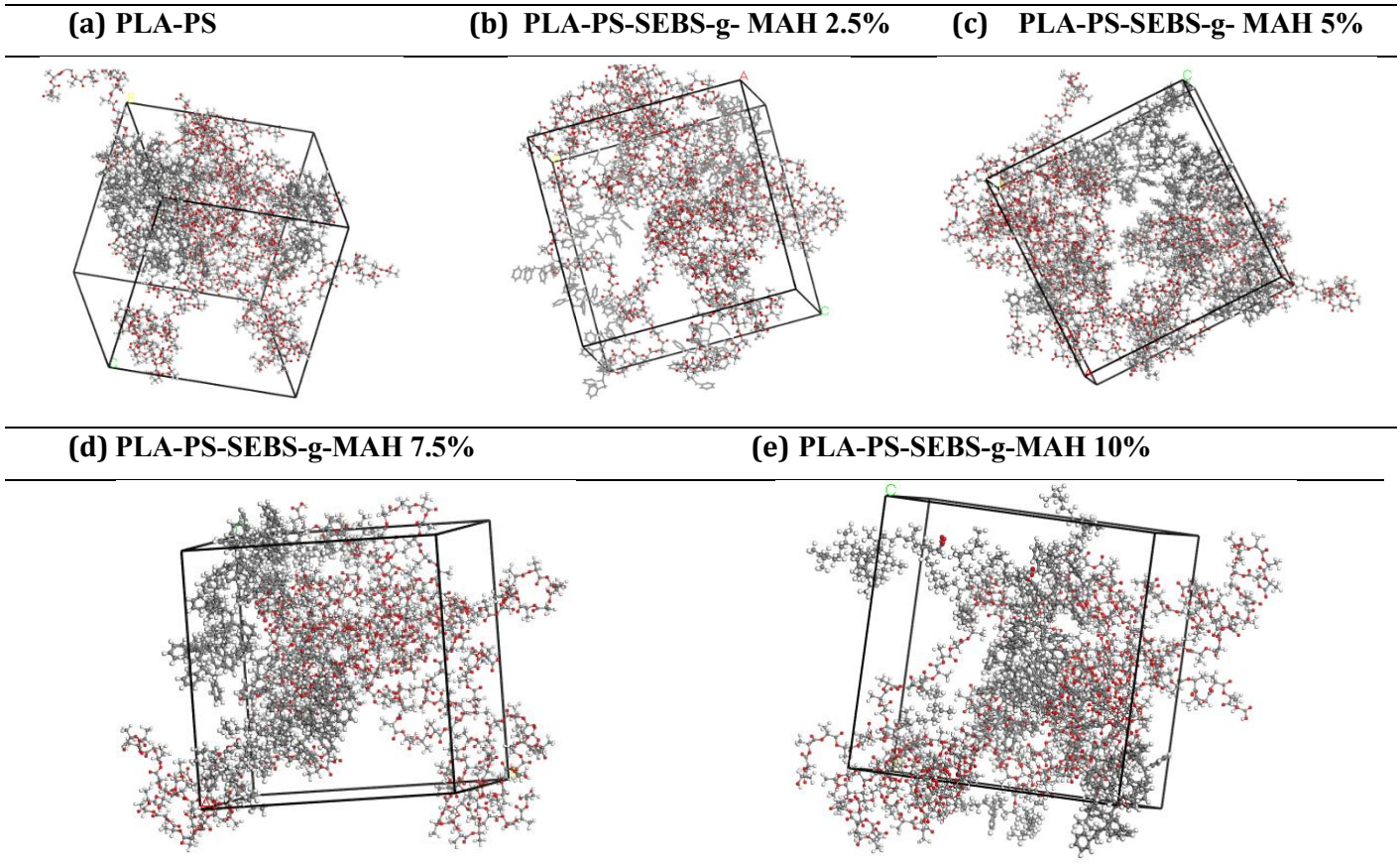

Figure IV.8. Ultimate stability structures derived through dynamic simulations for PS/PLA blends formulation, representing the structures after stabilization and density equilibration.

IV.3.1.1. Binding energy

Calculating and comparing the binding energies between the different formulations will help us understand the interaction mechanism and the effect of the compatibilizer agent on the intermolecular distribution of bioblend. The binding energies of the PLA-PS and PLA-PS-SEBS-g-MAH interaction models can be calculated using equations (1) .

$$E_{bind} = -E_{inter} = -E_{total} - E_1 - E_2 \qquad (1)$$

E_{total}, E_1, and E_2 are the energies of the blends studied. The binding energies of different blends are given in Table IV.5

Table.IV.5. Binding interaction energies (kcal/mol).

N° Sys	System	E(Total)	E(PLA)	E(PS)	E(SEBS-g-MAH)	E_{bind}	E_{Inter}
1	PLA-PS	-2706,566	-622,052	-46,542	----	2037,972	-2037,972
2	PLA-PS(2,5)	-3319,494	-800,639	75,774	-151,681	2442,948	-2442,948
3	PLA-PS(5)	-3456,22	-641,444	317,527	-305,357	2826,946	-2826,946
4	PLA-PS(7,5)	-3157,474	-880,603	-106,606	-311,682	1858,583	-1858,583
5	PLA-PS(10)	-2588,433	114,38	-106,606	-311,682	2284,525	-2284,525

The effect of the compatibilizing agent SEBS-g-MAH on the binding energy and interfacial interactions within the PLA/PS bioblends was examined. Table IV.5 demonstrates that the addition of SEBS-g-MAH increases the binding energy of the blends, indicating stronger interfacial interaction between PS-SEBS-g-MA and PLA-SEBS-g-MA compared to PLA-PS alone. Among the different compositions, the PLA-PS-SEBS-g-MAH blend with a 5% concentration exhibited the highest binding energy of 2826.946 kcal/mol, while PLA-PS blend had a binding energy of 2037.972 kcal/mol. This suggests that the interfacial interaction strength in the PLA-PS-SEBS-g-MA system is higher than in the PLA-PS blend. Additionally, figures and S (1-5) in the Supporting Data Information illustrate the molecular distribution of PLA-PS with and without the compatibilizing agent. The blends without the compatibilizer show a non-uniform molecular distribution, with phase segregation between PLA and PS, where the majority phase consists of PLA with PS chains entangled within it. This phase segregation is attributed to the immiscibility of the two polymers. However, the addition of SEBS-g-MAH improves the compatibility of the blends by enhancing interfacial interactions and promoting the diffusion of PS chains into the PLA matrix, thereby increasing the binding energy.

IV.3.1.2. Intermolecular interactions

The binding energies between PLA and PS in the blended systems are weak. However, with the addition of SEBS-g-MAH compatibilizer, the binding energies increase. This can be attributed to the influence of SEBS-g-MAH on the interfacial properties of the blends, enhancing the interactions between PLA and PS. Table IV.6 summarizes the non-bonded interaction energies ΔE (Kcal/mol) for the various molecular systems, indicating the changes in binding energies upon the addition of SEBS-g-MAH.

Table IV.6. Non-bonded interaction energies ΔE (Kcal/mol) for the different molecular systems

N° Sys	System	$\Delta E_{non\text{-}bond}$	$\Delta E_{H\text{-}bond}$	ΔE_{VdW}	$\Delta E_{electrostatic}$
1	PLA-PS	-6454,719	-2,203	184,093	-6636,609
2	PLA-PS(2,5)	-7633,596	-4,207	103,09	-7732,479
3	PLA-PS(5)	-8768,75	-2,202	341,119	-9107,667
4	PLA-PS(7,5)	-5992,566	-1,478	15,299	-6006,387
5	PLA-PS(10)	-5747,323	-5,893	82,883	-5824,313

The energies of non-bonded interactions ($E_{non\text{-}bond}$) in the PLA-PS blends were calculated using the DREIDING Force Field, which includes precise values for hydrogen bond energy and other energy components [16]. Enon-bond is determined by the sum of the hydrogen bond energy ($E_{H\text{-}bond}$), van der Waals energy (EVdW), and electrostatic energy ($E_{electrostatic}$) according to equation (2).

$$E_{non\text{-}bond} = E_{H\text{-}bond} + E_{VdW} + E_{electrostatic} \qquad (2)$$

In the case of PLA-PS blends, the dominant nature of the interaction is electrostatic, which is influenced by the chemical nature of PS. This supports the selection of SEBS-g-MAH as a compatibilizer due to its styrene segment, which enhances its chemical affinity with PS. Furthermore, maleic anhydride in SEBS-g-MAH enhances the interaction energies with PLA, resulting in strong interfacial interactions in the blend. These findings indicate that SEBS-g-MAH can be a compatibilizer for PLA/PS blends and other polymer blends with similar chemical structures.

IV.3.2. Density of state

Density of state (DOS) calculations were performed on PLA-PS-based complexes to examine the impact of SEBS-g-MAH on the properties of PLA/PS blends. Figure IV.9 illustrates the results obtained for PLA, PS, and their blends.

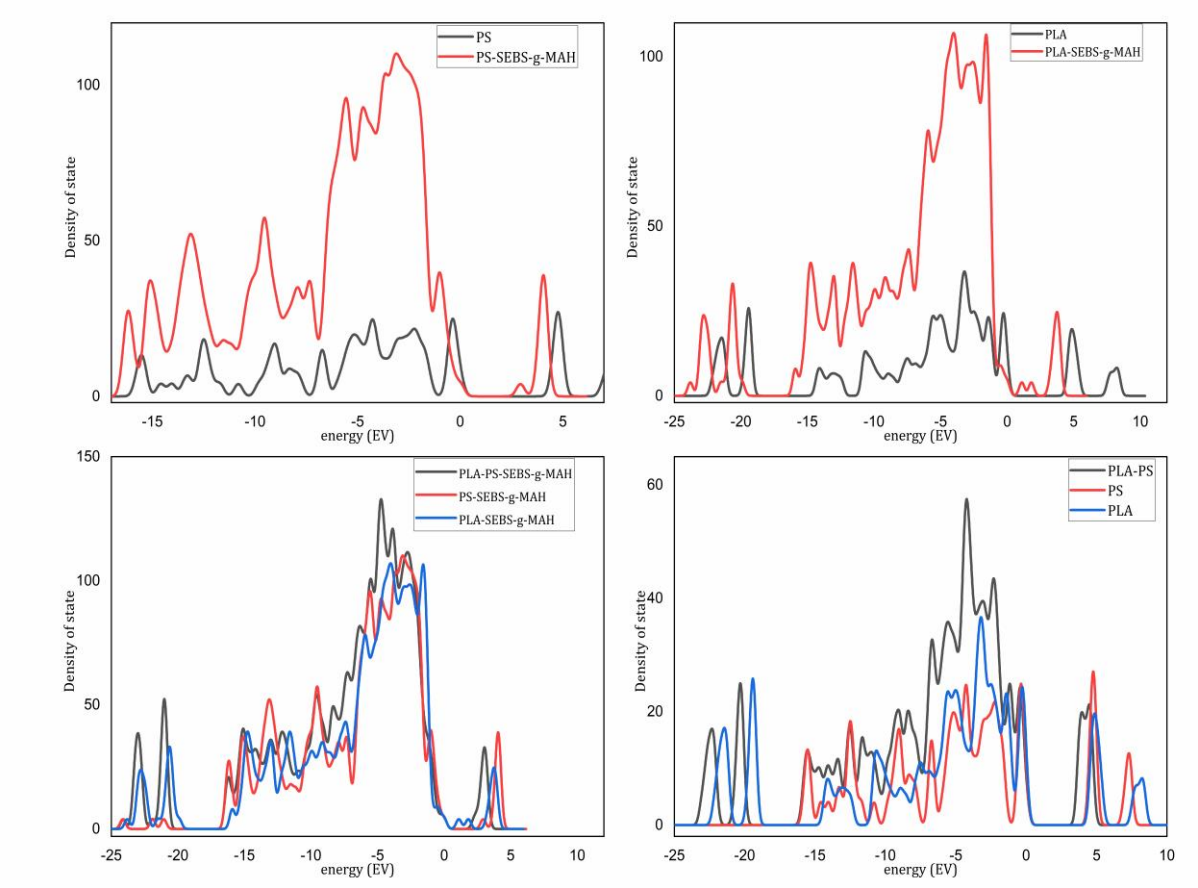

Figure IV.9. Density of state of PLA, PS, PLA-PS, and their Blends.

By comparing the density of state (DOS) plots of PLA, PS, and their mixtures, notable differences in the energy level positions and shapes can be observed. Figure IV.9 reveals that PLA exhibits the highest HOMO-LUMO deviation of 5.027 eV, indicating superior stability within the ternary mixture. On the other hand, PS demonstrates the lowest energy gap, suggesting a higher reactivity compared to the other molecules. The average energy gap of SEBS-g-MAH indicates that it acts as an intermediary component, enhancing the compatibility of the blend between PLA and PS.

When examining the DOS plots of PLA-PS-SEBS-g-MAH and PLA-PS, it is evident that the presence of the compatibilizer causes changes in the energy levels due to its charge. This alteration is attributed to the improved compatibility between PLA and PS at the interface. From a chemical standpoint, including styrene molecules in SEBS-g-MAH enhances the affinity with PS. At the same time, the presence of maleic anhydride increases the affinity with PLA in the PLA-SEBS-g-MAH system.

IV.3.3. COSMO-RS Study

In the Dmol3 quantum computation, methylene chloride was utilized as the solvent with a dielectric constant of 9.08. The COSMO calculation method was employed to determine the σ-profile values and examine the polarity of the polymers and their blends. The σ-profile values represent a distribution function that describes the relative surface area with σ-polarity for the molecule under investigation [2]. Figure IV.10 displays the COSMO surfaces for PLA, PS, and their blends, showcasing various colors to represent different regions of the molecules. The green regions indicate the non-polar "neutral" sections, the red regions represent the negatively charged "hydrogen accepting" areas, and the blue regions correspond to the positively charged "hydrogen donor" regions [2,17]. Furthermore, Figure IV.11 also depicts the σ-profile curves, which provide further insights into the distribution of σ-polarity within the molecules and their blends.

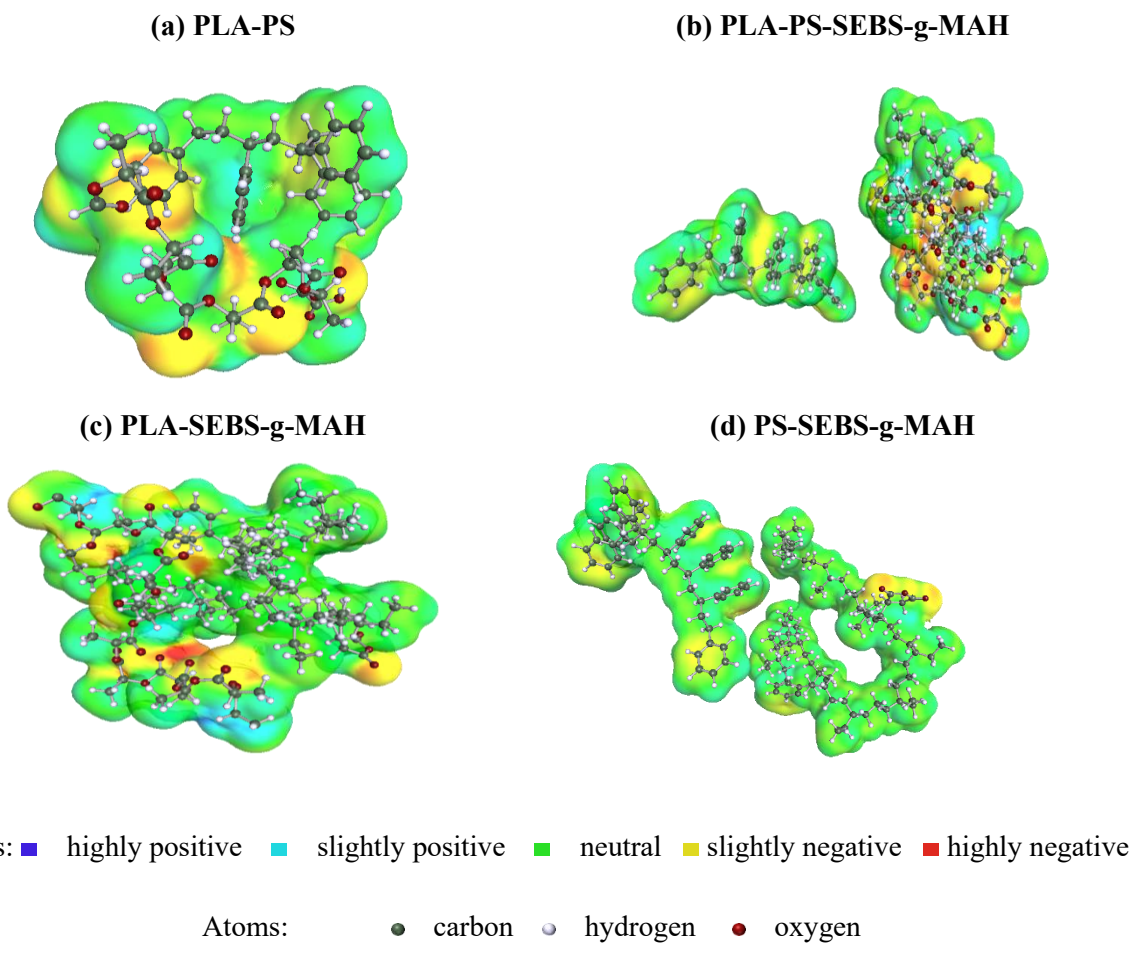

Figure IV.10 COSMO surfaces for (a) PLA-PS, (b) PLA-PS-SEBS-g-MAH, (c) PLA-SEBS-g-MAH, (d) PS-SEBS-g-MAH.

The sigma profile curves of PLA, PS, and their blend were divided into three zones: hydrogen bond donor (HBD), non-polar, and hydrogen bond acceptor (HBA). The width of the sigma profile curve is associated with charge delocalization and the formation of hydrogen bonds. A narrower profile indicates lower polarity, while a larger absolute value suggests a higher concentration of hydrogen bond donor (HBD) or hydrogen bond acceptor (HBA) groups in the chemical structure. By analyzing the sigma profile curves, we can gain insights into the polarity and hydrogen bonding characteristics of the molecules and their blend

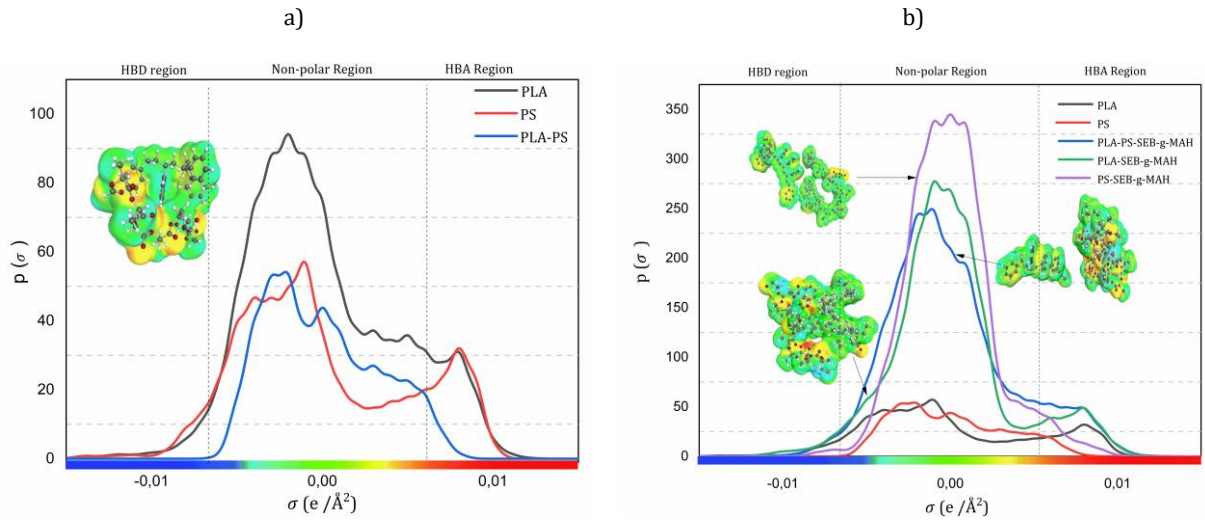

FigureIV.11 Sigma profiles for a) PLA-PS blends and b) PLA-PS-SEBS-g-MAH blends.

According to the COSMO results, the interfacial properties of the PLA/PS blend can be inferred. The preferential adsorption of SEBS-g-MAH at the interface between PLA and PS phases suggests a reduction in interfacial tension and improved compatibility. This is due to the lower solvation-free energy of SEBS-g-MAH at the interface compared to the bulk phases. In Figure IV.11(a), it can be observed that PLA exhibits a higher affinity for hydrogen bond donors (HBDs) and a lower affinity for hydrogen bond acceptors (HBAs), while PS shows the lowest affinity for both HBAs and HBDs but the highest affinity for the non-polar region. Figure IV.11(b) demonstrates that the presence of SEBS-g-MAH in the system enhances the affinity of PS towards HBAs. This indicates the role of SEBS-g-MAH as an intermediary, improving the compatibility between PLA and PS by facilitating interactions at the interface.

REFERENCES

[1] J. Xu, J. Zhang, W. Gao, H. Liang, H. Wang, and J. Li, "Preparation of chitosan/PLA blend micro/nanofibers by electrospinning," Mater. Lett., vol. 63, no. 8, pp. 658–660, 2009.

[2] A. Deghiche et al., "Effect of the stearic acid-modified TiO2 on PLA nanocomposites: Morphological and thermal properties at the microscopic scale," J. Environ. Chem. Eng., vol. 9, no. 6, pp. 106541, 2021.

[3] K. A. da S. Aquino, F. F. da Silva, and E. S. Araújo, "Investigation of poly(vinyl chloride)/polystyrene mixture miscibility: Comparison of viscometry criteria with Fourier transform infrared spectroscopy and refractive index measurements," J. Appl. Polym. Sci., vol. 119, no. 5, pp. 2770–2777, 2011.

[4] C. P. Wu, C. C. Wang, and C. Y. Chen, "Enhancing the PLA Crystallization Rate and Mechanical Properties by Melt Blending with Poly(styrene-butadiene-styrene) Copolymer," Polym. - Plast. Technol. Eng., vol. 54, no. 10, pp. 1043–1050, 2015.

[5] A. Mohamed, S. H. Gordon, and G. Biresaw, "Poly(lactic acid)/polystyrene bioblends characterized by thermogravimetric analysis, differential scanning calorimetry, and photoacoustic infrared spectroscopy," J. Appl. Polym. Sci., vol. 106, no. 3, pp. 1689–1696, 2007.

[6] R. Nehra, S. N. Maiti, and J. Jacob, "Analytical interpretations of static and dynamic mechanical properties of thermoplastic elastomer toughened PLA blends," J. Appl. Polym. Sci., vol. 135, no. 1, pp. 1–13, 2018.

[7] L. Qiu, W. Chen, and B. Qu, "Structural characterisation and thermal properties of exfoliated polystyrene/ZnAl layered double hydroxide nanocomposites prepared via solution intercalation," Polym. Degrad. Stab., vol. 87, no. 3, pp. 433–440, 2005.

[8] R. Avolio et al., "Plasticization of poly(lactic acid) through blending with oligomers of lactic acid: Effect of the physical aging on properties," Eur. Polym. J., vol. 66, pp. 533–542, 2015.

[9] J. C. C. Lima, E. A. G. Araújo, P. Agrawal, and T. J. A. Mélo, "PLA/SEBS Bioblends: Influence of SEBS Content and of Thermal Treatment on the Impact Strength and Morphology," Macromol. Symp., vol. 383, no. 1, pp. 1–6, 2019.

[10] G. Biresaw and C. J. Carriere, "Compatibility and mechanical properties of blends of polystyrene with biodegradable polyesters," Compos. Part A Appl. Sci. Manuf., vol. 35, no. 3, pp. 313–320, 2004.

[11] K. Hamad, M. Kaseem, F. Deri, and Y. G. Ko, "Mechanical properties and compatibility of polylactic acid/polystyrene polymer blend," Mater. Lett., vol. 164, pp. 409–412, 2016.

[12] T. Baouz, E. Acik, F. Rezgui, and U. Yilmazer, "Effects of mixing protocols on impact modified poly(lactic acid) layered silicate nanocomposites," J. Appl. Polym. Sci., vol. 132, no. 8, pp. 1–14, 2015.

[13] E. Tekay, "Preparation of tough, high modulus, and creep-resistant PS/SIS/halloysite blend nanocomposites," J. Thermoplast. Compos. Mater., vol. 33, no. 8, pp. 1125–1144, 2020.

[14] X. Liao, H. Zhang, Y. Wang, L. Wu, and G. Li, "Unique interfacial and confined porous morphology of PLA/PS blends in supercritical carbon dioxide," RSC Adv., vol. 4, no. 85, pp. 45109–45117,2014.

[15] J. Parameswaranpillai et al., "Toughened PS/LDPE/SEBS/xGnP ternary composites: morphology, mechanical and viscoelastic properties," Int. J. Light. Mater. Manuf., vol. 2, no. 1, pp. 64–71, 2019.

[16] L. Otmani, R. Doufnoune, Y. Benguerba, and A. Erto, "Experimental and theoretical investigation of the interaction of sulfonated graphene oxide with polyvinylalcohol/poly (4-styrenesulfonic) complex," J. Mol. Liq., vol. 284, pp. 599–606, 2019.

[17] W. Bououden et al., "Surface adsorption of Crizotinib on carbon and boron nitride nanotubes as Anti-Cancer drug Carriers: COSMO-RS and DFT molecular insights," J. Mol. Liq., vol. 338, pp. 116666, 2021.

Chapter V. Effect of the SEBS-g-MAH on (PLA/LDPE) biolends: Morphological and thermal properties at the microscopic scale

Chapter V. Effect of the SEBS-g-MAH on (PLA/LDPE) biolends: Morphological and thermal properties at the microscopic scale

V.1. Introduction

In this study, SEBS-g-MAH was chosen as a compatibilizing agent between PLA and LDPE due to the high reactivity of maleic anhydrides with PLA and the chemical affinity between LDPE and the copolymer SEBS during the melt blending process. Following this, samples were then obtained using a compression moulding machine. Compatibility and the microscopic behavior involving various proportions of the two components were subsequently investigated using the results from molecular dynamics simulations and experimental experiments.

V.2. Experimental characterization

V.2.1 Differential calorimetric analysis (DSC)

Modifying the crystallinity behavior of PLA/LDPE blends can improve their properties and expand their applications [1]. The DSC thermograms for the crystallization behavior of each sample, pure PLA, pure LDPE, and PLA/LDPE blend with and without SEBS-g-MAH are shown in Figure V.1 (a). The DSC curve of pure PLA (S1) as coded Table III-2 showed no signs of crystallization peaks because it does not crystallize easily during cooling [2]. On the other hand, The LDPE (S2), and the blend PLA/LDPE(S3) show a noticeable crystallization peak around 100 °C, which characterizes the crystallization of LDPE. After adding SEBS-g-MAH at different contents in the blend (S4-S7), the LDPE crystallization peak decreased slightly, suggesting that the SEBS-g-MAH ratio in the blends has little effect on the crystallization temperature.

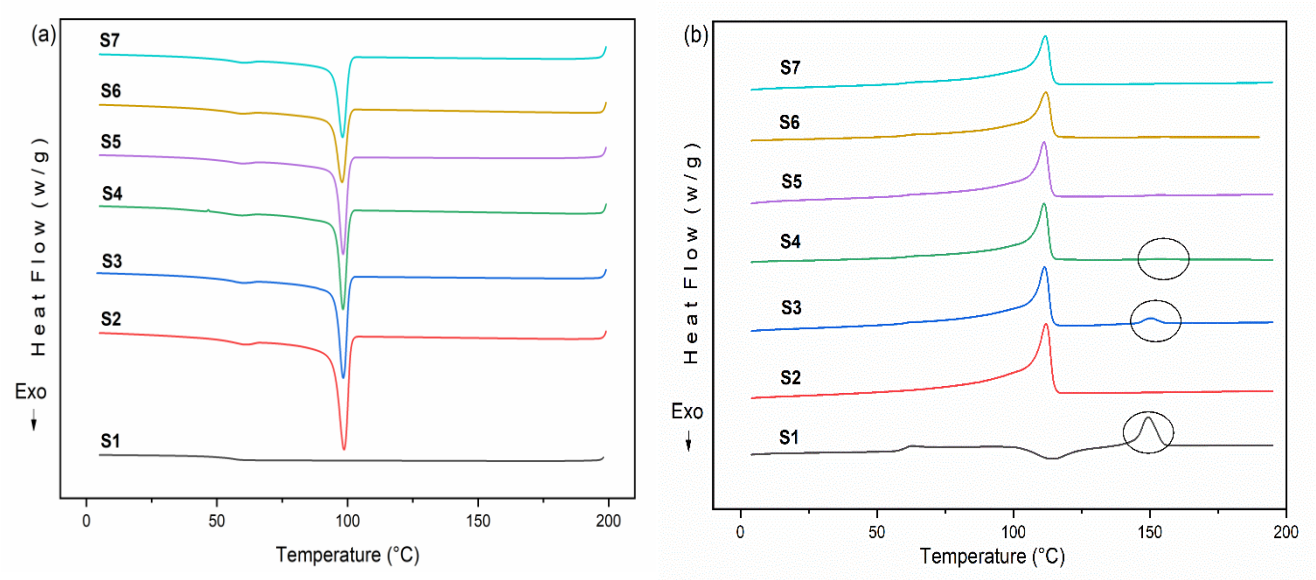

Figure V.1. DSC curves of pure PLA, pure LDPE, and PLA/LDPE blends at cooling (a) and heating (b) rate of 10 °C/min.

Figure V.1 (b) shows the second heating DSC curves, illustrating the samples' melting behavior. Table V.1 lists the numerical values of the characteristic temperatures and enthalpies obtained from the cooling and second heating scans and the (*Xc*)of the PLA and LDPE phases in the PLA/LDPE blends. The DSC curve of pure PLA shows a clear cold crystallization peak around 115 °C. This is due to the low PLA crystallization rate. With the addition of SEBS-g-MAH to the PLA/LDPE (20/80) blend, the cold crystallization peak of PLA disappeared in both PLA/LDPE blends with and without the compatibilizing agent. This phenomenon may be due to two reasons: first, the minimal percentage of PLA in the blend, and second, the LDPE melting process takes place at a temperature that overlaps with PLA's cold crystallization temperature (Tcc). This contrasts the DSC curves of pure PLA, as indicated in Table V.1.

Table V.1. Thermal properties of pure PLA, pure LDPE, and PLA/LDPE blends.

Samples	*Tc(LDPE) (°C)*	*Tm(LDPE) (°C)*	*Tcc(PLA) (°C)*	*Tm(PLA) (°C)*	*ΔHm(LDPE) (J/g)*	*ΔHcc(PLA) (J/g)*	*ΔHm(PLA) ((J/g)*	*Xc(LDPE) (%)*	*Xc(PLA) (%)*
S1	-	-	115	149	-	23.3	24.2	-	1.00
S2	99	112	-	-	110.2	-	-	37.6	-
S3	98	111	-	151	89.9	-	3.7	38.3	-
S4	97	113	-	154	70.9	-	0.6	31.0	-
S5	98	111	-	-	72.9	-	-	32.7	-
S6	98	112	-	-	63.6	-	-	29.3	-
S7	98	111	-	-	66.6	-	-	32.2	-

Pure PLA's melting peak (Tm) appears to be around 115 °C. The decrease of PLA Tm peak In the PLA / LDPE blend (20/80) is due to their low content. After adding SEBS-g-MAH, the characterized PLA Tm peaks completely disappeared in formulations (S4-S7). The SEBS-g-MAH mainly contributes to these results by improving the compatibility between PLA and LDPE blends. It possibly produces smaller droplet sizes, which hinder PLA crystallization[3].

V.2.2 Thermogravimetric analysis (TGA)

The results of the TGA analysis of neat homopolymers and the different compatibilized and un-compatibilized blends are illustrated in Figure V. 2. Table V.2 summarises the most relevant degradation temperatures. T_{onset} is the temperature at which 5% of the mass is lost; T_f is the temperature at which degradation stops due to a loss of 95% of the mass; and T_{dmax} is the temperature at which mass loss is at its maximum. TGA curves for pure PLA and LDPE showed single breakdown phases with T_{dmax} values of 366 °C and 480 °C, respectively. PLA starts to degrade degradation around T_{onset} =366 °C and ends around T_f =378 °C. While LDPE has excellent thermal stability, it degrades around T_{onset} =432 °C and ends around T_f =490 °C. LDPE is thermally more stable than PLA, as shown in Figure V.2 and Table V.2 because it degrades at higher temperatures[4].

The decomposition temperatures of the PLA/LDPE mixtures (20/80) range between those of LDPE and PLA, exhibiting an intermediate behavior between them (Figure V.2). LDPE decomposes at a higher temperature than PLA. The thermograms of the LDPE/PLA binary blend reveal a two-state decomposition process that may be attributed to PLA and LPDE degradation processes, respectively. Two prominent peaks appear at 367 and 472 °C [5].

Table V.2. Thermogravimetric Analysis Data.

Samples	T_{onset}(°C)	T_{dmax1} (°C)	T_{dmax2} (°C)	T_f (°C)
S1	336	366	-	378
S2	432	-	480	490
S3	349	367	472	490
S4	350	367	477	490
S5	349	366	474	488
S6	348	367	477	489
S7	351	365	477	489

When SEBS-g-MAH was added to the PLA/LDPE (20/80) blend, two decomposition stages were also observed Figure V.2, although they only slightly altered T_f compared to PLA/LDPE (20/80) blend. The potential existence of ethylene molecules in SEBS-g-MAH may enhance the affinity of LDPE. Similarly, in the case of PLA, the increase in affinity of PLA-SEBS-g-MAH might be attributed to maleic anhydride.

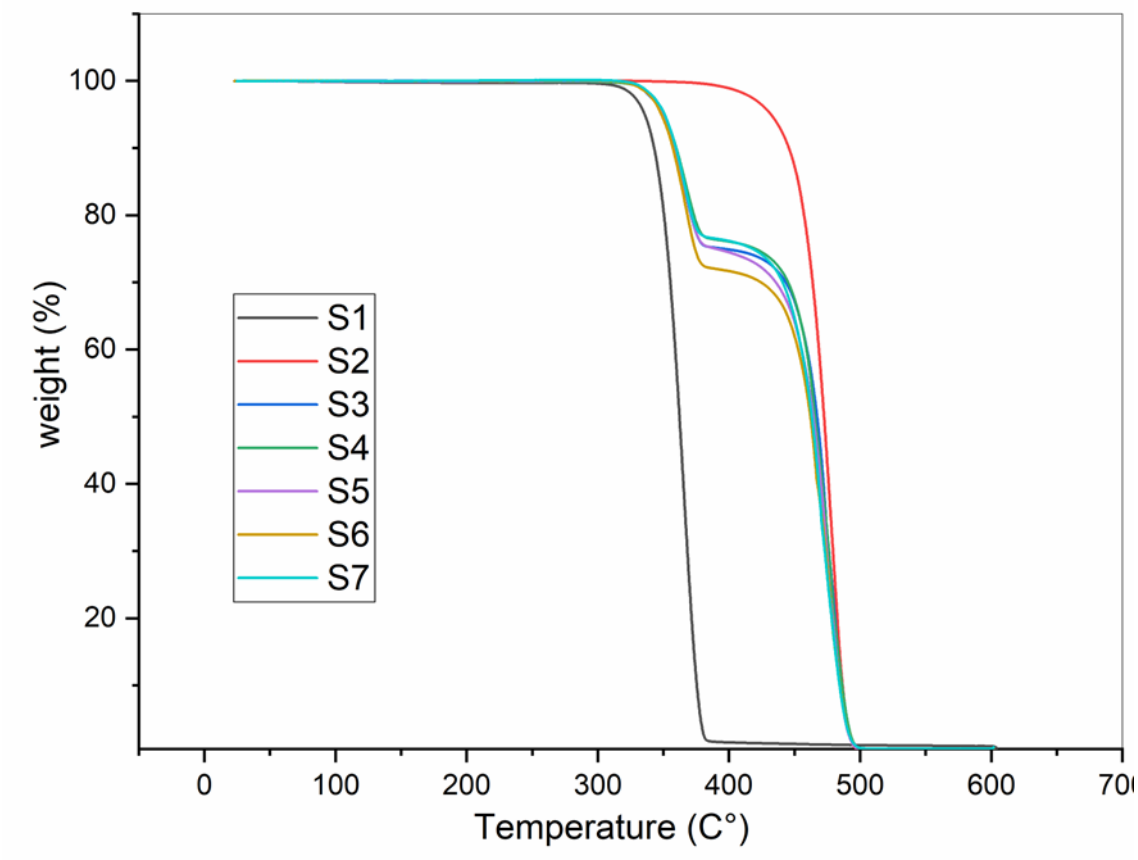

Figure V.2. TGA curves of PLA, LDPE, and their blends.

V.2.3 X-ray diffraction (XRD)

Figure V.3 shows the X-ray diffraction (XRD) spectra of pure PLA, LDPE, and LDPE/PLA blends with and without SEBS-g-MAH. The PLA (S1) has a fully amorphous structure, as shown by a broad double peak ranging from 5° to 40°, indicating the presence of amorphous regions. These peaks' positions align with the results reported in the published literature [6,7]. The diffraction scanning calorimetry thermogram exhibited a minor Xc value of around 1%. However, X-ray diffraction analysis revealed no discernible crystal structure. The diffraction pattern of pure LDPE polymer (S2) has a distinct peak at $2\theta = 21.34$, while another peak is observed at $2\theta = 23.72$, which may be attributed to the (110) and (200) crystallographic planes, respectively [4,8].

The crystallinity of the LDPE obtained by DSC analysis was 37.61%. The results are consistent with the previously established view that the LDPE crystallinity region is 30-50% [9].

In the case of the PLA/LDPE blend with and without compatibilizer (S3:S7), the broad halo indicating the amorphous phase of PLA disappeared due to the LDPE crystalline peak and the small amount of PLA used. The same peak position appeared in all blend formulations about the LDPE crystalline peak, meaning no new crystalline forms were formed. Furthermore, compared to the compatibilizer content, the crystalline phases decreased with increasing SEBS-g-MAH content, which improves the compatibility between PLA and LDPE, confirming the calculation result as previously indicated. The affinity between LDPE and the compatibilizer is located in the olefin part of the SEBS-g-MA compatibilizer due to the presence of the PE chain in the SEBS structure, and for PLA it is located between C=O in the PLA group and maleic anhydride in SEBS-g-MAH.

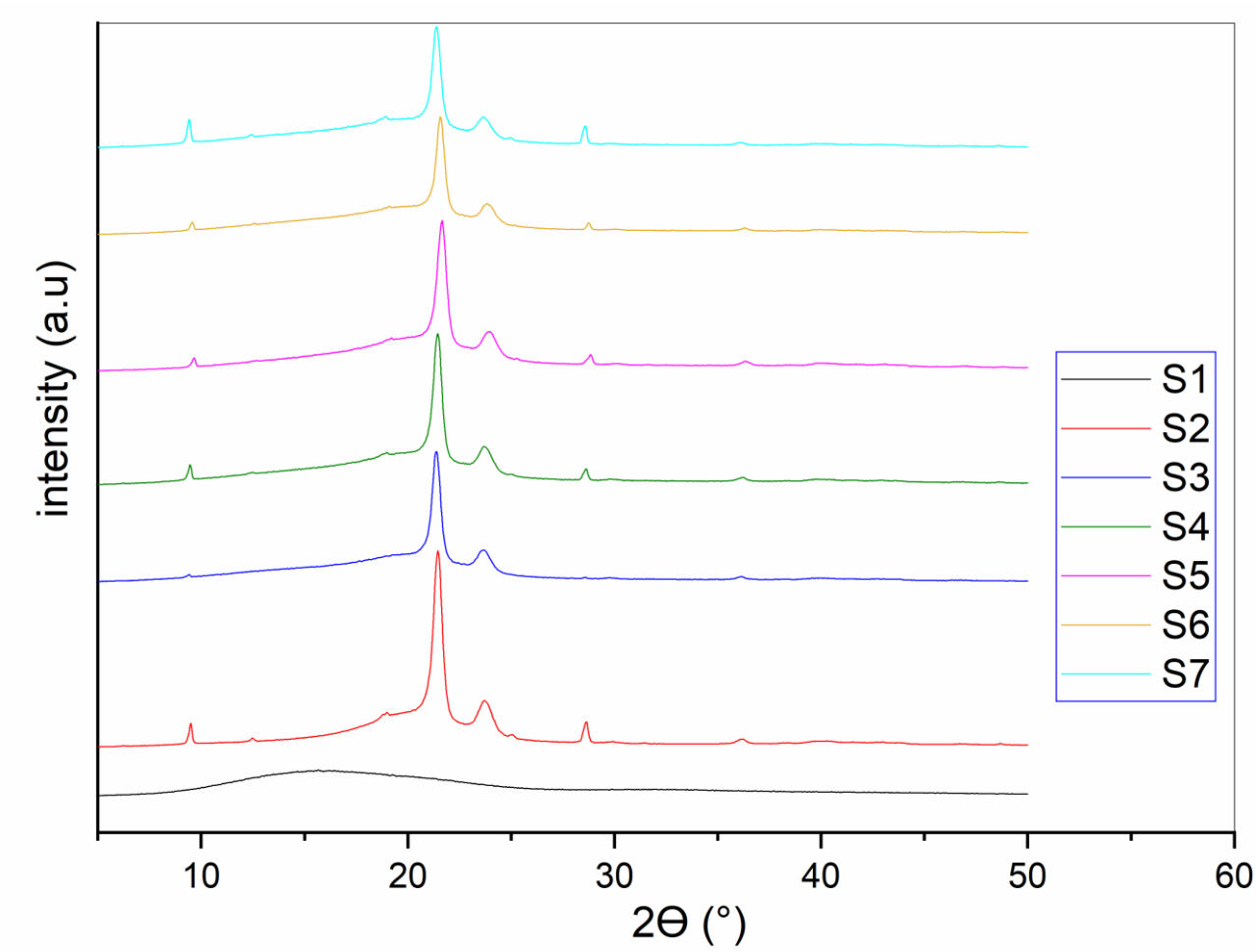

Figure V.3. XRD curves of PLA, LDPE, and their blends.

V.2.4 Scanning electron microscopy (SEM) analysis

The study of the morphology of polymer blends is of great importance for determining the relationship between structure and property. The morphology of the pure PLA, pure LDPE compatibilized and un-compatibilized blends was analyzed by scanning electron microscopy (SEM) as shown in Figure V.4. The fracture surfaces of pure PLA illustrated in Figure V.4(a) show brittle fracture surfaces characterized by little plastic deformation, showing a limited number of elongated threads of distorted PLA material. These findings align with previous research[10]. Furthermore, there was a deficiency in extensive plastic deformation [11].

In contrast, the image of pure LDPE shown in Figure V.4(b) has the characteristics of a material that has undergone plastic deformation. Polymer materials undergo plastic deformation when cracked or sheared.The fracture surface of cracking is often more brittle than the fracture surface for shear since it shows less observable plastic deformation [11].

Heterogeneous structures were expected from the studied blends, with particles of PLA dispersed in each matrix. The size of these particles indicates interactions between the blend partners, where larger particles are present when interactions are weak, and smaller sizes will result when good interactions are present[12]. The blend of PLA/LDPE Figure V.4(C) did not present homogeneous interfaces. Spherical and ellipsoidal dispersed phases were observed. The appearance of various voids shows the incompatible nature of PLA and LDPE [13].

It can be seen that large particles are formed in the case of blends without SEBS-g-MAH. On the contrary, PLA/LDPE blends with different ratios of SEBS-g-MAH Figure V.4(d, e, f, g) show relatively small PLA particles dispersed in LDPE matrices, confirming improved interactions of these material combinations.

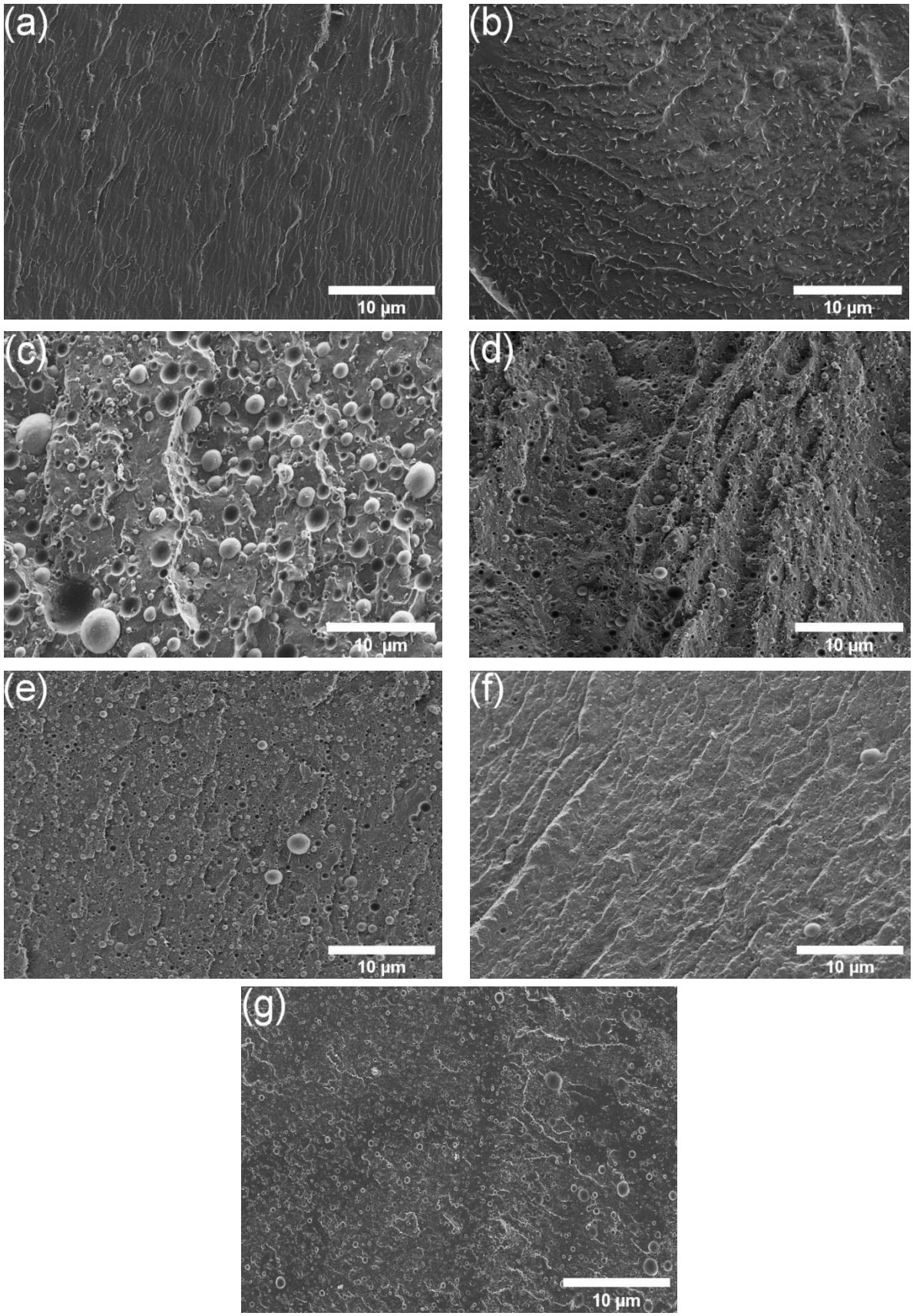

Figure V.4. SEM micrographs of (a) PLA, (b) LDPE, (c) PLA/LDPE, and (d)PLA/LDPE/SEBS-g-MAH 2.5%, (e) PLA/LDPE/SEBS-g-MAH 5%, (f) PLA/LDPE/SEBS-g MAH 7.5%, (g)PLA/LDPE/SEBS-g-MAH 10%.

V.3. Computational results

V.3.1. Molecular dynamic results

MD simulations explored the binding energy and the interaction mechanisms within the nanocomposites. Figure V.5 shows the structures obtained after equilibration and density stabilization. All the structures are composed of 15 LDPE chains and 3 PLA chains to keep the PLA/LDPE (20/80) formulation, varying the number of SEBS-g-MAH chains according to the 2.5, 5, 7.5 10 formulation and by 1, 2 3 4 chains, respectively.

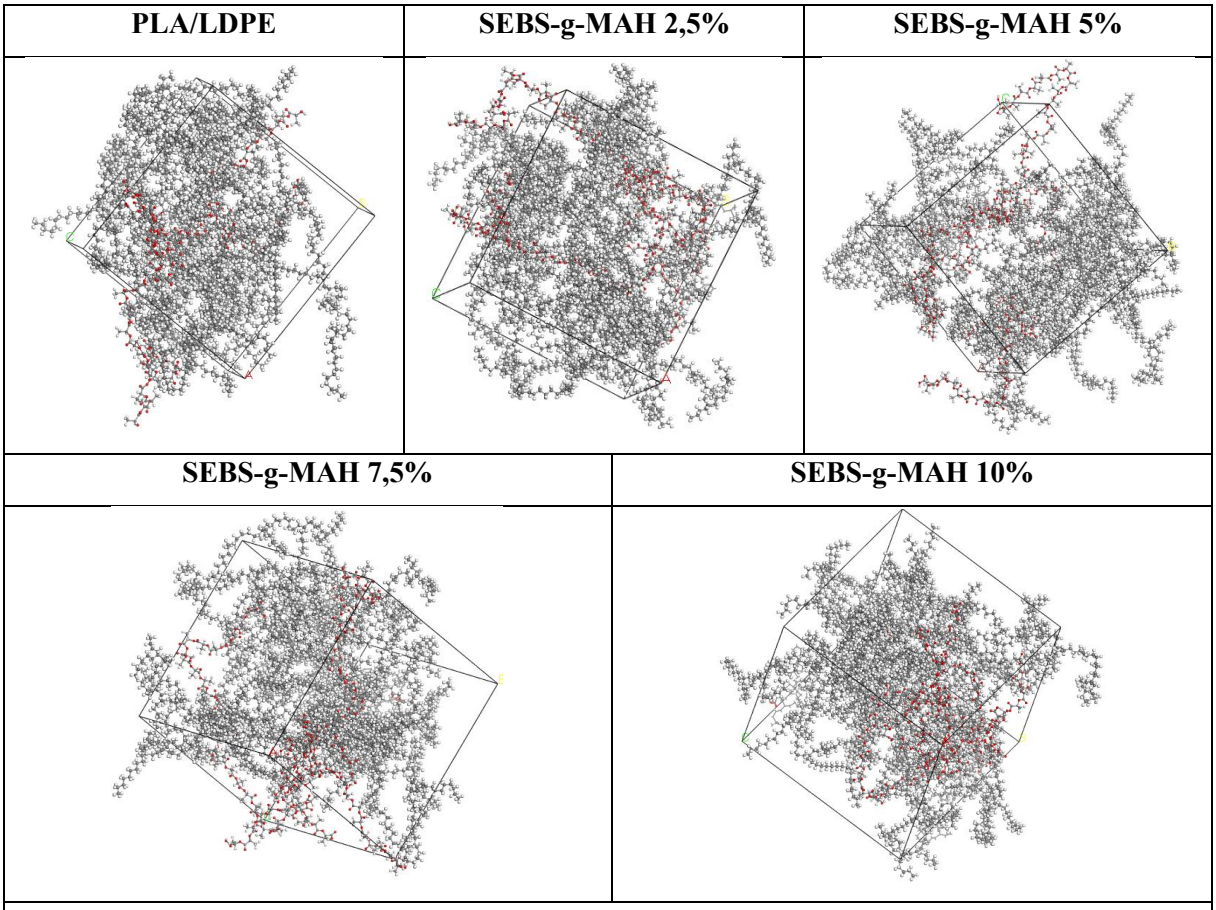

Figure V.5. Structures for PLA/LDPE and PLA/LDPE with 2.5, 5, 7.5 and 10 SEBS-g-MAH w%.

V.3.1.1Binding energy

The mechanism of the interactions can be better understood by calculating and comparing the binding energies between the different structures. LDPE/PLA interaction model binding energies with and without compatibilizer agents can be calculated using Equation 1.

$$E_{bind} = -E_{inter} = -E_{Total} - (E_{PLA} + E_{LDPE} + E_{SEBS\text{-}g\text{-}MAH}) \quad (1)$$

Where E_{Total} is the total potential energy of the system studied, E1, and E2 are the energies of the blends studied. The binding energies of different blends are given in TableV.3

Table V.3. Binding interaction energies (kcal/mol).

N° Sys	System	E(Total)	E(PLA)	E(SEBS-g-MAH)	ELDPE	E(bind)	E(Inter)
1	**LDPE/PLA**	-5392,25	1631,98	-	-5395,98	1628,25	-1628,25
2	**2,5%**	-6318,28	1001,62	-33,84	-5626,79	1659,27	-1659,27
3	**5%**	-8243,46	1688,22	-311,53	-6569,82	3050,33	-3050,33
4	**7,5%**	-10851,69	3298,86	-64,03	-2781.91	14086,52	-14086,52
5	**10%**	-9029,51	864,62	-670,6	-6564,55	2658,98	-2658,98

The binding energy of the blend complexes increases substantially with the addition of compatibilizer agent SEBS-g-MAH, reaching the highest value in the case of the fourth system containing 7.5 % of SEBS-g-MAH (E_{bind} = 14086,52 kcal/mol), compared with the lowest value of the system LDPE/PLA (1628,25 kcal/mol).

On the other hand, the presence of maleic anhydride in the system increases the compatibility between the polymers, but comparing systems 3, 4 and 5 when varying the number of SEBS-g-MAH chains, with E_{bind} of 3050.33, 1408652 and 2658.98 kcal/mol, respectively. We obtain an optimum value for the system with 3 SEBS-g-MAH chains, after which we have a shift in E_{bind} for the fifth system, which contains 4 chains of the compatibilizer agent, compared with the third system, which contains 2 chains. This means that increasing SEBS-g-MAH by more than 3 chains in the system affects the E_{bind} negatively and does not favor their interaction.

V.3.1.2 Intermolecular interactions

The binding energy results indicate that the polymers in the blending systems interact with the SEBS-g-MAH phase via the Van der Waals bond, which can be formed between the hydroxy groups of the grafted maleic anhydride and the functional group of the PLA, and via electrostatic bonds, which dominate between the ethylene chains in SEBS-g-MAH and LDPE. The results of the interaction energy of all the components are presented in Table V.4.

Table V.4. Non-bonded interaction energies ΔE (kcal/mol)

System	$\Delta E_{H\text{-}bond}$	ΔE_{VdW}	$\Delta E_{electrostatic}$	$\Delta E_{non\text{-}bond}$
0%	-0,134	-453,55	-1054,63	-1508,314
2,50%	-0,143	-724,54	-1773,34	-2498,023
5%	-0,089	-864,66	-2522,66	-3387,409
7,50%	-0,005	-812,375	-3225,039	-4037,419
10%	-0,199	-726,081	-2170,68	-2896,96

The energies $\Delta E_{H\text{-}bond}$, ΔE_{VdW}, $\Delta E_{electrostatic}$ and $\Delta E_{non\text{-}bond}$ represent the contributions from hydrogen bonding, van der Waals forces, electrostatic forces, and the total non-bonding interaction energy respectively. It has been calculated by the DREIDING force field, which represents the exact value of the energy of the hydrogen bond for all systems[14].

$$\Delta E_{non\text{-}bond} = \Delta E_{H\text{-}bond} + \Delta E_{VdW} + \Delta E_{electrostatic} \quad (2)$$

For the LDPE/PLA blend, the chemical affinity between the blend components is very weak. The E_{VdW} bond of the LDPE/PLA system equals -453,55 kcal/mol. The strongest interaction in this system is electrostatic, the energy of this interaction being $\Delta E_{electrostatic}$ = -3225,039kcal/mol of the fourth system. Adding SEBS-g-MAH to the blend increases the Van der Waals bonding energy from -453,55 to -864,66 kcal/mol for the LDPE/PLA and 7.5% SEBS-g-MAH content systems, respectively.

The hydrophobic behavior of LDPE, due to its saturated chemical nature, and the hydrophilic behavior of PLA, due to its functions existing in its structure, make them incompatible. Consequently, the hydrophobic and hydrophilic behavior of SEBS-g-MAH favors its intermediary role between PLA due to the presence of MAH and LDPE due to the presence of ethylene chains in the part of SEBS.

V.3.2 Density of state

Density of state (DOS) calculations were done on blends of PLA/LDPE, with and without SEBS-g-MA, PLA and LDPE, to determine how the compatibilizer will affect the final blend's properties. Figure V.6 displays the findings for the complexes of LDPE/PLA, PLA and LDPE.

With matching HOMO-LUMO energy gaps of 3.79, 3.93 and 7.01 eV, respectively, LDPE is anticipated to be insulators duo to their organic saturated structure. In contrast, PLA/LDPE-

SEBS-g-MA is gap values are 3.23 eV compared to PLA /LDPE with 3.79 eV. The decrease in gap energy in the presence of the compatibilizer is due to the presence of the phenyl group in the SEBS-g-MA structure. This impact validates the chemical composition of SEBS-g-MA concerning each PLA component. In the overall MDS picture, it is evident that the affinity between the LDPE and compatibilizer agent is located in the olefin part of the SEBS-g-MA compatibilizer due to the presence of the PE chain in the SEBS structure, which enhances the interaction, mainly of an electrostatic type, that favours the dispersion of the MDS cells. Maleic anhydride interacts more with the oxidation group of PLA , confirming also that the presence of MAH is responsible for the compatibilization.

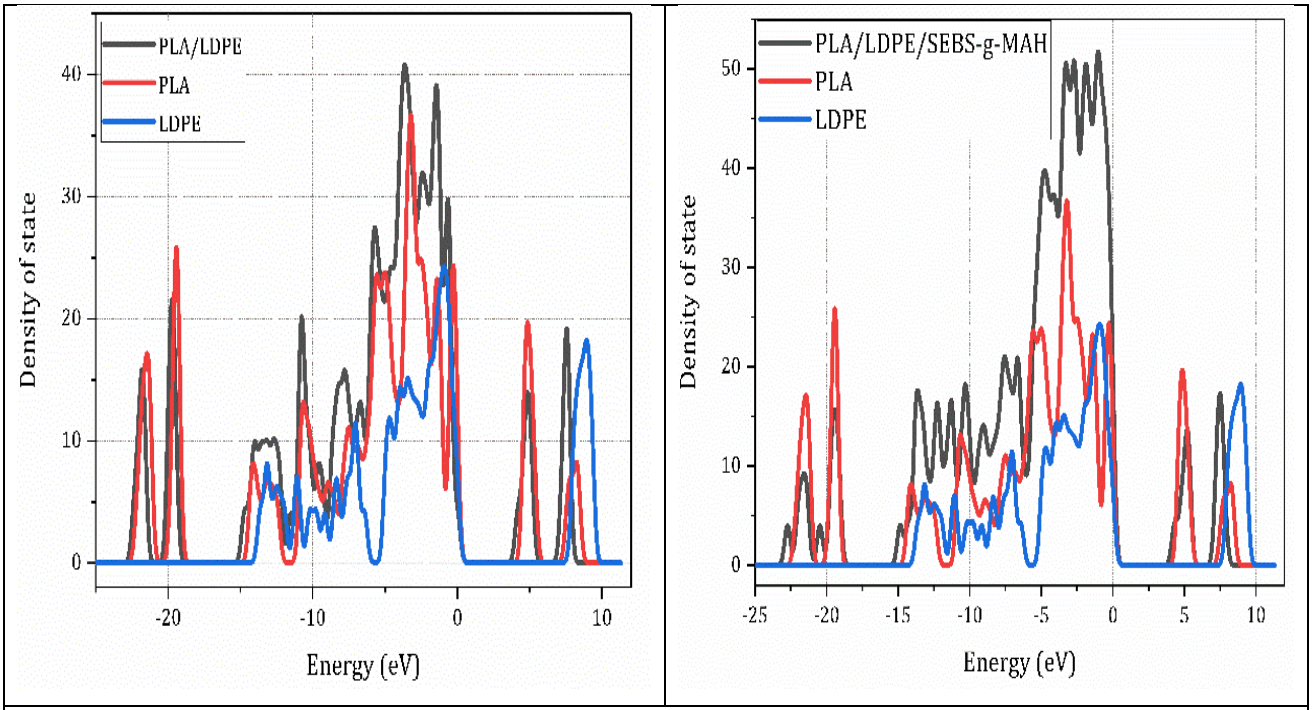

Figure V.6. DOS of PLA, LDPE and PLA/LDPE, with and without SEBS-g-MAH.

V.3.3. COSMO-RS study

Dimethyl chloride was used as the solvent in a Dmol3 quantum computation. The COSMO calculation option to build COSMO files is required to acquire σ-profile values to investigate the polarity of the blend with and without compatibilizer combination. The σ-profile values were described as a distribution function for the molecule under investigation that provides the relative surface area with polarity σ[15]. The COSMO surfaces for LDPE, PLA,

PLA/LDPE with and without SEBS-g-MAH are shown in Figure V.7, and the σ-profile curves are shown in Figure V.8.

Various colors represent the different regions of the molecules. The green portions represent the non-polar"neutral"sections, the red parts represent the molecule's negatively charged "hydrogen accepting"areas, while the blue segments indicate the positively charged "hydrogen donor" [16].

LDPE, PLA, and PLA/LDPE with and without SEBS-g-MAH sigma profile curves were split into three zones: HBD (hydrogen bond donors), non-polar, and HBA (hydrogen bond acceptors). Because charge delocalization is connected to hydrogen bond production, a narrow -profile implies less polarity. A greater absolute number suggests that the chemical is highly HBD or HBA.

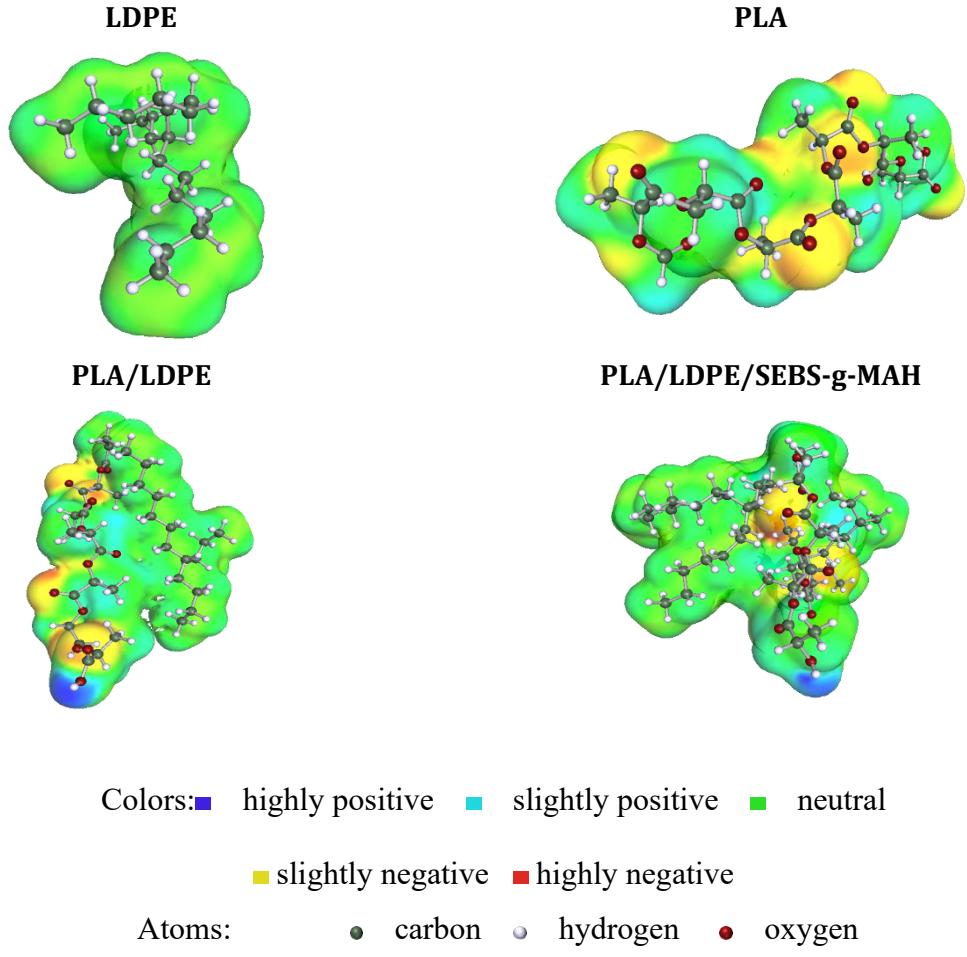

Figure V.7. COSMO surfaces of PLA, LDPE, PLA/LDPE and PLA/LDPE/SEBS-g-MAH.

PLA is represented by positive peaks in the sigma profiles in the range [0.0075, 0.025] e.Å-2t. The broad peaks imply that Oxygen atoms have a high electronegativity, which attracts a Hydrogen atom into the HBA domain. Meanwhile, LDPE is represented by non-polar peaks in the range [-0.0075, 0.0075].

The HBD domain corresponds to negative peaks in the range [-0.025, -0.008] e.Å-2. Their magnitude highlights the electropositivity of hydrogen atoms. Non-polar peaks between [-0.0075 and +0.0075 e.Å-2] reflect uncharged groups such as CH2 and CH3, predominantly present in the LDPE molecule and SEBS.

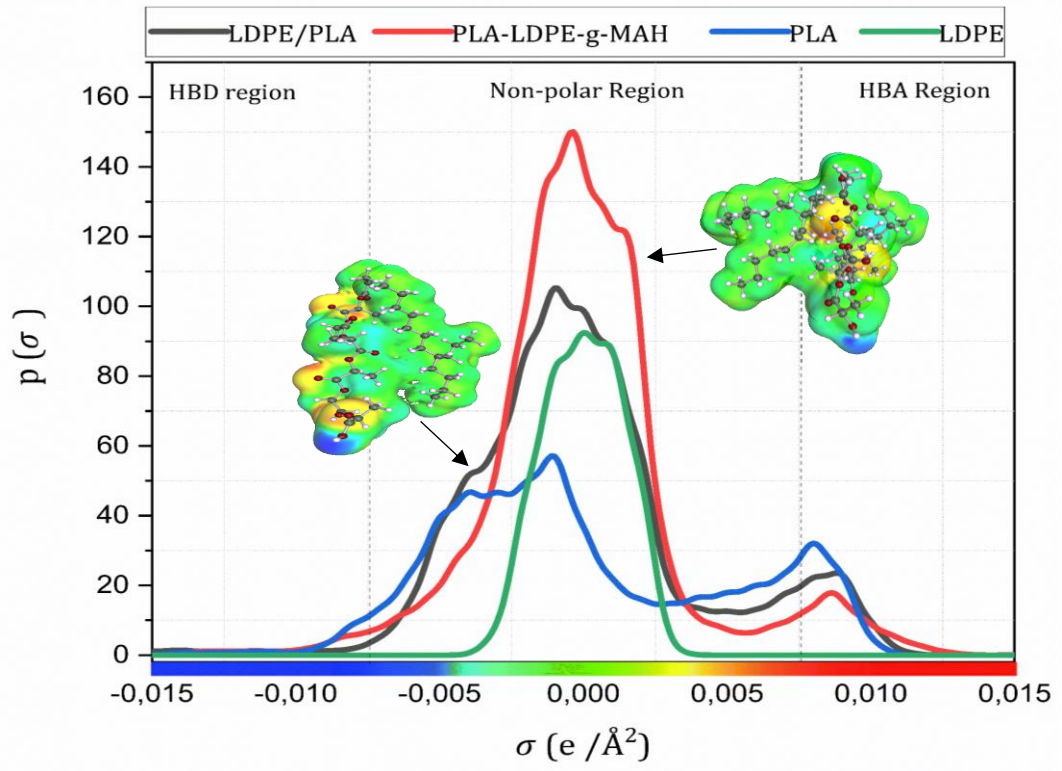

Figure V.8. Sigma profiles curves for LDPE, PLA, LDPE/PLA with and without SEBS-g-MAH

The comparison between LDPE/PLA and LDPE/PLA-SEBS-g-MAH shows that the compatibilizer's presence decreases PLA's electronegativity by reducing the peak in the HBA domain and increasing their non-polarity. This explains the MDS results that the majority of the bonds in the mixture are electrostatic as MAH reacts with the unsaturated PLA ester group and the SEBS ethylene groups interact with LDPE, which explains the decrease in the electronegativity of the LADPE/PLA mixture and the increase in its non-polarity. This Finding explains why SEBS-g-MAH was chosen as the intermediate between LDPE and PLA.

REFERENCES

[1] K. Hamad, M. Kaseem, and F. Deri, "Poly(lactic acid)/low density polyethylene polymer blends: preparation and characterization," Asia-Pacific J. Chem. Eng., vol. 7, no. pp.310-316. 2012.

[2] L. As'habi, S. H. Jafari, H. A. Khonakdar, L. Häussler, U. Wagenknecht, and G. Heinrich, "Non-isothermal crystallization behavior of PLA/LLDPE/nanoclay hybrid: Synergistic role of LLDPE and clay," Thermochim. Acta, vol. 565, pp. 102–113, 2013.

[3] L. Sangroniz et al., "Fractionated crystallization in semicrystalline polymers," Prog. Polym. Sci., vol. 115, pp. 101376, 2021.

[4] M. S. Khan, P. P. Dhavan, D. Ratna, S. S. Sonawane, and N. G. Shimpi, "LDPE:PLA and LDPE:PLA:OMMT polymer composites: Preparation, characterization, and its biodegradation using Bacillus species isolated from dumping yard," Polym. Adv. Technol., vol. 32, no. 9, pp. 3724–3739, 2021.

[5] S. Mooninta, S. Poompradub, and P. Prasassarakich, "Packaging Film of PP/LDPE/PLA/Clay Composite: Physical, Barrier and Degradable Properties," J. Polym. Environ., vol. 28, no. 12, pp. 3116–3128, 2020.

[6] M. Maiza, M. T. Benaniba, G. Quintard, and V. Massardier-Nageotte, "Biobased additive plasticizing Polylactic acid (PLA)," Polimeros, vol. 25, no. 6, pp. 581–590, 2015.

[7] N. Khitas, K. Aouachria, and M. T. Benaniba, "Blending and plasticising effects on the behaviour of poly(lactic acid)/poly(ϵ -caprolactone)," Polym. Polym. Compos., vol. 26, no. 5–6, pp. 337–345, 2018.

[8] K. Urman, T. Schweizer, and J. U. Otaigbe, "Uniaxial elongational flow effects and morphology development in LDPE/ phosphate glass hybrids," Rheol. Acta, vol. 46, no. 7, pp. 989–1001, 2007.

[9] Z. Yuan and X.-R. Xu, "Surface characteristics and biotoxicity of airborne microplastics," 2023, pp. 117–164.

[10] Z. Kulinski, E. Piorkowska, K. Gadzinowska, and M. Stasiak, "Plasticization of Poly (L -lactide) with Poly (propylene glycol)," pp. 2128–2135, 2006.

[11] D. Vrsaljko, D. Macut, and V. Kovačević, "Potential role of nanofillers as compatibilizers in immiscible PLA/LDPE Blends," J. Appl. Polym. Sci., vol. 132, no. 6, 2015.

[12] B. M. Lekube and C. Burgstaller, "Study of mechanical and rheological properties, morphology, and miscibility in polylactid acid blends with thermoplastic polymers," J. Appl. Polym. Sci., vol. 139, no. 8, pp. 1–10, 2022.

[13] B. Boubekeur, N. Belhaneche-Bensemra, and V. Massardier, "Valorization of waste jute fibers in developing low-density polyethylene /poly lactic acid bio-based composites," J. Reinf. Plast. Compos., vol. 34, no. 8, pp. 649–661, 2015.

[14] L. Otmani, R. Doufnoune, Y. Benguerba, and A. Erto, "Experimental and theoretical investigation of the interaction of sulfonated graphene oxide with polyvinylalcohol/poly (4-styrenesulfonic) complex," J. Mol. Liq., vol. 284, pp. 599–606, 2019.

[15] A. Zerriouh, A. Deghiche, W. Bououden, D. Cavallo, A. Erto, and N. Haddaoui, "A computational and experimental investigation of TEOS-treated graphene oxide-PVA interaction: molecular dynamics simulation and COSMO-RS insights," J. Mol. Liq., vol. 382, no. pp. 121914,2022.

[16] T. Aouissi et al., "Enhancing compatibility and properties of polylactic acid / polystyrene (PLA / PS) bioblend for sustainable food packaging : Experimental and quantum computational insights," Mater. Today Commun., vol. 37, pp. 107106, 2023.

General Conclusions & Perspectives

GENERAL CONCLUSION

The study of the thesis addressed in this dissertation is divided into two studies: the development of two different blends based on bio-sourced polymers (PLA/PS) and (PLA/LDPE) in the presence of a compatibilizer (SEBS-g-MAH) to improve interfacial adhesion.

The comprehensive investigation of PLA/PS blends, involving various analytical techniques, provided a thorough understanding of the influence of SEBS-g-MAH as a compatibilizing agent. Thermal analysis, including TGA and FTIR, highlighted the impact of n-π interactions on the crystallization process and thermal stability of PLA blends. DSC analysis confirmed a reduction in PLA crystallinity due to the addition of SEBS-g-MAH. Tensile testing demonstrated a decrease in hardness and Young's modulus, indicating enhanced flexibility and softening attributed to the presence of the compatibilizer.

SEM analysis revealed improved dispersion of the PS phase within the PLA matrix, especially notable at SEBS-g-MAH concentrations of 5 to 10% by weight, resulting in a single-phase behavior. MD simulations confirmed increased binding energy interaction, signifying improved compatibility, while COSMO-RS analysis supported SEBS-g-MAH's role as an intermediary between PLA and PS, enhancing their chemical compatibility. DOS and Blends investigations provided insights into molecular arrangement and structure, emphasizing the intermediate role of SEBS-g-MAH in enhancing PLA and PS compatibility.

Additional analyses in the (PLA/LDPE), blend including DSC and DRX, further confirmed a reduction in PLA crystallinity by adding SEBS-g-MAH. TGA results indicated that thermal stability was not significantly affected, and DRX demonstrated the reduction in crystalline phases, improving compatibility between PLA and LDPE. SEM observations highlighted the smaller particle size dispersion in the presence of SEBS-g-MAH compared with un-compatibilized LDPE/PLA blends.

Moreover, molecular dynamics simulations demonstrated a substantial increase in binding energy (Ebind) in systems containing 7.5% SEBS-g-MAH compared to LDPE/PLA. DFT results, including DOS and COSMO calculations, indicated an affinity between LDPE and the compatibilizer in the olefin part of SEBS-g-MAH. For PLA, affinity was identified between the ester group (C=O) and the O-H group in SEBS-g-MAH.

In conclusion, integrating these results establishes that SEBS-g-MAH is a powerful compatibilizing agent in PLA/PS and PLA/LDPE blends, enhancing thermal, mechanical, and interfacial properties. These results contribute significantly to developing biodegradable polymer blends with superior application performance.

PERSPECTIVES

Several research aspects need deep investigation for future research. In this regard, the following additional investigations could, therefore, be recommended:

Study the long-term durability of bio-based blends, considering the potential effects of exposure to external conditions, including UV light and humidity.

Extend mechanical tests to varied environmental conditions to evaluate the stability of mechanical properties in real-world situations.

Deepen studies on molecular interactions using more complex numerical simulations, such as multiscale modeling, to capture phenomena at different scales.

Investigate innovative applications for compatibilized blends, such as food packaging or biodegradable materials for electronic products.

Conduct life cycle analyses to assess the overall environmental impact of blends, from production to disposal.

Evaluate the economic viability of large-scale production of compatibilized blends, considering production costs, market demand, and long-term economic considerations.

Abstract

This work focuses on the study of the structural, thermal, rheological, morphological and mechanical properties of PLA/PS and PLA/LDPE polymers using a compatibilising agent, SEBS-g-MAH, in different proportions. The aim was to better understand the role of SEBS-g-MAH as a bonding agent between the two different blends. Theoretical calculation (simulation), in particular molecular modelling, was also used as an alternative to obtain results concerning structural and spectroscopic properties. Analysis, using X-ray difraction (XRD), differential scanning calorimetry (DSC) and scanning electron microscopy (SEM), confirmed a reduction in PLA crystallinity with the addition of SEBS-g-MAH in both types of blends. Theoretical calculations, in particular dynamic molecular MD, confirmed the increase in binding energy between PLA and PS and the role of SEBS-g-MAH in improving their compatibility. DFT results, including DOS and COSMO calculations, indicated an affinity between LDPE and the compatibiliser in the olefin part of SEBS-g-MAH. For PLA, an affinity was identified between the ester group (C=O) and the O-H group of SEBS-g-MAH.
Keywords: polylactic acid, blend, compatibiliser, simulation, molecular modelling

Résumé

Ce travail porte sur l'étude des propriétés structurelles, thermiques, rhéologiques, morphologiques et mécaniques des polymères PLA/PS et PLA/LDPE en utilisant un agent compatibilisant, le SEBS-g-MAH, dans différentes proportions. Afin de mieux comprendre le rôle du SEBS-g-MAH en tant qu'agent de liaison entre les deux différents mélanges. Le calcul théorique (simulation), en particulier la modélisation moléculaire, a également été utilisée comme alternative pour obtenir des résultats concernant les propriétés structurelles et spectroscopiques. L'analyse, réalisée à l'aide de la difraction des rayons X (XRD), de la calorimétrie différentielle à balayage (DSC) et de la microscopie électronique à balayage (SEM), a confirmé une réduction de la cristallinité du PLA par l'ajout de SEBS-g-MAH dans les deux types de mélanges. Les essais de traction ont montré une diminution de la dureté et du module de Young, indiquant une flexibilité et un assouplissement accrus attribués à la présence de l'agent de compatibilité.Le calcul théorique, en particulier dynamique moléculaire MD a confirmé l'augmentation de l'énergie de liaison entre le PLA et le PS et le rôle du SEBS-g-MAH dans l'amélioration de leur compatibilité. Les résultats DFT, y compris les calculs DOS et COSMO, ont indiqué une affinité entre le LDPE et le compatibilisant dans la partie oléfine du SEBS-g-MAH. Pour le PLA, une affinité a été identifiée entre le groupe ester (C=O) et le groupe O-H du SEBS-g-MAH.

Mots clés : acide polylactique, mélange, compatibilisant, simulation, modélisation moléculaire

ملخص

يركز هذا العمل على دراسة الخواص الهيكلية والحرارية والانسيابية والمورفولوجية والميكانيكية لبوليمرات PLA/PS وPLA/LDPE باستخدام عامل توافقي، SEBS-g-MAH، بنسب مختلفة. من أجل فهم أفضل لدور SEBS-g-MAH كعامل ربط بين الخليطين المختلفين. كما تم استخدام الحساب النظري (المحاكاة)، وخاصة النمذجة الجزيئية، كبديل للحصول على نتائج فيما يتعلق بالخصائص الهيكلية والطيفية. أكد التحليل، الذي تم إجراؤه باستخدام حيود الأشعة السينية (XRD)، وقياس سعرات المسح التفاضلي (DSC) والمجهر الإلكتروني الماسح (SEM)، انخفاضًا في بلورة PLA عن طريق إضافة SEBS-g-MAH في كلا النوعين من المخاليط. . أظهر اختبار الشد انخفاضًا في الصلابة ومعامل يونج، مما يشير إلى زيادة المرونة والليونة المنسوبة إلى وجود المتوافق. أكدت الحسابات النظرية، وخاصة النمذجة الجزيئية MD، زيادة طاقة الربط بين PLA وPS ودور SEBS-g-MAH في تحسين توافقها. أشارت نتائج DFT، بما في ذلك حسابات DOS وCOSMO، إلى وجود تقارب بين LDPE والمتوافق في جزء الأوليفين من SEBS-g-MAH. بالنسبة لـ PLA، تم تحديد تقارب بين مجموعة الإستر (C = O) ومجموعة OH من SEBS-g-MAH.

الكلمات المفتاحية :بوليمر حمض اللاكتيك,مزيج, المتوافق، المحاكاة، النمذجة الجزيئية.